Development of mucoadhesive carrier systems for flavoring agents and cannabidiol

Dissertation

der Mathematisch-Naturwissenschaftlichen Fakultät

der Eberhard Karls Universität Tübingen

zur Erlangung des Grades eines

Doktors der Naturwissenschaften

(Dr. rer. nat.)

vorgelegt von

Ulrike Söpper

aus Münster

Tübingen

2021

Gedruckt mit Genehmigung der Mathematisch-Naturwissenschaftlichen Fakultät der Eberhard Karls Universität Tübingen.

Tag der mündlichen Qualifikation:	28.10.2021
Dekan:	Prof. Dr. Thilo Stehle
1. Berichterstatter:	Prof. Dr. Rolf Daniels
2. Berichterstatter:	Prof. Dr. Dominique Lunter

Publications and presentations

Poster presentation

Ulrike Söpper, Anja Hoffmann, Rolf Daniels

Development of mucoadhesive carrier systems for flavoring agents

12th World Meeting on Pharmaceutics, Biopharmaceutics and Pharmaceutical Technology 11-14 May 2021/ Online Conference

Publication

Ulrike Söpper, Anja Hoffmann, Rolf Daniels

Mucoadhesion and Mucopenetration of Cannabidiol (CBD)-Loaded Mesoporous Carrier Systems for Buccal Drug Delivery, Sci. Pharm. 2021, 89, 35

Special notes

Legally protected trademarks are used without special identification.

Statement of ethics

Porcine buccal mucosa was received from the department of experimental medicine of the University Hospital Tübingen, where the pigs were sacrificed in the course of experiments, that had been approved by the ethics committee of the University Hospital Tübingen. Alternatively, porcine buccal mucosa was supplied by a local butcher and the tissue was isolated immediately after the pig's slaughter.

The Chair of Pharmaceutical Technology and Biopharmacy at the Eberhard Karls University of Tübingen is registered for the use of animal materials with the Regierungspräsidium Tübingen (registration number DE 08 416 1052 21).

TABLE OF CONTENTS

ABBREVIATIONS ..... **VIII**

1 INTRODUCTION **1**

1.1 SILICA CARRIERS 1

1.2 ANATOMY AND PHYSIOLOGY OF THE ORAL MUCOSA 4

1.3 MUCOADHESION 8

1.4 MUCOADHESIVE POLYMERS 10

1.5 BUCCAL TRANSMUCOSAL DRUG DELIVERY 13

1.6 CANNABIDIOL 18

1.7 AIM 20

2 MATERIAL AND METHODS **22**

2.1 MATERIAL 22

2.1.1 Chemicals 22

2.1.2 Consumables 24

2.1.3 Devices 25

2.2 METHODS 27

2.2.1 Characterization of silica carriers 27

2.2.1.1 Scanning electron microscopy 27

2.2.1.2 Mercury intrusion porosimetry 27

2.2.1.3 Particle size 27

2.2.1.4 Oil absorption 27

2.2.1.5 Density measurement of triacetin and sunflower oil 28

2.2.2 Loading of silica carriers 29

2.2.2.1 Loading of thymol as a model drug 29

2.2.2.2 Loading of Optamint 29

2.2.2.3 Loading of CBD 30

2.2.3 Preparation of mucoadhesive carrier systems 31

2.2.3.1 Coating with a polymer suspension 31

2.2.3.2 Coating with high shear mixing 31

2.2.3.3 Coating with low- melting polymer 31
2.2.4 Preparation of toothpaste 32
2.2.5 Drug load quantification 33
2.2.6 HPLC assay 33
2.2.7 Differential scanning calorimetry (DSC) 33
2.2.8 Dissolution 33
2.2.9 Microscopy 34
2.2.10 Mucoadhesion test 35
2.2.10.1 Mucoadhesion test of flavor-loaded carrier systems 35
2.2.10.2 Mucoadhesion test of CBD-loaded carrier systems 36
2.2.11 Mucopenetration test 37
2.2.12 Rheometric characterization of toothpastes 38
2.2.13 Stability studies 38
2.2.13.1 Stability studies of flavor- loaded silica carriers 38
2.2.13.2 Stability studies of toothpaste 39
3 RESULTS AND DISCUSSION 40
3.1 FLAVOR-LOADED CARRIER SYSTEMS 40
3.1.1 Characterization of silica carriers 40
3.1.1.1 Particle size and morphology of silica carriers 40
3.1.2 Surface area and porosity 42
3.1.2.1 Oil absorption 44
3.1.3 Flavor loaded silica carriers 46
3.1.3.1 Loading and release of thymol as a model drug 46
3.1.3.2 Loading of Optamint flavors 51
3.1.4 Flavor-loaded mucoadhesive carrier systems 66
3.1.4.1 Development of mucoadhesive carrier systems 66
3.1.4.2 Optimization of the formulation 78
3.1.4.3 Mucoadhesive carrier systems with Sident 9 88
3.1.4.4 Influence of the type of flavoring agent on mucoadhesion 94
3.1.4.5 Mucoadhesion kinetic 95
3.1.4.6 Mucoadhesion after storage of carrier systems 98

3.1.5 Toothpastes 99
3.1.5.1 Stability studies of toothpastes 99
3.1.5.2 Mucoadhesion test of toothpastes 101
3.1.6 Flavor-loaded carrier systems - Interim conclusion 104
3.2 CBD-LOADED CARRIER SYSTEMS 107
3.2.1 CBD loaded silica carrier systems 107
3.2.1.1 Loading of CBD 107
3.2.1.2 Loading capacity 109
3.2.1.3 CBD release from silica carrier systems 111
3.2.2 CBD loaded mucoadhesive and mucopenetrating carrier systems 112
3.2.2.1 CBD release from mucoadhesive carrier systems 112
3.2.2.2 Mucoadhesion tests of CBD loaded mucoadhesive carrier systems 115
3.2.2.3 Mucopenetration tests of CBD loaded mucoadhesive carrier systems 117
3.2.3 Mucopenetration enhancer 121
3.2.3.1 CBD-loaded silica carrier systems with penetration enhancers 121
3.2.3.2 CBD loaded mucoadhesive carrier systems with propylene glycol 128
3.2.4 CBD-loaded carrier systems - Interim conclusion 134
3.3 FLAVOR- AND CBD-LOADED CARRIER SYSTEMS 136
3.3.1 Mucoadhesive carrier systems combining CBD and flavor 136
3.3.1.1 Flavor- and CBD-loaded carrier system - Interim conclusion 140
4 SUMMARY AND CONCLUSION 141
5 INDICES 143
5.1 LIST OF FIGURES 143
5.2 LIST OF TABLES 151
5.3 LIST OF EQUATION 154
5.4 REFERENCES 155
6 APPENDIX 160
6.1 HPLC UV-CALIBRATION 160
6.2 MUCOADHESION TEST OF FLAVOR-LOADED SILICA CARRIERS 162

6.3 COMPOSITION OF MUCOADHESIVE CARRIER SYSTEMS 163

Abbreviations

API	Active Pharmaceutical Ingredient
CBD	Cannabidiol
cm, cm^2	Centimeter, square centimeter
DSC	Differential scanning calorimetry
EtOH	Ethanol
FDA	Food and Drug Administration
g, mg	Gram, milligram
G′	Storage modulus
G′′	Loss modulus
h	Hour
HPLC	High performance liquid chromatography
HPMC	Hydroxypropyl methylcellulose
Hz	Hertz
IUPAC	International Union of Pure and Applied Chemistry
K	Kelvin
kDa	Kilodalton
kV	Kilovolt
LOD	Limit of Detection
LOQ	Limit of Quantification
mA	Milliampere
MC	Mucoadhesion coefficient
mm, μm	Millimeter, micrometer
min	Minute
mL, μL	Milliliter, microliter

N	Newton
nm	Nanometer
PE	Penetration enhancement ratio
PEG	Polyethylene glycol
pH	Negative log of activity of hydrogen ions
Ph.Eur.	European Pharmacopoeia
PP	Polypropylene
PTFE	Polytetrafluorethylene
RP	Reversed phase
RT	Room temperature
rpm	Revolutions per minute
s	Second
SD	Standard deviation
SEM	Scanning electron microscopy
SLS	Sodium lauryl sulfate
TC	Temperature cycle
UV	Ultraviolet radiation
V	Volume
%	Percent

1 Introduction

1.1 Silica carriers

Silicon dioxide, also referred to as silica, is a substance with the stoichiometric composition SiO_2 or SiO_2* X H_2O [1]. Synthetic amorphous silica is mainly produced by precipitation or flame hydrolysis processes; the latter being called pyrogenic or fumed silica. Oxides obtained by precipitation are called precipitated silica, silica sols or silica gels, depending on the process conditions [2]. Due to the possibility to control and customize the physical properties during the manufacturing process [3], synthetic silica materials cover an extremely wide range of applications. Its great biocompatibility and the classification as "generally recognized as safe (GRAS)" by the FDA are attracting increasing interest in the pharmaceutical, food and cosmetics industries [4]. Silica-based particles have emerged in the field of drug delivery as potential and promising materials for the incorporation of functional components [5]. Their huge surface area enables substantial adsorption of substances to the silica carrier. Compared to the surface of non-porous silica, the surface of porous silica is significantly enlarged due to the inner surface area of the pore system, resulting in the higher drug loadings [6]. Therefore, porous silica have proven to be excellent carriers promoting controlled and fast release [7]. According to the IUPAC porous materials are classified based on the average pore size. Pores with a width less than 2 nm are defined as micropores, for mesopores the diameter ranges between 2 and 50 nm and those exceeding 50 nm are called macropores [8].

Various different types of porous silica are commercially available [9], such as Aeroperl 300, Sident 9 and Sident 22s. Both Sident 9 and Sident 22s are precipitated silica specially developed for toothpaste applications. Aeroperl 300 is classified as mesoporous and granulated hydrophilic fumed silica. Owing to their internal porosity, the granules are capable of absorbing large quantities of various substances and hence act as a carrier material [10].

Several methods are available for incorporation of drugs into silica carriers (Table 1). Loading is achieved by temporary mobilization of the drug [7]. Melting the drug, using intense mechanical work, or loading the drug from a solution can enable the incorporation. The first technique, known as melt method, is based on the capillary forces drawing the melt into the pores [11]. Several common techniques for loading the drug from a solution have been established. These include loading from supercritical solvents as well as solvent immersion and solvent evaporation. The two latter methods rely on the equilibrium absorption from an excess of loading solution. In the solvent immersion method, the loading is followed by filtration and drying of the obtained carrier. Using the solvent evaporation method, the solvent is removed completely by evaporation [6]. Deposition of the loaded molecules in the incipient

wetness method is achieved by filling the pores with a precise amount of high concentrated drug solution and subsequently removing the solvent by drying or evaporation [11].

Table 1. Overview of drug loading techniques [12, 13]

	Method	**Loading**	**Advantages**	**Disadvantages**
Solvent- free methods	Melt method	Absorption of the melted drug by capillarity	No solvent residues, easy prediction of final drug load, short processing time, simple	Thermal stability of the drug required, risk of pore blocking by high viscous molten drug
	Physical mixing	Mechanical work	No solvent residues, short processing time, simple, easy prediction of final drug load	Drug in crystalline state, slower release rate
Solvent-based methods	Solvent immersion	Filling of the pores by capillarity and later adsorption on the pore walls from solvent + filtration and drying of residual solvent	Fastest release kinetics, time for drug to rearrange and aggregate inside the mesopores, limited risk of recrystallisation of the drug, non-organic solvents possible	Inefficient, time consuming, loading degree difficult to predict, drug loss by filtration

Method	Loading	Advantages	Disadvantages
Solvent evaporation	Filling of the pores by capillarity and later adsorption on the pore walls from a volatile organic solvent + solvent evaporation	Fastest release kinetics, time for drug to rearrange and aggregate inside the mesopores	Evaporation can affect the physical state of the drug, organic solvents necessary, less drug loss then solvent immersion
Incipient wetness	Absorption of concentrated drug solution by capillarity + drying/ evaporation	More efficient than the traditional solvent immersion (less time consuming, less drug loss), easy prediction of final drug loading	Risk of drug recrystallization, uniform distribution is difficult to control
Supercritical carbon dioxide technology	Impregnation of silica with drug solubilized in supercritical carbon dioxide + fluid evacuation	Non-toxic, non-flammable, easy removal, deeper penetration into the pores, no solvent residual	Poor solubility of drugs in supercritical carbon dioxide, more complex process

Despite growing interest in the pharmaceutical use of porous silica, the underlying mechanism of pore loading and consecutive drug desorption and release are still not sufficiently understood [5]. Nevertheless, it is understood that the efficiency of drug loading depends on texture properties of the carrier particles, the drug itself and also on the solvent used for loading [6, 14].

1.2 Anatomy and physiology of the oral mucosa

Similar to other body cavities that communicate with the exterior, the mouth is covered by a biological membrane, the oral mucosa. It is a moist surface lining the walls of the entire oral cavity with the exception of the teeth [15]. The oral mucosa has a total surface area of about 200 cm^2 and shows distinct variations in structure, thickness and blood flow in different regions of the oral cavity [16]. Three types of mucosa can be distinguished according to their primary function: masticatory mucosa, lining mucosa and specialized mucosa. The anatomical location of each type is illustrated in Figure 1. The lining mucosa represents the largest part of the oral mucosa, covering about 60% of the total area. The masticatory and the specialized mucosa cover a significantly smaller area of the oral cavity with 25% and 15%, respectively [17].

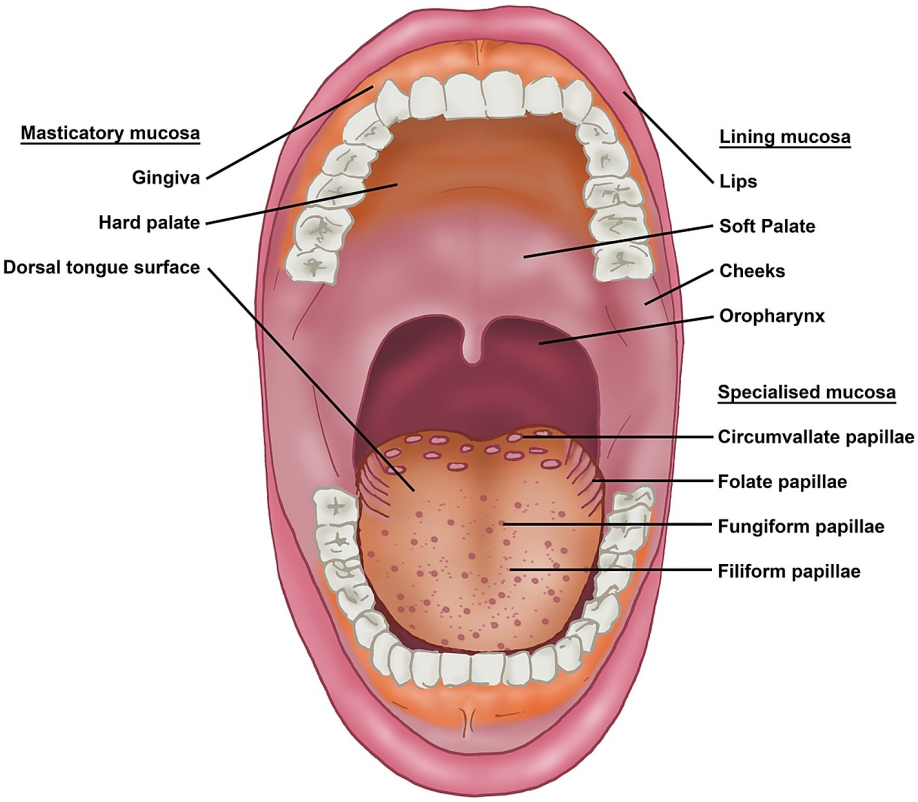

Figure 1. Classification and localization of the oral mucosa [15]

The masticatory mucosa, subject to mechanical stress, is keratinized and covers the gingiva and hard plate [15]. The epithelium of the lining mucosa is non-keratinized and covers the remaining regions, except for the dorsal part of the tongue. The latter is the specialized mucosa featuring characteristics of both the masticatory and the lining mucosa [15].

Anatomically, the oral mucosa is divided into three distinctive layers (Figure 2). The outermost layer is the epithelium followed by the basement membrane and the connective tissue. The connective tissue can be further subdivided into the lamina propria and the submucosa [18]. Depending on the location in the oral cavity, the composition of the epithelium varies. The buccal epithelium consists of approximately 40 - 50 layers of stratified squamous epithelia cells. Epithelia cells, produced by the basal layers, migrate to the surface and during this process undergo maturation. Cells are then shed at the surface of the epithelium [19]. The turnover time for the buccal epithelium has been estimated at 5 - 6 days [20]. The basement membrane, a proteinaceous fibrous extracellular matrix, functions as a mechanical support to the overlying epithelium and enables its connection with the subordinate lamina propria [21]. The lamina propria is a supporting layer of connective tissue, rich in fibrous fibers. In the lamina propria lymphatic and blood vessels, nerves and glands are present. The high blood supply of the lamina propria is derived from the external carotid artery [16]. Depending on its location in the oral cavity, the submucosa is situated beneath the lamina propria and, if present, attaches the upper tissues with the underlying bone or muscle. The submucosa contains fatty tissue, blood vessels, nerves and minor salivary glands [22].

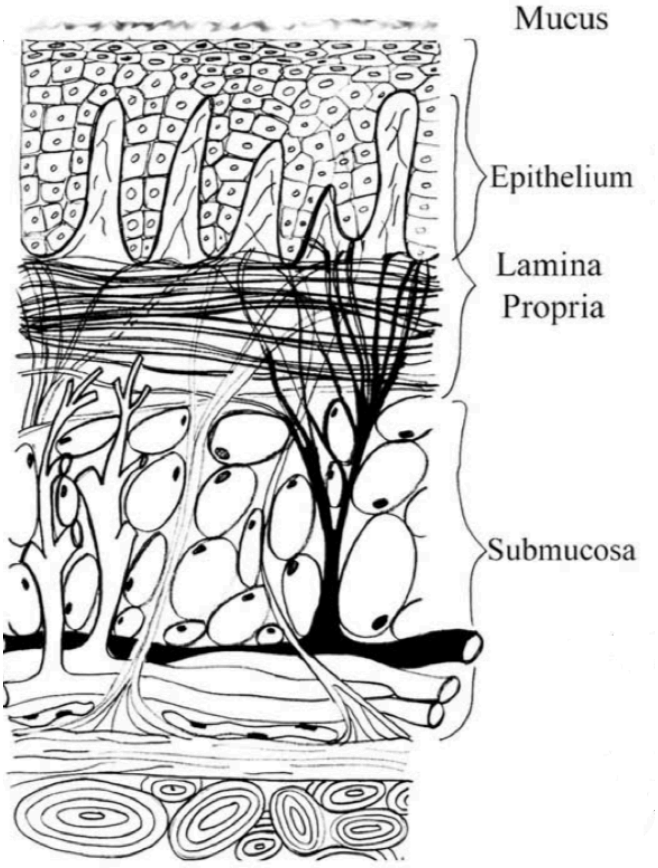

Figure 2. Cross section through the buccal mucosa [16]

The moist surface of the oral mucosa results from a mucus layer adhering to the epithelial surfaces of the oral cavity [23, 24]. Mucus is a highly viscous adherent secretion that is continuously produced by mucus secreting cells belonging to the sublingual and minor saliva glands [24-26]. The main functions of the mucus are to protect the supporting epithelia layer from physical and chemical damage, to provide lubrication and to control the water content in the underlying tissue [20, 25, 27, 28]. The major components of the mucus layer are glycoproteins termed mucins, inorganics salts, proteins, lipids, mucopolysaccharides and water [20, 24]. Water accounts for the largest part of the composition with over 95% [21, 25, 29]. Mucins are hydrophilic high molecular macromolecules consisting of a large polypeptide backbone with side chains of oligosaccharides [21, 30]. The side chains are covalently linked to the hydroxy amino acids, serine and threonine along the polypeptide backbone and often terminate in either sialic acid, sulfonic acid, or L-fructose [23]. In the oral cavity, a pH value in the range of 6.2 to 7.4 causes the mucins to be negatively charged and to behave as anionic polyelectrolytes [23, 26].

To maintain and preserve the oral tissue, the minor and major salivary glands provide a continuous flow of saliva into the oral cavity [31]. Salivation shows great individual variability and is influenced by various factors. The secretion of saliva is controlled by a salivary center in the medulla. Specific triggers including olfactory, gustatory, and mechanical stimuli can increase the flow rate to up to 7 mL/min [32]. The average resting or unstimulated salivary flow is approximate 0.5 mL/min [33]. Saliva is a highly aqueous solute composed of more than 99% water with the remainder comprising a various of electrolytes (including sodium, potassium, calcium, magnesium, bicarbonate, and phosphates), proteins, enzymes, immunoglobulins, mucins, and nitrogenous products [15, 32]. As a result of this complex composition, the saliva fulfills a multitude of functions. The saliva is responsible for taste and digestives functions, protective functions by lubrication and demulcent properties, buffer capacity, clearance, antibacterial activity and maintaining tooth integrity [32, 34].

The oral mucosa serves a variety of functions. The main function is the protection of the underlying tissue against environmental influences. This includes protection against mechanical forces as well as the penetration of harmful substances and microorganisms. The oral mucosa also functions as the site of secretion and sensory perception, including pain, temperature, taste and touch [19]. Adapted to the variety of functions, regional differences in the morphology of the mucosa in the oral cavity result in a variability in their potential utility for drug delivery [35]. The sublingual mucosa is thin and highly permeable and enables a rapid onset of action. The buccal mucosa is less permeable and thus suitable for retentive and sustained drug release [18, 36]. In general, the oral cavity is an attractive location for drug

delivery with both local and systemic effects. Therefore, a variety of oral drug delivery systems such as tablets, lozenges, sprays, and films have been developed (Table 2) [37].

Table 2. Examples of oral mucosal drug delivery systems [37, 38]

Mucosal site	**Dosage form**	**Drug**	**Product name**	**Manufacturer**
Sublingual	Tablet	Fentanyl citrate	Abstral	Orexo AB
	Spray	Fentanyl citrate	Subsys	INSYS Therapeutics
	Film/ Tablet	Buprenorphine Naloxone	Suboxone	INDIVIOR
Buccal	Tablet	Fentanyl citrate	Fentora	Cephalon
	Film	Fentanyl citrate	Onsolis	Meda Pharmaceuticals, Inc.
	Lozenge	Fentanyl citrate	Atiq	Cephalon
	Chewing gum	Nicotine	Nicorette	GSK Consumer Health
	Oromucosal solution	Midazolam	Buccolam	ViroPharma
	Spray	Insulin	Ora-lyn	Generex Biotechnology

1.3 Mucoadhesion

Adhesion is defined as the state in which two surfaces are held together by interfacial forces for extended periods of time [20, 28]. Bioadhesion is a specific case of adhesion in which at least one of the two substrates is of biological nature [29]. If the adhesive attachment is to mucus or a mucus membrane, the phenomenon is specifically referred to as mucoadhesion [28, 36].

Despite intensive research, the mechanisms behind the process of mucoadhesion are still not entirely understood. In general, the process is divided into two steps: the contact stage and the consolidation stage [25]. In the contact stage an intimate contact between the mucoadhesive and the mucus membrane occurs. This stage is characterized by spreading and swelling of the formulation initiating the close contact with the mucus layer [39]. In the consolidation stage the adhesion is strengthened through several physicochemical interactions [28].

Numerous theories have been proposed to explain the complex process of mucoadhesion and the mechanisms involved [26].

Wetting theory:

The wetting theory is primarily applicable to liquid or low viscosity mucoadhesive systems and considers surface and interfacial energies [20, 28]. It defines the energy required to counter the surface tension at the interface allowing the polymer to spread over the mucus surface [24]. The spreadability of the polymer on the surface is a prerequisite for an intimate contact and therefore for the development of adhesion. The ability of the polymer to spread across the surface increases with decreasing contact angles and is optimal with a contact angle equal or close to zero degree [24, 40].

Diffusion theory:

This theory describes the time-dependent interpenetration and entanglement of the mucoadhesive macromolecule and the mucin chains. At a sufficient interpenetration depth (0.2 - 0.5 μm), the two-way diffusion creates a semi-permanent adhesive bond [16]. The penetration rate depends on the contact time and characteristics of the two interacting polymers, including diffusion coefficients and chain flexibility [20, 41].

Electronic theory:

The electronic theory explains the adhesion based on electron transfer between the mucus and the mucoadhesive polymer generated by differences in their electronic structures. The electron transfer results in a formation of an electrical double layer and electrostatic attraction between oppositely charged surfaces [20, 29].

Absorption theory:

The adsorption theory posits that adhesion is the result of interactions between the adhesive and the mucus substrate. The chemical bonds can be categorized into primary and secondary bonds. On account of their durability, primary bonds, which include ionic, covalent, and metallic bonds, are generally undesirable. Secondary bonds on the other hand have the advantage of being semi-permanent. They are generated by van der Waals forces, hydrophobic interactions and hydrogen bonds and are predominant in mucoadhesion processes [28, 42].

Fracture theory:

According to fracture theory, the adhesive strength is related to the forces required for polymer detachment from the mucus after adhesion is established [43].

In isolation, none of these theories can completely explain the process of mucoadhesion. Therefore, the theories should not be considered separately but as complementary processes involved in different stages of the interaction between the adhesive polymers and the mucosa [26].

The concept of mucoadhesion offers several advantages in the field of drug delivery. Mucoadhesive drug delivery systems provide the possibility of localized drug release by retaining the dosage form at the site of action over an extended period of time [28]. As a result of the prolonged and intimate contact to the absorption side, mucoadhesive drug delivery systems also enable improved systemic absorption of drugs via the mucosa.

1.4 Mucoadhesive polymers

Mucoadhesive polymers are generally identified as macromolecular organic hydrocolloids featuring properties that enable interactions with the mucus surface [25]. The mucoadhesive properties of polymers are dependent on various factors, including molecular weight, chain flexibility, functional groups, concentration and the extent of swelling/hydration [20]. High molecular weight promotes physical entanglement by increasing the internal cohesiveness of the polymer. Studies have shown that the optimal molecular weight differs for each polymer. In general, a threshold of at least 100 kDa is assumed to be required for a desirable level of mucoadhesion [21, 36, 44]. On the other hand, high molecular weight reduces flexibility and thus impairs diffusion and interpenetration into the mucus layer [20]. The same applies for the degree of cross-linking. A high degree of cross-linking minimizes polymer chain flexibility and thus reduces the penetration of the chains into the mucin network. The degree of cross-linking also affects the resistance to dissolution. Cross-linked hydrophilic polymers swell and retain their structure in aqueous environments, whereas non-crosslinked polymers tend to disperse rapidly forming a colloidal solution [16, 18, 25, 40]. According to the adsorption theory the polymer attaches to the mucosa by formation of secondary non-covalent bonds. Therefore, the presence of respective functional groups is mandatory and consequently facilitates mucoadhesion [24]. An increased concentration of polymer leads to improved mucoadhesion due to a higher number of functional groups. If a certain concentration is exceeded, the mucoadhesive strength drops rapidly, since the polymer chains interact strongly with each other, limiting the chains available for interpenetration. The optimum concentration varies from polymer to polymer [36, 45]. An optimum degree of hydration is required for mucoadhesion to occur [23]. Polymer swelling permits relaxation of the polymer chains and enhances the interpenetration process between the polymer and the mucin molecules [16, 21, 25]. High swelling capacity can achieve higher levels of entanglement within the mucus layer [24]. However, overhydration results in a loss of mucoadhesion due to a formation of a slippery mucilage [16, 25]. Consequently, there is a critical degree of hydration of the mucoadhesive polymer leading to optimal adhesion [21].

Besides polymer-specific factors, external factors can also affect mucoadhesion of polymers in the oral cavity. These include the pH value, which can influence the dissociation of functional groups, the duration of initial contact, the mucus turnover rate, as well as tissue movement like speaking or consumption of food and other [21].

Polymers commonly used for mucoadhesive drug delivery systems can be classified as first- and second-generation polymers, among others [24]. The traditional or first-generation polymers can be further divided into cationic, anionic and neutral polymers [20, 25]. In the

first category, chitosan is the most extensively studied polymer in current literature [20]. Chitosan is a natural cationic polymer derived from the deacetylation of chitin [18, 40]. The mucoadhesion of chitosan is associated with several mechanisms [27]. Electrostatic attraction between the positively charged amines and the negative sialic acid residues of glycoproteins seems to be the primary mechanism. The complex interaction with the mucosa also involves hydrogen bonding and hydrophobic effects [18, 23, 27].

Anionic polymers comprise carbomers, synthetic, high-molecular polymers which are widely used in designing mucoadhesive delivery systems [18, 46]. They are polymers of acrylic acid cross-linked with polyalkenyl ethers or divinylglycol [46]. The mucoadhesive properties of carbomers are based on a number of physicochemical properties, including high hydration and excellent swelling levels allowing entanglement within the mucus layer and promoting mucoadhesion [16]. Depending on the prevailing pH and pK_a value of the polymer and the resulting number of ionized carboxyl groups, adhesion is also related to the ability to form hydrogen bonds with oligosaccharide chains of the mucins [26].

Hypromellose is a semi-synthetic, non-ionic cellulose derivate and is also extensively used outside the field of mucoadhesion for controlled drug delivery [40]. Apart from the ability of some polymers to form hydrogen bonds, the adhesion of non-ionic polymers to the mucosa is based on interpenetration followed by polymer chain entanglement [47].

In contrast to first-generation polymers, second-generation polymers offer specificity for certain chemical target structures on the mucosal surface, and hence exhibit improved chemical interactions [20, 24]. Lectins, bacterial adhesion, thiolated polymers and thiomers are representatives of this group [16]. The last two possess thiol-bearing functional groups and, by means of the covalent bonds between the thiol groups and the cysteine-rich subdomains of the mucus layer, achieve a prolonged retention time on the mucosa [16, 21, 26]. On the downside, lectins are associated with toxicity and immunogenic reactions, and cytotoxicity is also discussed in context of some thiolated polymers [16, 48].

For the assessment of mucoadhesive properties of polymers, various testing methods have been postulated. Traditionally the intensity of mucoadhesive characteristics are evaluated by in vitro test methods [26]. The testing methods can be divided into direct and indirect methods. The former measure the force or time required to detach or remove the mucoadhesive from a mucosal surface [49]. Indirect methods determine the interactions between the mucoadhesive system and mucins. Among the commonly used methods are: tensile studies, flow-through method, rheological method and fluorescence detection [16].

For tensile studies the force necessary to detach a formulation from a mucosal surface after they are brought into contact, is measured [50]. A flow through simulation quantifies the

binding ability of a polymer to the mucosa under shear forces exerted by a continuous flow. The strength of interactions between a mucus gel and a mucoadhesive polymer can be evaluated by rheological measurements [30].

In addition to the different set ups, the choice of an appropriate mucosal tissue or replacement is challenging and influences the results. Beside from human gastric mucosa, mucin disc (compressed mucin), animal mucosa and mucosa mimetic materials (hydrogels) are used [49]. Animal mucosa offers the advantage of structural similarity to human mucosa. Due to the differences in the keratinization of the mucosal lining, however, not all animal tissues are equally suitable as test substrates [51]. In addition, mucosal tissue varies greatly depending on its location in the body. Thus, the intestinal mucosa is structurally not identical to the oral mucosa. [19]. The oral mucosal membranes of pigs, monkeys and dogs provide the greatest resemblance to those of humans and are therefore most appropriate for mimicking the physiological conditions in the human oral cavity [52]. Disadvantages of biological materials are, besides the ethical point of view, the large variability, and the associated lower reproducibility. Synthetic mucosal mimetic materials are cost-effective and homogeneous alternatives to animal tissue and are particularly attractive in terms of ethical aspects [53]. Fully synthetic materials such as hydroxyethyl methacrylate have shown promise as test substrates for determining mucoadhesive performances [54]. However, few synthetic materials are currently available, and they require validation under a variety of conditions before they can be accepted as an alternative to mucosal tissue [55]. Overall, the multitude and the strongly varying test conditions lead to a large heterogeneity of the test results and preclude a feasible comparison of the mucoadhesive properties of polymers [49].

1.5 Buccal transmucosal drug delivery

Oral transmucosal drug delivery is the administration of APIs through the oral mucosa with the aim of attaining therapeutic levels in the blood to achieve systemic effects [56]. The buccal mucosa is generally employed as the site of absorption when a sustained and prolonged drug release is desired [57]. The buccal mucosa provides a smooth and relatively immobile surface [38], as well as a reduced enzymatic activity with respect to other mucosal tissues [58]. Additionally, the buccal mucosa is robust and shows short recovery times after stress or damage [52]. Owing the ease of access and administration buccal drug delivery is highly accepted by patients [58]. Moreover, the relative permeability and the rich blood supply of the buccal mucosa provide direct access to the systemic circulation, thus bypassing hepatic first-pass effect and avoiding presystemic elimination within the gastrointestinal tract. [16, 23]. Consequently, the buccal mucosa is an attractive path when conventional routes do not allow for adequate therapy [59].

Disadvantages results from the continuous salivary flow and the mechanical stress in the oral cavity, causing shorter residence times on the mucosa [16]. To obtain the therapeutic action, it is therefore necessary to prolong and improve the contact between the drug and the mucosa and minimize the drug loss by salivary flow [58]. Another major limitation in the development of transmucosal drug delivery systems is the permeability barrier in the buccal mucosa [60]. Although the basement membrane provides some resistance to mucosal permeation, the outer epithelium is still considered to be the relevant barrier to the penetration of substances [52]. The permeability barrier is attributed to extruded material from membrane coating granules. During differentiation, these fuse with the plasma membrane of the apical cell surface and discharge their contents (mainly cholesterol esters, cholesterol, and glycosphingolipids) into the intracellular spaces in the outermost superficial layers [52]. The oral mucosa also presents an enzymatic barrier formed by enzymes such as aminopeptidases, carboxypeptidases and esterases. However, this barrier is considerably less effective than the one of the gastrointestinal tract [61].

Absorption of a drug into the oral mucosa is predominantly based on a passive diffusion process. Drug molecules in contact with the mucosa can permeate by two possible routes: transcellular (intracellular) and paracellular (intercellular) [38]. The route taken depends on the physicochemical properties of the diffusing substance. Lipophilic agents are able to pass through the lipid structures of membranes and usually show permeation via the transcellular pathway. For hydrophilic substances, the hydrophilic intercellular spaces and thus the paracellular pathway is the main route of transportation [52]. Compared to intestinal tissue, the presence of tight junctions in the oral mucosa is rare. Hence, drug transport via the

paracellular route is more favorable in the oral mucosa then in the intestinal mucosa, as with the tight junctions the primary barrier to intercellular passage is absent [62].

Buccal penetration enhancer

The current transmucosal route of administration is limited to a small number of drugs that provide the appropriate characteristics to readily cross the mucosa [63]. A list of drugs available in commercially buccal dosage forms is shown in Table 3. Most drugs that are successfully administered via the buccal route are small and lipophilic, while large hydrophilic molecules are generally poorly absorbed [64]. In order to extend the accessibility of the buccal route to a wider range of drugs by facilitating permeation through the buccal mucosa, enhancers are used [65].

Table 3. Examples of commercially available transbuccal drug delivery systems [37, 38, 66]

Drug	**Product name**	**Dosage form**	**Manufacturer**
Fentanyl citrate	Atiq	Lozenge	Cephalon
	Fentora	Tablet	Cephalon
	Onsolis	Film	Meda Pharmaceuticals, Inc
Buprenorphine hydrochloride	Subutex	Tablet	Reckitt Benckiser
Buprenorphine hydrochloride /Naloxone	Suboxane	Tablet	Reckitt Benckiser
Prochlorperazine	Buccastem	Tablet	Reckitt Benckiser
Triamcinolone	Aphtac	Tablet	Teijin Ltd
Testosterone	Striant SR	Tablet	Columbia Pharmaceuticals
Nitroglycerine	Nitrostat	Tablet	W Lambert-P Davis-Pfizer Pharmaceuticals
Glyceryl trinitrate	Suscard	Tablet	Forest Laboratories
Nicotine	Nicorette	Chewing gum	GSK Consumer Health
	Nicotinelle	Lozenge	Novartis Consumer Health
Miconazole	Loramyc	Tablet	BioAlliance Pharma SA
Cannabis-derived (THC, CBD)	Sativex	Spray	GW Pharmaceuticals, PLC
Midazolam	Buccolam	Oromucosal solution	ViroPharma
Insulin	Ora-lyn	Spray	Generex Biotechnology

Penetration enhancers can promote buccal absorption via different techniques, which include drug-saturated systems, physical approaches, and chemical penetration enhancers [62]. Physical enhancement techniques comprise iontophoresis and phonophoresis, approaches that are currently very expensive and associated with technical challenges and compliance issues [57, 67]. Therefore, the most common approach is the use of chemical substances with penetration-enhancing properties. Ideally, the chemicals should provide a safe and non-toxic, pharmacologically, and chemically inert, non-irritating and non-allergenic profile. In addition, they should not permanently alter membrane properties [57]. Table 4 gives an overview of typical substances studied as mucosal enhancers.

Table 4. Penetration enhancers used for buccal drug delivery [57]

Type	Example
Surfactants	Sodium lauryl sulfate, laureth-9, polyoxyethylene-9-laurylether, polysorbates
Bile slats	Sodium deoxycholate, sodium glycocholate, sodium tauro cholate
Fatty acids	Oleic acid, caprylic acid, lauric acid
Polymers	Chitosan and derivates
Polyols	Glycerol, propylene glycol
Chelators	Ethylene diamine tetra acetic acid, citric acid, salicylates
Others	Azone, cyclodextrin

In general, chemical enhancers can act through many different mechanisms. They can increase cell membrane fluidity, extract structural intercellular and intracellular lipids, and alter cellular proteins or mucus structure. Enhancers can also act by overcoming the enzymatic barrier or by increasing thermodynamic activity of the permeant [61]. There are only a few works specifically targeting the buccal mucosa and therefore the exact mechanism of action of most buccal enhancers has not been fully elucidated [60].

Bile salts and surfactants

For bile salts and surfactants various mechanisms are proposed, including extraction of lipid or protein components, enzyme interaction, membrane fluidization and reverse micellization [57]. It is suggested that the effects of bile salts and surfactants are concentration dependent. At lower concentrations, the lipid-solubilizing effect generally modifies paracellular transport. At higher concentrations, transcellular transport is proposed to be affected by extraction of membrane lipids [62]. The beneficial effect of surfactants and bile salts on buccal mucosal absorption has been reported in several studies [62]. However, one of the problems associated

with chemical permeation enhancers, especially surfactants and bile salts, is their potential toxicity [57]. The increase in membrane fluidity has been linked to the irritation potential of surfactants. Typically, ionic surfactants tend to be more potent enhancers than nonionic surfactants, but they are also considered more toxic because they can damage the permeability barrier even at relatively low concentrations [61].

Fatty acids

Fatty acids - in particular unsaturated fatty acids -are endogenous molecules, which have been extensively investigated as enhancers in dermal formulations [68]. For buccal delivery, there are only limited reports [57]. Studies focused primarily on oleic acid, which has been shown to increase mucosal uptake of several active ingredients [68]. With respect to biocompatibility, tests showed no adverse tissue effects from oleic acid [69]. It is suggested that the fatty acids act by altering membrane fluidity, disturbance of the lipid packing, and increasing partitioning into the tissue [57, 62, 68].

Chitosan

Chitosan is a biocompatible and biodegradable polymer that offers the unique feature of combining a mucoadhesive and a mucopenetration enhancing effect [70]. In the literature, studies with chitosan have demonstrated the enhancing effect on drug penetration through various mucosal tissues including the buccal mucosa [70]. However, the mechanism of penetration enhancement through the mucosa of the oral cavity has not yet been fully understood. The enhancing effect is often attributed to the bioadhesive properties of chitosan [57]. Within the intestinal mucosa, the penetration enhancement is ascribed to the binding of chitosan to the epithelial membrane by a charge-dependent effect leading to opening of tight junctions [71]. Such a mechanism of action cannot be extrapolated to buccal penetration enhancement, since tight junctions in the buccal mucosa are rare and do not contribute to its barrier function [62]. Theories that chitosan interferes with the intercellular organization in the buccal epithelium have still to be demonstrated [62].

Propylene glycol

Propylene glycol is a frequently used skin penetration enhancer, but its mechanism underlying its ability to promote permeation has not been explored in detail. In addition to affecting the drug solubility in the vehicle, it is suggested in literature that propylene glycol increases permeant partitioning into and solubility within the intercellular lipids [72]. Studies demonstrate that the use of propylene glycol as a penetration promoting substance did not result in tissue damage of the buccal mucosa [69].

Current and future development of transmucosal drug delivery

Intensive research has been conducted in the field of oromucosal delivery and numerous substances have been investigated, yet only a few products are currently available on the market (Table 3) [64, 73]. But despite the small number of drugs administered via this route to date, buccal drug delivery remains an attractive and feasible route when enteral administration is inefficient or impractical [38, 56]. Recently the opportunity to exploit the buccal route as a non- invasive alternative for protein drug molecules is investigated as well [66]. Consequently, there is still an increasing interest in the development of formulations that are able to overcome the barriers and enable successful transmucosal drug delivery.

1.6 Cannabidiol

Cannabidiol is a major phytocannabinoid isolated from the *Cannabis sativa* plant [74] or derived by chemical synthesis [75]. It is a non-psychoactive component and displays favorable safety and tolerability profiles in humans. At this point, the precise mechanism of action is not fully understood, and little is known about possible CBD receptor-mediated signaling pathways. In addition to the two cannabinoid receptors, CB1 and CB2, a variety of other receptors, such as the G-protein coupled receptor GPR55, are being studied in association with the effects of CBD [76].

CBD has attracted extensive and growing scientific and commercial interest due to its wide range of beneficial effects, including effects on anxiety, memory, locomotion, inflammatory reactions and pain perception [77]. Despite the variety of possible indications only a few licensed medicinal products are available. To date, two CBD-based products have been approved by the FDA and EMA [74]. Epidiolex, a pure CBD oral solution, is approved in connection with a rare pediatric from of epilepsy [78]. The second product, Sativex, is a combination of CBD and delta-9-tetrahydrocannabinol that is available as an oromucosal spray [79].

Per oral administration of CBD is most convenient, yet strongly influenced by the challenging pharmacokinetic properties [80]. With both a high lipophilicity and a pronounced first pass effect, CBD features a low bioavailability and variable pharmacokinetic profiles. The bioavailability of CBD after per oral administration is estimated at 6%- 20% [80-82] and is highly susceptible to food effects [83]. Therefore, alternative drug delivery systems that increase the bioavailability are essential for a successful therapy of CBD. Administration via the oral transmucosal route can overcome some of the problems of CBD delivery by bypassing the digestive tract and the first-pass metabolism. However, recent studies for the oromucosal spray Sativex have implied that a substantial portion of the administered dose is washed from the mucosa by salivary flow and may subsequently be absorbed through the gastrointestinal tract [80, 81]. The pharmacokinetic data of Sativex showed a dependence on food intake, although the pharmacokinetic profiles should not be significantly affected when administered transmucosally [84]. Supporting these findings is a study by Guy et al. demonstrating that the pharmacokinetic parameters of Sativex were similar for oromucosal and oral administration [85]. Nevertheless, since CBD is able to permeate through the mucosa with clinically relevant plasma levels, it is suggested that the oromucosal route of administration remains viable as long as exposure times to the oral mucosa are adequate and washout by saliva is prevented [80]. Intrapulmonary administration is also considered an effective route of administration as it results in rapid onset of action and high systemic bioavailability [86]. Regarding inhalation,

the major limitations are caused by the variability in inter-patient efficiency and irritation of the respiratory tract [86].

Formulations currently under development by commercial companies include oral dosage forms with formulation strategies to improve pharmacokinetic profiles, as well as dosage forms increasing bioavailability by utilizing alternative routes of administration, such as transdermal, oromucosal, nasal and intravenous systems [81].

1.7 Aim

The buccal region of the oral cavity is an attractive site for drug delivery to achieve mucosal (local) and transmucosal (systemic) effects. But despite having many advantages, there are still some challenges encountered while developing dosage forms for the buccal route. One main obstacle associated with buccal drug delivery is the salivary flow and the resulting difficulty in keeping the dosage form at the site of action. Therefore, the concept of mucoadhesion is considered a critical factor in the formulation of buccal dosage forms.

Traditionally, mucoadhesion is a concept used in the field of drug delivery systems. In recent years, mucoadhesion has also attracted considerable interest in other industries, like the food sector, to modify perception and sensory characteristics of food products. In general, flavoring agents have rather unfavorable adhesion and release profiles on physiological surfaces, especially the oral mucosa. Consequently, high concentrations or highly effective flavoring agents are usually required to improve the duration and intensity of taste perception. In addition, the volatility of the flavoring agents poses a major challenge in the preparation and storage stability of dosage forms.

The aim of the first part of this thesis was to develop and characterize mucoadhesive carrier systems for flavoring agents to optimize the adverse adhesion and release profiles of flavors on oral mucosa. It was hypothesized that by developing a flavor-loaded silica carrier system with mucoadhesive properties, an optimized residence time of the flavor in the oral cavity could be achieved, thus allowing a reduction in the concentration of the flavor and the avoidance of highly potent substances. Additionally, the loading of the flavor into a silica carrier is intended to achieve durable binding of flavor to the carrier system to enable sufficient stability of the flavor content. The presence of mucoadhesive polymers is crucial to protect the formulation from physiological removal mechanisms in the oral cavity and hence achieve adequate mucoadhesion. Therefore, special emphasis is placed on the development of a suitable coating method to functionalize the flavor-loaded silica systems with a mucoadhesive polymer without compromising flavor stability. The resulting mucoadhesive carrier systems are characterized with a focus on mucoadhesion, storage stability and release of the flavoring agents. Furthermore, the performance of the mucoadhesive carrier systems has to be optimized by investigating different types of silica as well as different coating mediums and types of mucoadhesive polymers. Finally, the mucoadhesive carrier systems should be incorporated into toothpastes, as an example of application, and the aforementioned critical quality attributes need to be reevaluated.

In addition to providing a prolonged local effect, the buccal mucosa offers an attractive alternative route for systemic drug delivery when enteral administration is inefficient or

impractical. With direct access to the systemic circulation, transmucosal administration can bypass degradation by the first pass effect and in the gastrointestinal tract, resulting in increased drug bioavailability. However, formulation developed for systemic use in the oral cavity are limited by the barrier function of the mucosa and require the utilization of appropriate absorption enhancement strategies to obtain suitable penetration profiles. Beyond penetration, buccal drug delivery systems must maintain intimate contact with the mucosa long enough to allow drug release and absorption. Otherwise, saliva flow in the oral cavity may result in drug loss and thus further reduce absorption. Given these limitations, the development of an effective buccal dosage forms requires both sufficient mucosal penetration and buccal retention in order to allow sufficient mucosal absorption of the drug.

The second aim for this thesis was to develop and characterize mucoadhesive and mucopenetrating carrier systems for APIs, based on the mucoadhesive formulations developed for flavoring agents. Although CBD is attracting increasing interest due to its potential value in the treatment of several medical conditions, a successful therapy is challenging because of its low oral bioavailability. Additionally, recent studies on the commercially available CBD- based oromucosal spray (Sativex) have implied that a substantial portion of the administered dose is washed from the mucosa and may subsequently be absorbed through the gastrointestinal tract. Therefore, CBD should be investigated as a model drug.

It was hypothesized that the mucoadhesive formulation will prevent washout by saliva flow and increase penetration of CBD into the mucosa due to the prolonged residence time at the site of absorption. For the preparation of the CBD-loaded carrier systems, transferability of the loading and coating methods developed for the flavoring agents are to be examined. The prepared mucoadhesive carrier systems have to be investigated with regard to the dissolution of the drug and the mucoadhesive properties. A special focus needs to be placed on the penetration behavior of CBD into the mucosa to gain insights into the suitability of the mucoadhesive carrier systems for systemic application. Therefore, a method needs to be developed to test the CBD-loaded mucoadhesive carrier systems and to investigate the penetrated amount of the drug and the penetration depth. To ensure adequate penetration of CBD, the influence of various penetration enhancers on mucosal absorption of CBD should be included in the investigation.

When it comes to buccal delivery, molecules with a strong taste are not desirable and therefore taste issues must be considered. Hence, the concluding objective of this thesis is to investigate whether a mucoadhesive carrier system with a combination of drug and flavoring agent is a feasible approach.

2 Material and methods

2.1 Material

2.1.1 Chemicals

α- Amylase from *Bacillus subtilis*	Sigma-Aldrich Chemie GmbH
Acetonitrile (HPLC- grade)	Fisher Scientific GmbH
Acidum oleinicum	Caesar & Loretz GmbH
Aeroperl 300	Evonik Industries
Carbopol 971P NF	Lubrizol Deutschland GmbH
Chitosan food grade	Harke Pharma GmbH Sigma-Aldrich Chemie GmbH
di-Potassium hydrogen phosphate trihydrate	Merck KGaA
Ethanol (HPLC- grade)	Sigma-Aldrich Chemie GmbH
Glycerol Ph.Eur.	Dr. Willmar Schwabe GmbH & Co. KG
Hydrochloride acid	Sigma-Aldrich Chemie GmbH
Isopropyl alcohol	Fisher Scientific GmbH
Kolliphor PS 80	BASF SE
Methanol (HPLC-grade)	Sigma-Aldrich Chemie GmbH
Metolose 65SH50	Shin-Etsu Chemical Co.
Mucin from porcine stomach, Type III	Sigma-Aldrich Chemie GmbH
Mucosa (porcine)	Department of Experimental Medicine Tübingen, Local butcher Tübingen (Grießhaber)
Nitrogen	Westfalen AG
Optamint liquid 678368	Symrise AG

Optamint solid 678367	Symrise AG
Polyethylene glycol 1000	Sigma-Aldrich Chemie GmbH
Potassium chloride	VWR International GmbH
Propylene glycol	Dr. Willmar Schwabe GmbH & Co. KG
Refined sunflower oil	Caesar & Loretz GmbH
Sodium chloride	Caesar & Loretz GmbH
Sodium hydrogen carbonate	Caesar & Loretz GmbH
Sident 9	Grace GmbH
Sident 22s	Grace GmbH
Texapon V95G	BASF SE
Thymol	Caesar & Loretz GmbH
Toothpaste base (SAG19102501)	Symrise AG
Triacetin	Sigma-Aldrich Chemie GmbH

2.1.2 Consumables

Aluminum foil	FORA GmbH
Aluminum tube 3 mL	WEPA GmbH & Co. KG
BAYHA- Sterile surgical blades	C. Bruno Bayha GmbH
Cannula Sterican 20 G x 1 ½	B. Braun Deutschland GmbH & Co. KG
Eppendorf tubes 2 mL	Eppendorf AG
Cellstar-Tubes 15 mL, 50 mL	Fisher Scientific™ GmbH
Chromafil Xtra H-PTFE-20/25	Macherey-Nagel GmbH & Co. KG
Glass plate 20 x 20 cm	Workshop University of Tübingen
HPLC vials 1.5 mL with N11 crimps	Macherey-Nagel GmbH & Co. KG
Injection vial 20 mL	Zscheile & Klinger GmbH
Microscope slides	VWR International GmbH
MX35 Premier+ Microtome Blade 34/ 80 mm	Thermo Fisher Scientific Inc.
NEG-50	Thermo Fisher Scientific Inc.
Nucleosil 100-5 C18 125/4	Macherey-Nagel GmbH & Co. KG
Parafilm M	Bemis Company Inc.
Pipette tips 200 µL, 1000 µL, 5000 µL	Brand GmbH & Co. KG, Eppendorf AG
Rubber stopper for injection vials	Zscheile & Klinger GmbH
Schott glasses 100 mL, 250 mL	Schott AG
SpeedMixer vessels	Hausschild & Co. KG
Swab 15x15 cm	Fuhrmann GmbH
Syringe, Omnifix 1 mL, 2 mL, 10 mL, 20 mL	B. Braun GmbH & Co. KG

2.1.3 Devices

Analytical balance XPE 205	Mettler Toledo GmbH
Balance Sartorius excellence	Sartorius AG
Centrifuge Mini Spin	Eppendorf AG
Cryostat Microm CryoStar HM560	Thermo Fisher Scientific Inc.
Dissolution apparatus PT-DT	Pharma Test Apparatebau AG
DSC 820	Mettler Toledo GmbH
Freezer (-28 °C)	Liebherr GmbH
Hot air oven TU 60/60	W.C. Heraeus GmbH
HPLC LC-20AT prominence Degasser DGU-20A5R Autosampler SIL-20AC HT Oven CTO-10ASVP UV/Vis-Detector SPD-20A Com. bus Modul CBM-20A (Software LabSolutions)	Shimadzu GmbH
HPLC pump 510	Waters Corporation
Magnetic stirring hotplate MR 3001K	Heidolph Instruments GmbH & Co. KG
Microscope Axio Imager Z 1 AxioCam MRm (Software AxioVision v 4.6)	Carl Zeiss Microscopy GmbH
Mucoadhesion cell	Workshop University of Tübingen
pH- Meter Seveneasy	Mettler Toledo GmbH
Pipette Eppendorf research 20-100 µL, 200 - 1000 µL	Eppendorf AG
Pipette Transferpette 2000 µL – 5000 µl	Brand GmbH & Co. KG
Purelab option-Q	Elga LabWater
Quantachrome Poremaster 60-GT	Quantachrome GmbH
Rheometer Physika MCR501	Anton Paar GmbH & Co. KG

Schaukelschrank Typ 3401	Rubarth Apparate GmbH
SEM Zeiss DSM 940 (Software Orion 5.25)	Carl Zeiss Microscopy GmbH
Somakon LabMixer	Somakon Verfahrenstechnik UG
SpeedMixer DAC 150.1 FVZ	Hausschild & Co. KG
Sputtercoater E5100	Bio Rad GmbH & Co. KG
Testo 830-T2 Infrared thermometer	Testo SE & Co. KGaA
Thermostat E11	Funke medingen
Vortex 2	IKA-Werke
Water bath Memmert W200	Memmert GmbH + Co. KG

2.2 Methods

2.2.1 Characterization of silica carriers

2.2.1.1 Scanning electron microscopy

Prior to imaging, the samples were fixed on studs with double-sided adhesive tape and coated with gold four times for 60 s each at 2.1 kV and about 20 mA. Subsequently, the sputtered preparations were examined at an accelerating voltage of 5 kV on a scanning electron microscope.

2.2.1.2 Mercury intrusion porosimetry

Experiments for pore size measurement on silica samples were conducted by an external contract laboratory (3P Instruments GmbH) using a Quantachrome Poremaster 60-GT. First, the samples were dried under vacuum at 200 °C for 2 h and then measured after cooling to room temperature. The Washburn equation was used to calculate the relationship between pore size and pressure, using 4.8 N/cm and 140 ° for mercury surface tension and contact angle, respectively.

2.2.1.3 Particle size

Laser diffraction was used to determine the particle size of the porous silica. By means of a vibrating dry powder feeder, a dry dispersion was obtained. A disperser pressure of 1 bar and an obscuration range between 2% and 6% were used for the measurements. The evaluation was performed according to the Mie theory, assuming a refractive index of 1.52 and an absorption index of 0.1. The mean value from three measurements was calculated.

2.2.1.4 Oil absorption

According to the ASTM International D281-95 "Standard Test Method for Oil Absorption of Pigments by Spatula Rub-Out" [87], the oil absorption capacity of the porous silica materials for triacetin and sunflower oil was assessed. Prior to the measurement, the silica samples were dried at 110 °C for 30 min. Subsequently, a sample quantity of 1 g was placed on a glass plate. Either triacetin or sunflower oil was added in dropwise manner to the silica powder using a burette. After each drop, the oil was thoroughly mixed into the powder with two spatulas, until sufficient oil was incorporated to form a stiff, putty-like paste. The required volume of oil was determined from the burette, converted to mass using the density (2.2.1.5) and expressed as oil absorption capacity in grams of oil per 100 g of silica. For each silica and oil, the absorption capacity was determined in triplicate. In an adaptation of the method, the volume of sunflower oil that the silica can absorb without losing the properties of a free-

flowing powder was determined. The measurement was carried out according to the method described above. The end point was chosen as the point at which the powder particles begin to visibly aggregate.

$$w\ [g/100\ g] = \frac{\Delta V\ (Oil) * \rho\ (Oil)}{m(Silica)} * 100$$

Equation 1. Oil absorption capacity

w= Oil absorption capacity
ΔV= Volume oil [mL]
P= Density [g/mL]
m= Mass [g]

2.2.1.5 Density measurement of triacetin and sunflower oil

A density meter was used to determine the density of triacetin and sunflower oil for the oil absorption capacity measurements. The samples were appropriately tempered by the instrument to the required temperatures and measured three times each.

2.2.2 Loading of silica carriers

2.2.2.1 Loading of thymol as a model drug

Three different methods were used to load thymol into the pores of the silica carrier, namely: solvent filtration method, incipient wetness and melt method. Before loading, the silica carrier was dried in the hot air oven for 30 min at 110 °C. After loading, the thymol content in the loaded silica samples was analyzed by HPLC after extraction (2.2.5, 2.2.6).

In the solvent method, loading of the dried silica carrier was achieved by dispersing 100 mg silica particles in 5 mL of a thymol solution in ethanol at the desired concentration. In a closed glass vial, the suspension was brought to equilibrium under gentle stirring for at least 1 h. Afterwards the suspension was filtered, and the obtained powder dried at 35 °C to evaporate the residual ethanol.

For the incipient wetness method, dried silica materials were impregnated in a glass vial with a concentrated solution of the drug in ethanol whilst stirring continuously. The vial was closed, and the mixture stirred for 5 min at 1000 rpm with a magnetic stirrer. After loading, the powders were dried at 35 °C until mass constancy was reached. To study effects of the loading method on loading efficiency, the ratio of drug to carrier particles (1:1, 1:2 and 1:3) and the concentration of the loading solution (10, 30 and 50 mg/mL) were varied. Silica carriers were loaded with thymol aiming at drug contents of 25, 33 and 50% theoretical loading. The loading efficiency was assessed based on the difference between the determined load and the theoretical load.

In the melting method, physical mixtures of drug and dried silica were prepared and heated in a closed glass container for 15 min at a temperature slightly above the melting temperature of the drug (thymol: 55 °C).

2.2.2.2 Loading of Optamint

Bevor the loading process, the silica carrier was dried in the hot air oven for 30 min at 110 °C. The flavoring agent was dripped in small amounts to the carrier particles. During the addition, the powder was intensively mixed with a magnetic stirrer. The loaded carrier was subsequently mixed at 1000 rpm for 5 min. For a larger batch size, the loading was carried out using a LabMixer. To this end, 15 g of silica carrier were placed in the mixer and loading was done by steadily syringing 3 g Optamint to the carrier whilst mixing at low speed for 4 min. Finally, the loaded carrier was mixed for another 10 min at 600 rpm with the scraper (level 2) turned on additionally. For investigating the influence of the drug-to-carrier ratio, carriers with a ratio of 1:1 to 1:5 were prepared. The powder obtained was extracted to determine the actual load (2.2.5 Drug load quantification).

2.2.2.3 Loading of CBD

Prior to the loading process, the silica was dried at 110 °C for 30 min. Loading of Aeroperl 300 with CBD was conducted in a LabMixer. An amount of 15 g of silica carrier was placed in the mixer and loading was achieved by steadily syringing a concentrated ethanolic CBD solution onto the silica within 4 min of mixing at low speed. Subsequently, mixing of the loaded carrier was continued for another 10 min at 600 rpm with the scraper (level 2) turned on additionally. Finally, the silica carrier was dried at room temperature until the ethanol was evaporated and mass constancy was reached.

2.2.2.3.1 Preparation of CBD-loaded carrier systems with penetration enhancers

CBD-loaded carrier systems with propylene glycol, SLS or oleic acid were obtained by adding the enhancer to the ethanolic CBD solution. The concentration of enhancer in the solution was chosen depending on the desired final concentration in the carrier system. Loading of Aeroperl 300 was accomplished as described above (2.2.2.3).

2.2.3 Preparation of mucoadhesive carrier systems

2.2.3.1 Coating with a polymer suspension

Mucoadhesive carrier systems were prepared by firstly loading the silica carrier with Optamint or CBD and afterwards coating with a mucoadhesive polymer. Loading of the flavor or the API was accomplished in advance by means of a magnetic stirrer or in line with the polymer coating in the LabMixer (2.2.2.2 Loading of Optamint, 2.2.2.3 Loading of CBD). A suspension consisting of a mucoadhesive polymer and sunflower oil, triacetin, glycerol, or water was prepared. The final concentration of polymer in the carrier system was controlled by the amount of suspension and its concentration. Subsequently, the suspension was dosed dropwise to 15 g of loaded carrier. While adding of the polymer suspension, the rotational speed was first adjusted to 400 rpm for 5 min and then raised to 600 rpm for 2 min. Finally, the scraper was additionally set to level 2 for 5 min.

When using the flavoring agent as a suspension medium, the first step of loading the silica carrier with flavoring agent was omitted and the coating was directly carried out with the suspension of polymer and flavor as described above.

2.2.3.2 Coating with high shear mixing

For the dry coating of the carrier with the mucoadhesive polymer by high shear mixing, 15 g flavor-loaded silica carrier and 3% HPMC were mixed in the LabMixer for 2 min at 400 rpm and then at 1500 rpm for additional 3 min with the scraper (level 2) additionally turned on. Thereafter the speed was increased to 3000 rpm for 30 min.

2.2.3.3 Coating with low- melting polymer

A batch of 15 g CBD-/flavor-loaded silica carrier was mixed with the mucoadhesive polymer in the LabMixer at 400 rpm for 2 min and at 1500 rpm for another 3 min with the scraper (level 2). Subsequently, 5, 10 or 20% of PEG 1000 was added. After 5 min homogenization at 400 rpm, the batch was heated to 45 °C, slightly above the melting range of PEG 1000, and mixed for 25 min at 1500 rpm. The mixture was then slowly cooled to 20 °C at a stirring speed of 1500 rpm.

2.2.4 Preparation of toothpaste

As an application example, the mucoadhesive carrier systems were blended into a toothpaste base. The composition of the toothpaste base (Table 5) was selected in a way that the base did not contain any flavoring substances and had a 10% silica carrier deficit compared to the ready-to-use product. To compensate for the absence of preservatives, the toothpaste base was first pasteurized in a water bath for three min at 65 °C. After cooling to ambient temperature, the toothpaste base was mixed with the carrier systems for 4 min in the SpeedMixer at 2000 rpm. The added amount of mucoadhesive carrier system corresponds to 10% silica carrier, 1% flavor and 1% polymer based on the total mass of the toothpaste. The content of flavoring agents in the toothpastes was assayed by HPLC-UV after extraction (2.2.5 Drug load quantification).

Table 5. Composition of toothpaste base

Components	**[%]**	**Components**	**[%]**
Water demin.	21.81	Sident 22 s	8.00
Sorbitol 70%	45.00	Sodium carboxy methylcellulose	1.10
Trisodium phosphate	0.10	Titanium (IV) oxide	0.50
Saccharin 450 -fold	0.20	Water demineralized	4.50
Sodium monofluorophosphate	1.14	Sodium lauryl sulfate	1.50
PEG 1500	5.00		

2.2.5 Drug load quantification

The content of flavoring agents or CBD in the silica particles was quantified by HPLC. Therefore, three aliquots of the samples of about 10 mg each were mixed with 1 mL ethanol, vortexed for 10 s and extracted for at least 1 h. After centrifuging for 5 min at 13400 rpm, the supernatant was analyzed. Flavor load and CBD load, respectively, are expressed in % (m/m).

2.2.6 HPLC assay

Quantitative analysis of the CBD or the flavor concentration in the samples was performed with a HPLC system equipped with an UV-detector. The separation was conducted on a RP-18 column at 30 °C. The mobile phase during determination was adjusted to a flow rate of 1 mL/min and was composed of acetonitrile: water (55: 45 v/v). To determine Optamint liquid, carvone was used as an analytical marker and detected at a wavelength of 259 nm. The content of Optamint solid was assessed using thymol as reference substance at 270 nm. A wavelength of 220 nm was used for the quantitation of CBD. For analysis, samples volumes of 20 µL were injected. The calibration data are summarized in Table 26 and Table 27.

2.2.7 Differential scanning calorimetry (DSC)

To investigate the physical state of the flavoring agents or the CBD in the silica matrix, the loaded powders were analyzed by means of differential scanning calorimetry. The samples were weighed in 40 µL aluminum crucibles and sealed. The scans were performed at a heating rate of 20 K/min under N_2 gas purging with a flow rate of 80 mL/min. The melting point of thymol at 51 °C was determined by heating from -20 °C to 70 °C. Samples containing Optamint liquid were heated from -50 °C to 20 °C to detect the melting event of eucalyptol at 1.5 °C. Carriers loaded with Optamint solid were heated from -150 °C to 0 °C, with a melting peak occurring at approximately -50 °C. For measuring the melting peak of CBD at 66-67 °C, the samples were heated from -30 °C to 90 °C. The thermal events were recorded using the STAR^e Evaluation- Software.

For the determination of the loading capacity, flavor or CBD loaded samples with different concentrations were analyzed by DSC. The obtained melting peaks were integrated, and resulting specific enthalpy was plotted against the determined flavor content. The maximum amount of loading was calculated from the intercept of a linear regression with the x-axes.

2.2.8 Dissolution

To assess the dissolution behavior of the prepared carrier systems, a Ph.Eur. paddle dissolution apparatus was used. Dissolution tests were carried out at 37 °C with a stirring speed of 65 rpm and 100 mL of purified water or artificial saliva as the dissolution medium.

The composition of the used artificial saliva was adapted from Hoffmann et al. [88] and is listed in Table 6. To ensure sink conditions, the sample weight differed depending on the amount of Optamint or CBD loaded into the carrier system. Aliquots of 2 mL were collected after set time points for the quantification. After filtration through a 0.20 μm hydrophilic PTFE filter, 300 μL of the aliquots were blended with 300 μL cold acetonitrile to precipitate the proteins. For further processing, the samples were vortexed for 10 s and then centrifuged at 13400 rpm for 5 min. The supernatants were analyzed by HPLC (2.2.6 HPLC assay). Results were obtained from 3 replicates. The extracted Optamint and CBD quantities were used as the basis for calculating the percentage release in the dissolution experiments. For Optamint, sampling was performed after 1, 2.5, 4, 6, 8, 10 and 15 min. To quantify the amount of CBD released, 0.5% polysorbate 80 was added to the dissolution medium to improve the poor water solubility of the API. The sampling intervals for CBD were set as 2.5, 5, 10, 15, 30, 45, 60, 90 and 120 min.

Table 6. Composition of artificial saliva

Constituent basic solution	**Amount [g]**
NaCl	0.84
KCl	1.20
$K_2HPO_4 \bullet 3H_2O$	0.34
H_2O	1000
HCl (1 M)	adjust pH to 6.9
Addition to basic solution	
α- Amylase	0.02
Mucin	0.01
Basic solution	ad 100.00

2.2.9 Microscopy

Images were taken with a light microscope. For this purpose, the samples were spread thinly to the microscope slide and covered with a cover slip. A magnification of 20- or 40-fold was used to capture the microscopic images of the samples.

2.2.10 Mucoadhesion test

2.2.10.1 Mucoadhesion test of flavor-loaded carrier systems

Mucoadhesion of the prepared carrier systems was measured based on the method described by Hoffmann et al. [88], using a slightly modified mucoadhesion cell to allow sampling of the released flavor during the test.

The tests were conducted with porcine buccal mucosa. Due to its great resemblance in structure and composition compared to that of human, porcine mucosa is an attractive animal model for buccal drug delivery studies [52]. The mucosa has been provided by a local butcher and the department of Experimental Medicine of the University Hospital Tübingen. The majority of the underlying connective tissue was removed from the mucosa using a scalpel blade before the tissue was stored frozen at -28 °C. The final preparation of the mucosa took place immediately before the experiment. For this purpose, the mucosa was slowly thawed at room temperature. To facilitate further preparation, the mucosa was processed in a half-frozen state and fixed with the help of arterial clamps. The mucosa was separated from the remaining connective tissue and cut to a thickness of 2 mm ± 1 mm. A piece of porcine mucosa with a diameter of 2.5 cm was punched out and secured in a holder enabling the mucosa to be positioned on a metal disc within the mucoadhesion cell. Together with a reservoir of artificial saliva, the mucoadhesion cell was placed in a water bath (40 °C) as shown in Figure 3. After an equilibration time of 15 min the mucosa was warmed up to 36.5 °C ± 1 °C. Wetting the surface of the mucosa and the holder with 1 mL of artificial saliva (2.2.8 Dissolution) prevented drying out during temperature regulation. Simultaneously, 10 mL of artificial saliva were added to the mucoadhesion cell to allow subsequent sampling. Approximately 20 mg of the samples were placed on the buccal mucosa and flushed with artificial saliva using an HPLC pump with a flow rate of 0.5 mL/min. Optamint was extracted from the collected saliva after 2, 4, 6, 8, 10 and 12 min and after 12 min additionally from the mucosa. The remaining carrier was removed from the mucosa with a swab and 1 mL EtOH. The swab was extracted with 5 mL EtOH. For the extended mucoadhesion testing, the mucosa was removed after 30 respective 60 min testing time and the amount of flavor remaining was extracted from the mucosa as mentioned above. All samples were filtered with 0.20 μm hydrophilic PTFE filters. The saliva samples were then mixed with cold acetonitrile in equal parts, vortexed for 10 s and centrifuged at 13400 rpm for 5 min, to precipitate the proteins. The flavor content of the samples was assayed by HPLC-UV (2.2.6 HPLC assay). Each sample was tested in triplicate. The mucoadhesion value represents the amount of flavor retained, expressed as percentage of the total initial amount of flavor in the carrier system. To allow comparison, the different carrier systems, a mucoadhesion coefficient (MC) was calculated by dividing the

mucoadhesion value of the mucoadhesive carrier system by the mucoadhesion value of the corresponding carrier system without mucoadhesive additives.

$$MC = \frac{\text{Mucoadhesion [\%] mucoadhesive carrier system}}{\text{Mucoadhesion [\%] polymer-free reference carrier system}}$$

Equation 2. Mucoadhesion coefficient (MC)

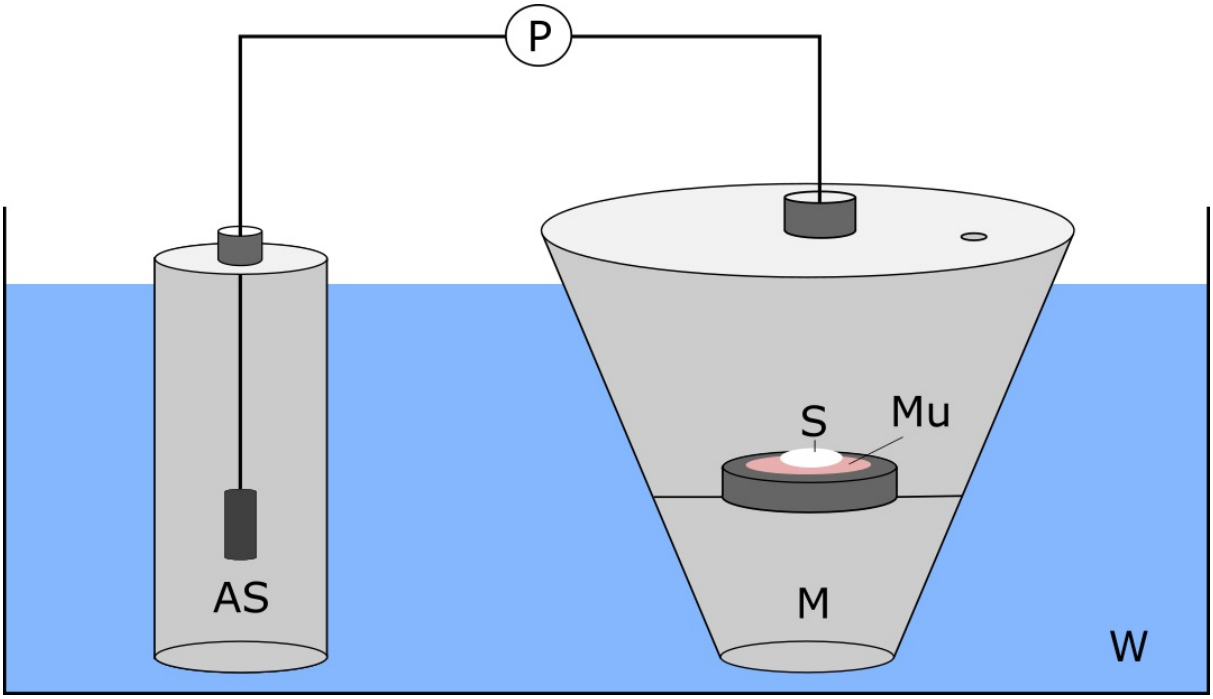

Figure 3. Mucoadhesion test system, AS: artificial saliva, P: pump, S: sample, Mu: mucosa, M: mucoadhesion cell, W: water bath

2.2.10.2 Mucoadhesion test of CBD-loaded carrier systems

The mucoadhesion test for CBD-loaded carrier systems was performed analogously to the mucoadhesion test for Optamint-loaded carrier systems (2.2.10.1). Due to the poor water solubility of CBD, sampling during the measurement was not possible. Hence, the collected saliva was withdrawn from the mucoadhesion cell after the testing time. Subsequently, the mucoadhesion cell was rinsed with 16 mL ethanol (respectively 25 mL and 40 mL for 30 min and 60 min testing time) which was then combined with the saliva to quantify the amount of CBD flushed from the mucosa.

2.2.11 Mucopenetration test

To assess penetration of CBD in the mucosa, the mucosa from the mucoadhesion test (2.2.10 Mucoadhesion test) was removed then weighed and immediately frozen in liquid nitrogen. The frozen mucosa was placed in a container made of aluminum foil with the mucosal surface facing down. Afterwards, the lower surface was covered with a smooth layer of frozen sectioning medium. The object was flash frozen at -50 °C to cure the medium. With a few more drops of NEG 50, the mucosa was attached to the sample holder of the cryo microtome. The object temperature was set to -30 °C and the knife temperature to -32 °C to obtain an optimal longitudinal slice and to prevent thawing of the mucosa. The section thickness was set to 100 μm. The mucosa was then segmented slice by slice. The first slice, with a thickness of 100 μm, was taken as the first sample. Thereafter, five slices are prepared and reunited as the second sample. This process of collecting and pooling five slices was repeated until the complete mucosa was sectioned. For extraction of the drug from the mucosa, 1 mL of acetonitrile was added to each sample. After vortexing the samples for 5 s, they were subjected to the ultrasonic bath for 30 min. Afterwards, the samples were filtered (0.20 μm hydrophilic PTFE) and analyzed by HPLC (2.2.6 HPLC assay).

Calculation of the amount penetrated per area was performed by normalizing the amount of CBD obtained to the quantity of CBD used, the weight of the mucosa and the area of mucosa exposed to the sample. To this end, an average mucosal weight of 1200 mg, an average applied amount of 3 mg of CDB and a penetration area of 2.08 cm^2 were assumed. Penetration experiments were carried out in triplicate. The total amount of drug penetrated the mucosal tissue was calculated by the sum of all sample contents. For the depth profiles, the CBD amounts of the individual samples were examined separately. To simplify comparison, a penetration enhancement ratio (PE) was calculated by dividing the penetrated amount of CBD from the carrier system by the penetrated amount of pure CBD.

$$PE = \frac{\text{Penetrated CBD } \left[\frac{\mu g}{cm^2}\right] \text{ of carrier system}}{\text{Penetrated CBD } \left[\frac{\mu g}{cm^2}\right] \text{ of pure CBD}}$$

Equation 3. Penetration enhancement ratio (PE)

2.2.12 Rheometric characterization of toothpastes

Oscillation measurements were performed to investigate the influence of the viscosity of the manufactured toothpastes on mucoadhesion. As a characteristic value, the flow point was determined from the cross over (G''=G') of an amplitude sweep. The oscillation measurements were conducted with a rheometer equipped with a plate-plate geometry (diameter: 25 mm; gap size: 0.2 mm). The operating temperature was set to 37 °C. The deformation was increased from 0.01 to 100% while maintaining the frequency constant at 1 Hz. The flow point was calculated as the value of the shear stress at the cross-over of loss and storage modulus (G''=G'). The flow point was determined in triplicate for each toothpaste. For rheological characterization of the silica, dispersions of silica in water were measured under the same conditions 2 h after preparation

2.2.13 Stability studies

2.2.13.1 Stability studies of flavor- loaded silica carriers

For stability testing, the samples were stored in sealed glass containers protected from light. Samples were either kept at room temperature or exposed to a temperature cycle. Over a period of 24 h, the samples were heated from -5 to 40 °C and then cooled down to -5 °C (Figure 4).

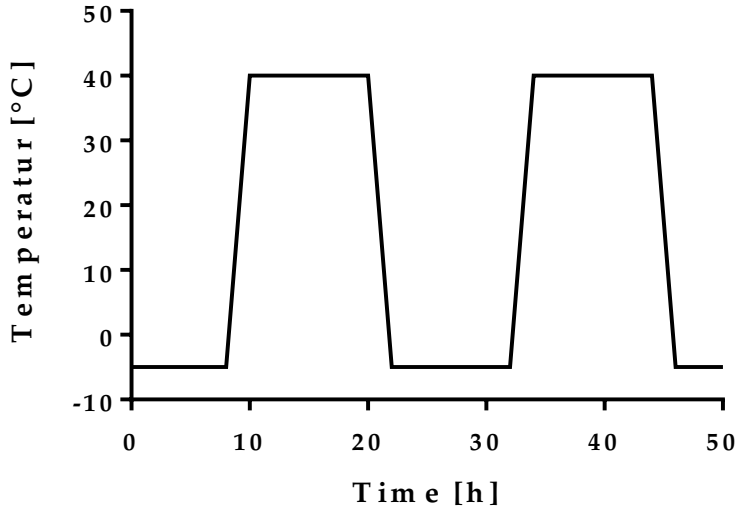

Figure 4. Temperature profile over time during the temperature cycle

Directly after preparation and after 1 week, 2 weeks, 1 month, 2 months, 3 months, and 6 months the stored samples were analyzed for both, the quantity of flavoring agent and the physical state in the carrier system. The former was determined after extraction of the samples (2.2.5 Drug load quantification) by HPLC (2.2.6 HPLC assay) and the latter using DSC measurements (2.2.7 Differential scanning calorimetry (DSC)).

For selected mucoadhesive carrier systems, mucoadhesion tests (2.2.10 Mucoadhesion test) were repeated after 6 months.

2.2.13.2 Stability studies of toothpaste

For the stability tests of the toothpastes, samples were stored in either polypropylene containers or aluminum tubes at room temperature and in a temperature cycle test as described above. Over a period of 6 months, the amount of flavor remaining in the toothpastes was assayed by HPLC-UV after extraction (2.2.6 HPLC assay).

Note: All data are represented as arithmetic mean ± standard deviation

3 Results and discussion

3.1 Flavor-loaded carrier systems

3.1.1 Characterization of silica carriers

Three different porous silica were selected as carrier materials for this study: Aeroperl 300, Sident 9 and Sident 22s. Since their different physicochemical properties can significantly affect drug loading and drug release, it is crucial to characterize each carrier in terms of particle size, surface area, pore size and pore volume.

3.1.1.1 Particle size and morphology of silica carriers

The SEM images (Figure 5) show the general morphology of Aeroperl 300, Sident 9 and Sident 22s. Aeroperl 300 exhibit spherical shaped particles with a roughened surface on a smooth underground and thus differs visually from the two Sident types. The latter two appear visually nearly identical, with irregularly shaped particles and a rather sponge-like, porous surface. No visual difference between Sident 9 and Sident 22s was noticeable regarding the particle size. In comparison to Aeroperl 300, the particles of the two Sident carriers were significantly smaller. The characteristic particle shape and the larger particle size of Aeroperl 300 can be attributed to granulation in the manufacturing process.

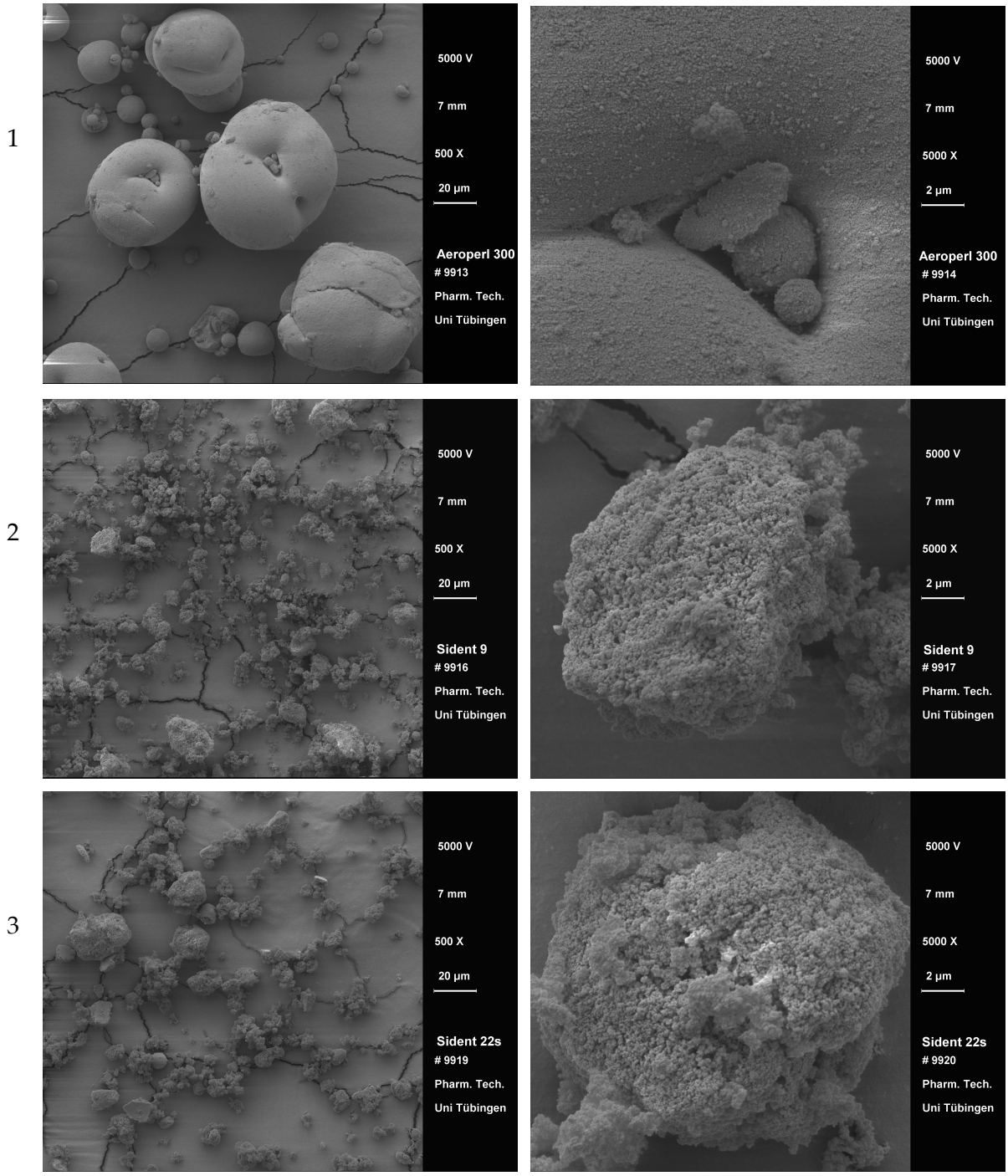

Figure 5. SEM images of (1) Aeroperl 300, (2) Sident 9, (3) Sident 22s at different magnifications. Left: 500x magnification, right: 5000x magnification

To accurately determine particle size, laser diffraction measurements were performed. The results are shown in Figure 6. Aeroperl 300 exhibited the largest mean particle size, followed by Sident 9 and Sident 22s. This confirms the optical impression from the SEM images. With respect to the particle size distribution, particle size measurements showed the broadest distribution for Sident 9 and the narrowest for Sident 22s.

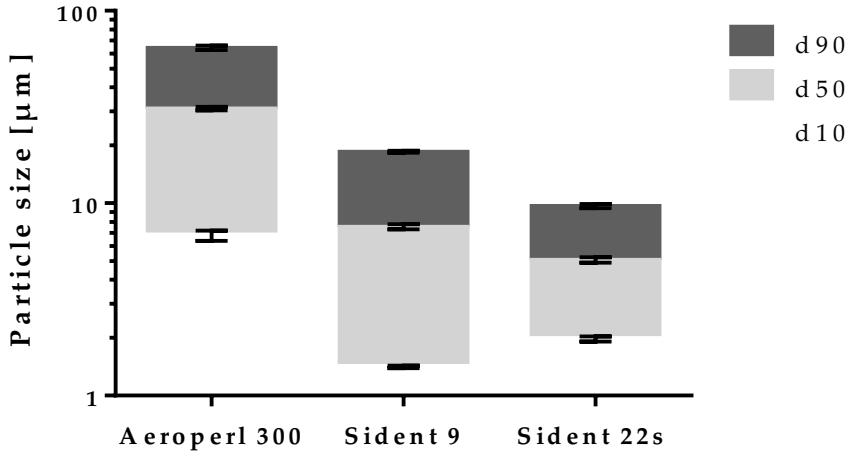

Figure 6. Particle size of Aeroperl 300, Sident 9 and Sident 22s[1]

3.1.2 Surface area and porosity

The utility of porous silica as carrier materials is determined by their loading capacity. Loading capacity is dependent on the amount of drug that is adsorbed onto the surface of the carrier material and/or that fills the pores [89]. Therefore, both the surface area and the pore volume are key properties for determining the ability of a carrier to incorporate a high amount of drug. Depending on the size of the drug, the diameter of the pores controls the availability of the pore volume and subsequently influences the release of the drug. Larger pore sizes encourage higher drug release rates [90].

The surface area data of the three silica studied (Table 7) reveal that Aeroperl 300 exhibits the largest surface area, followed by Sident 22s. Sident 9 offers by far the smallest surface area.

Table 7. Product specification of Aeroperl 300, Sident 9 and Sident 22s (provided by manufacturer Evonik)

	Aeroperl 300	**Sident 9**	**Sident 22**
Surface area [m^2/g]	260 - 320	45	190

Table 8 lists data on pore volume and pore diameter obtained by mercury intrusion porosimetry. The specific pore volume of Aeroperl 300 is almost twice as large as the pore volume of Sident 22s and Sident 9, whilst the pore volume of Sident 9 is still slightly lower

[1] This data was created as part of a master's thesis (Characterization of silica-based mucoadhesive carrier systems: focusing on particle size and rheological behavior; Mona Mamo 2021)

than that of Sident 22s. In terms of pore diameter, Aeroperl 300 and Sident 22s show similar values, being in the range of mesopores with an average diameter of approximately 30 nm. With an average pore diameter of one decade above 50 nm, the pores of Sident 9 fall within the range of macropores.

Table 8. Specific pore volume and pore diameter measured by mercury intrusion porosimetry

	Aeroperl 300	**Sident 9**	**Sident 22**
Specific pore volume [cm^3/g]	1.764	0.784	0.937
Average pore diameter [μm]	0.029	0.29	0.026

Based on its physical properties, Aeroperl 300 offers the best prerequisites for a high loading capacity, having the largest surface area and the largest pore volume. Sident 9 accordingly has the lowest potential for drug loading, whilst Sident 22s has intermediate drug loading capacity. In comparison, it still offers a relatively large surface area for adsorption, but a significantly lower pore volume than Aeroperl 300.

3.1.2.1 Oil absorption

The oil absorption capacities, characterized by the mass of absorbed oil per 100 g silica of Aeroperl 300, Sident 9 and Sident 22s for triacetin and sunflower oil were determined. The results in Figure 7 reveal that Aeroperl 300 and Sident 22s were able to absorb a substantially higher amount of liquid compared to Sident 9. While Sident 9 absorbed an amount of oil equal to its own weight, Aeroperl 300 and Sident 22s absorbed three times their own weight in fluid. The slightly higher absorption capacities for triacetin compared to sunflower oil are based on the calculation of capacity. For both oils, the same values were obtained in terms of the absorbed volume. The higher density of triacetin, however, resulted in the calculation of higher absorption capacities for triacetin.

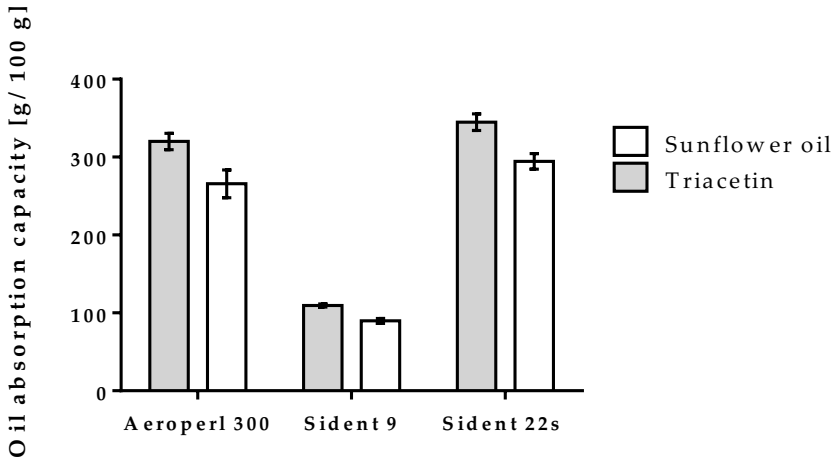

Figure 7. Oil absorption capacity of Aeroperl 300, Sident 9 and Sident 22s for triacetin and sunflower oil[2]

Carrier with larger pore volume hold of more liquid mass. Therefore, the low absorption capacity of Sident 9 is explained by the comparatively small pore volume among the silica carriers studied (Table 8). Consequently, Aeroperl 300, having the largest pore volume, is expected to have the highest absorption capacity. However, Sident 22s, which has a much smaller pore volume and a smaller surface area than Aeroperl 300, showed equally high to even slightly higher absorption capacities compared to Aeroperl 300. The discrepancy between the experimentally determined absorption capacities and the pore volume data could be due to the fact that the required volume oil needed to form a uniform paste was determined. Figure 8 shows the results when determining the amount of sunflower oil absorbed by the silica without losing its character as a free-flowing powder. The results are in good agreement

[2] This data was created as part of a master's thesis (Characterization of silica-based mucoadhesive carrier systems: focusing on particle size and rheological behavior; Mona Mamo 2021)

with the data on the pore volume of the respective silica. Aeroperl 300 showed the highest absorbed amount and, analogous to the pore volume, Sident 22s and Sident 9 had correspondingly lower absorption capacities. It is noticeable that there is a much greater difference between the amount of oil absorbed by Sident 22s to remain a flowable powder and the amount required to form a cohesive paste compared to the other silica.

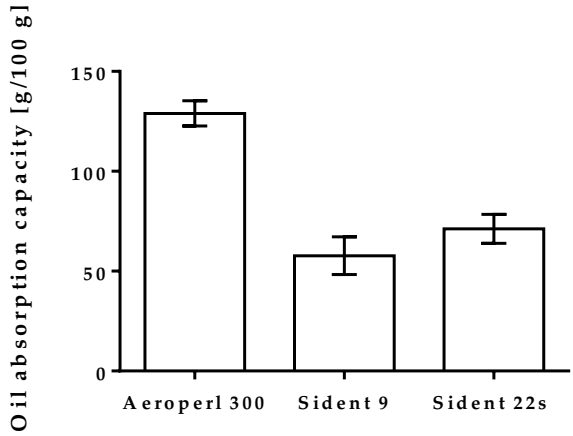

Figure 8. Absorption capacity of Aeroperl 300, Sident 9 and Sident 22s for sunflower oil with free-flowing powder as the endpoint

Figure 9 shows the determined absorption capacity of sunflower oil from Figure 8 calculated in relation to the surface area and pore volume of the silica materials. While the amount of oil bound by the carrier materials per m^2 of surface area differed, the amount absorbed in terms of pore volume was comparable for all three silica types. The fact that all silica types studied absorbed approximately the same amount of oil per pore volume suggests that pore volume, rather than the surface area, is the decisive parameter for liquid absorption.

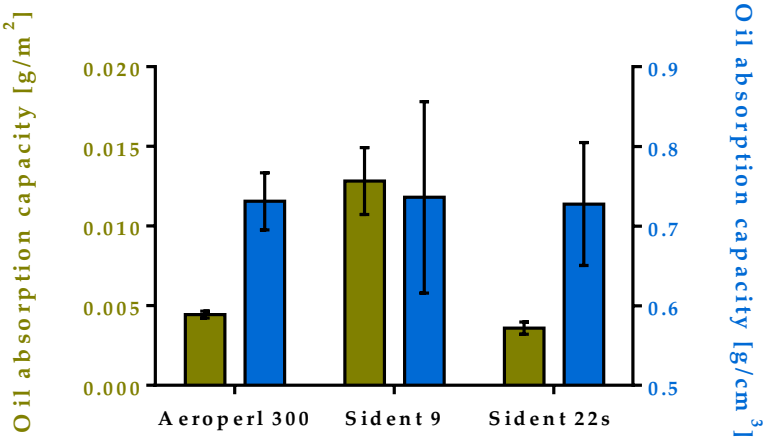

Figure 9. Absorption capacity of 100 mg Aeroperl 300, Sident 9, Sident 22s for sunflower oil with free-flowing powder as the endpoint dependent on pore volume and surface area

3.1.3 Flavor loaded silica carriers

3.1.3.1 Loading and release of thymol as a model drug

Loading of actives into mesoporous silica can be achieved by several methods. The suitability of three methods, namely solvent filtration method, incipient wetness method and melt method, for the loading of a volatile active was tested with thymol as a model drug and Aeroperl 300 as an example of a silica carrier. The results are shown in Figure 10.

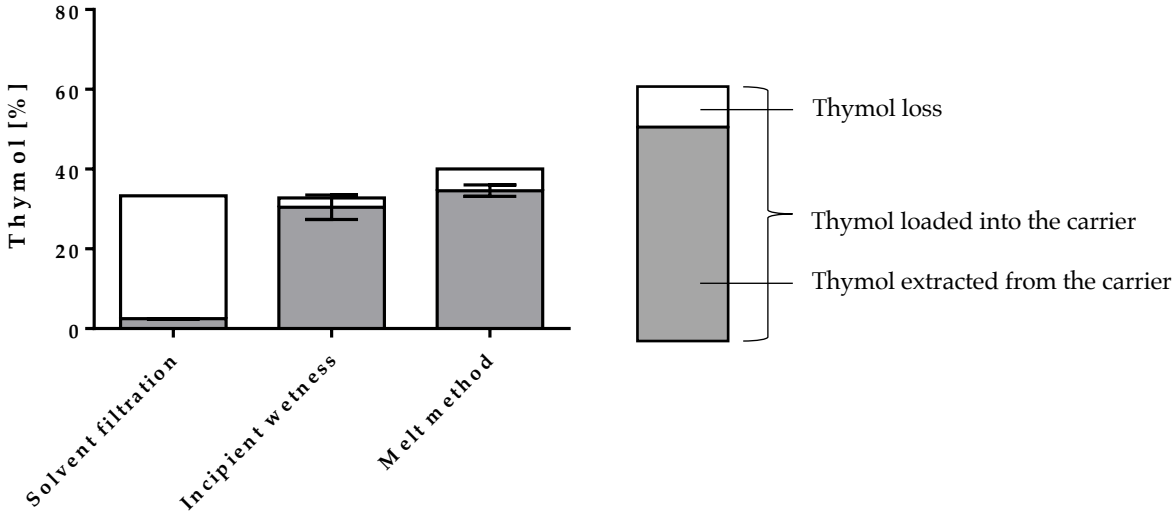

Figure 10. Comparison of loading methods for loading thymol into Aeroperl 300
(The entire bar represents the theoretical amount of thymol loaded into the carrier, the grey bar the actual amount that could be extracted from the loaded carrier and the white bar the loss of drug during the loading).

Compared to the theoretical thymol load, the measured contents after loading were systematically lower. This discrepancy was due to the loss of thymol in the loading process either by residues on the wall of the glass ware or by its volatility. When using the melt method or the incipient wetness method the discrepancies were minor, because no or only a minimal removal of solvent was necessary. Using the solvent filtration method, significantly larger differences were observed between the calculated and actual load of thymol. A main difference between the solvent method and the incipient wetness method is the necessary removal of the solvent. In the first method, thymol molecules were immediately introduced into the pores, followed by direct evaporation of the solvent. In the solvent method, loading is a two-step process that requires the establishment of an equilibrium between the quantity of thymol in the carrier and that of the loading solution. The subsequent removal of the solvent is much more complex due to the larger liquid quantity. The additional filtration step followed by a

prolonged evacuation time to remove residual solvent were critical parameters for the loss of volatile compounds. Furthermore, an excess amount of thymol in the loading solution was necessary, resulting in the loading being less effective using the solvent filtration method for the same initial amount of thymol.

The ratio of drug-to-carrier and the concentration of the loading solution are decisive parameters that influence the efficiency of the loading process using the incipient wetness method. Junmin Lai et al. reported that a lower ratio of the drug-to-carrier and a higher initial concentration of the loading solution are favorable for a higher quantity of drug deposited at the surface and into the pores [91]. To identify the optimum parameters, loading was performed with solutions containing 10, 30, and 50 mg/mL thymol and with a drug-to-carrier ratio of 1:1, 1:2, and 1:3, respectively. Based on the results illustrated in Figure 11 an increased concentration of the loading solution led to a more efficient loading. The improved loading with higher concentrated loading solutions could be explained by the lower ethanol volume. This allowed a faster removal of the solvent resulting in faster loading and a decreased risk of volatilization of the flavor. Moreover, higher loading efficiencies were obtained with a higher proportion of silica carrier in relation to thymol. If the proportion of carrier is increased compared to the drug substance, this provides a larger available surface area and pore volume and hence a higher or more effective loading [6]. In contrast the highest percentage of thymol was deposited on the carriers by using a drug-to-carrier ration of 1:1, but as discussed before, this was achieved at the expense of a high thymol loss.

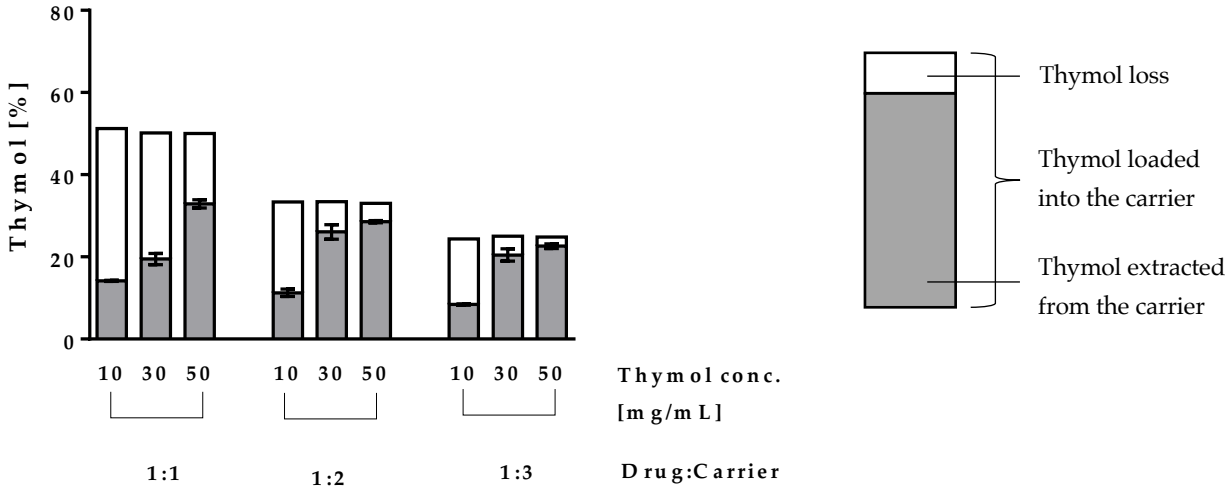

Figure 11. Influence of drug-to-carrier ratio and concentration of the loading solution on loading efficiency of thymol into Aeroperl 300 (The entire bar represents the theoretical amount of thymol loaded into the carrier, the grey bar the actual amount that could be extracted from the loaded carrier and the white bar the loss of drug during the loading)

Loading of substances into a silica carrier can cause the transformation of the molecules into an amorphous state by breaking up the intermolecular interactions of the drug through separation on the silica surface [11]. The behavior of drug molecules confined to porous media is different from those in bulk. This relates to finite-size effects, preventing the drug molecules from rearranging themselves in a crystal lattice. The flavor that remains outside of the pore system can crystallize on the outer surface or into separated crystals [92].

DSC is a common technique for the characterization of the physical state of substances. While the absence of phase transitions is indicative for a completely amorphous state, the occurrence of a melting event implies molecules in a crystalline form. Conclusions on the physical state of the loaded drug were drawn by examining carriers with different concentrations using DSC. Additionally, the thermograms of the loaded carriers were compared to the DSC curve of pure thymol with a quantity corresponding to 10% drug load (Figure 12). Regarding the thermograms, a sharp melting peak at 51 °C can be observed for pure thymol. The slightly visible melting peaks of the carrier systems with 20% drug load and 30% drug load allow the conclusion that part of thymol molecules recrystallized. However, no melting event occurred for the carrier systems with 10% thymol, indicating that the drug was completely in the amorphous state. The results of the DSC curves were consistent with the fact that the risk of recrystallization tends to increase with increasing concentration of the loading solution [6].

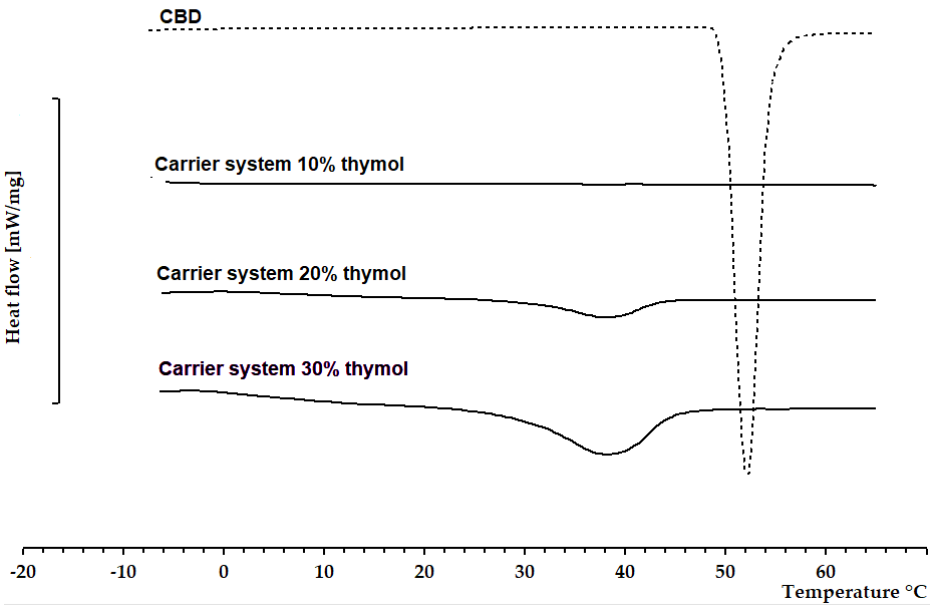

Figure 12. Comparison of DSC curves obtained by Aeroperl 300 carriers loaded with 10, 20 and 30% thymol in contrast to pure thymol

The in vitro release of the prepared carrier systems was investigated next. A comparison of the dissolution profiles of pure thymol and thymol loaded onto Aeroperl 300 are presented in Figure 13. Dissolution from thymol loaded into silica was so rapid that a 100% release was detected already after 5 min. The dissolution profile of pure crystalline thymol, on the other hand, reached its maximum value after 10 min. The enhanced dissolution rate of loaded molecules compared with the bulk drug can be attributed to the increased surface and an altered physical state [93]. As a result of the loading process, the formation of crystalline material is limited by the confined space of the pores, leaving the drug in its non-crystalline, amorphous form. It is understood that the amorphous form exhibits altered thermodynamic properties and therefore higher dissolution rates than the crystalline phase [7, 9, 93]. Furthermore the rapid release kinetics from the silica surfaces can be explained by the competitive adsorption of drug molecules and water in favor for the latter [11]. This displacement of thymol from the pores occurs instantaneously upon influx of water and leads to a fast release [94].

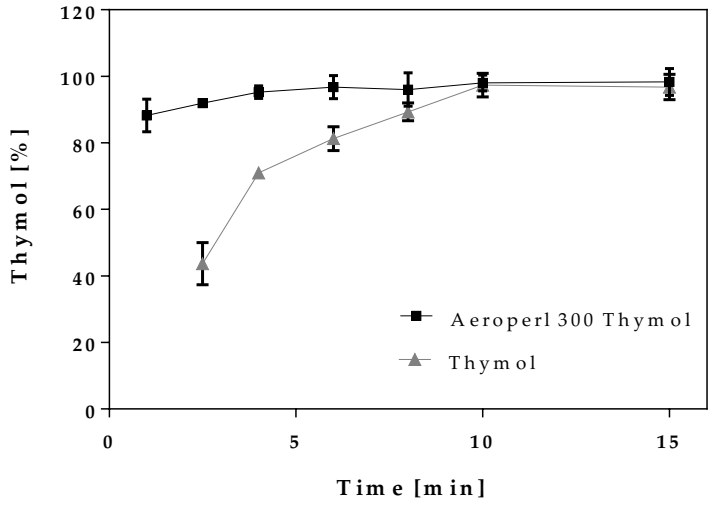

Figure 13. Comparison of dissolution profiles of pure thymol and thymol loaded onto Aeroperl 300 (Aeroperl 300 Thymol)

3.1.3.2 Loading of Optamint flavors

Based on the results from chapter 3.1.3.1 and considering the fact that the Optamint flavors used are liquids, the incipient wetness method was selected for loading the carriers with Optamint liquid and Optamint solid (0

Loading of Optamint). In the following experiments, the quantity of carvone as an analytical marker was analyzed for both flavors and used to calculate the total amount of Optamint.

3.1.3.2.1 Loading of Optamint liquid

Figure 14 displays the results from loading Optamint liquid to Aeroperl 300 with different drug-to-carrier ratios. As expected, the bar plot reveals an increased loading efficiency with a lower drug-to-carrier ratio. When using a ratio of 1:3 or lower, the loss of flavor during the loading process was reduced to 1.98% or less. These results are in good resemblance with the findings of the preliminary trials with thymol.

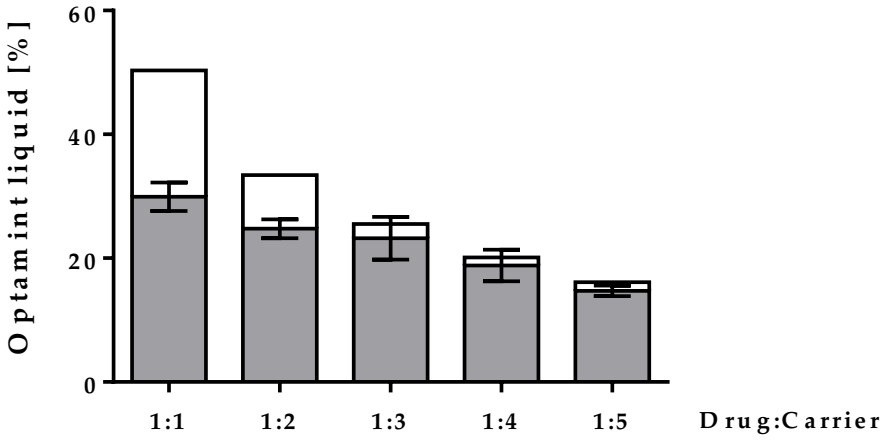

Figure 14. Influence of drug-to-carrier ratio on loading efficiency of Optamint liquid into Aeroperl 300

As shown in Figure 15, the efficiency of the loading was robust with regards to a scale up from 100 mg to 15 g sample and the preparation with other stirring systems. The marginally higher loss of Optamint liquid during the loading in the LabMixer is caused by the larger surface of the product vessel, mixer, and scraper compared to the loading process with the magnetic stirrer in a glass vial.

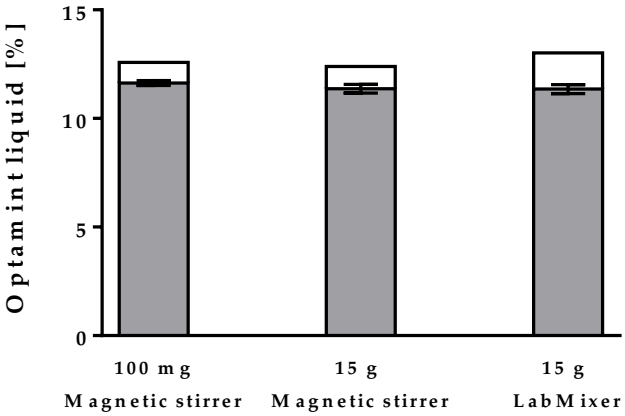

Figure 15. Comparison of loading efficiency using different sample size or different machinery for loading

To assess the influence of different carrier characteristics, Optamint liquid was also loaded into Sident 9 or Sident 22s using the incipient wetness method. The loaded samples were characterized in terms of drug content, the loading capacity, dissolution, storage stability and mucoadhesive properties. Figure 16 illustrates similar loads with comparable effectiveness for all silica carriers. As opposed to the thermograms of the carrier systems, prepared with the Sident carriers, the DSC curve of Aeroperl 300 (Figure 17) showed no melting event for the same amount of loaded flavor. The crystalline fractions observed in the curves of the silica carrier systems are in good agreement with the surface area and pore volume data from chapter 3.1.2. As surface area and pore volume increase from Sident 9 to Sident 22s to Aeroperl 300, so does the adsorbed drug quantity.

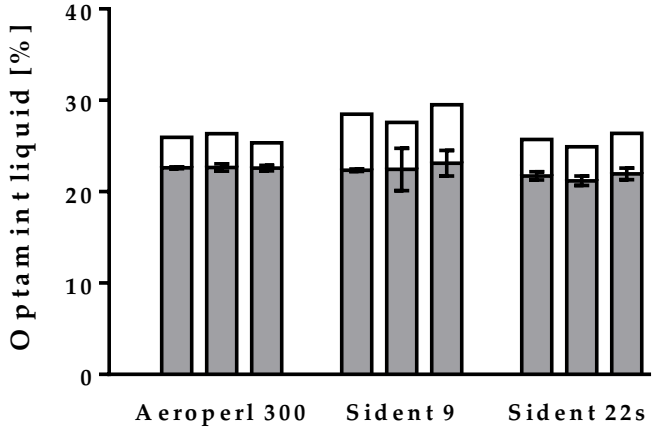

Figure 16. Loading of Optamint into different silica carriers (Aeroperl 300, Sident 9 and Sident 22s)

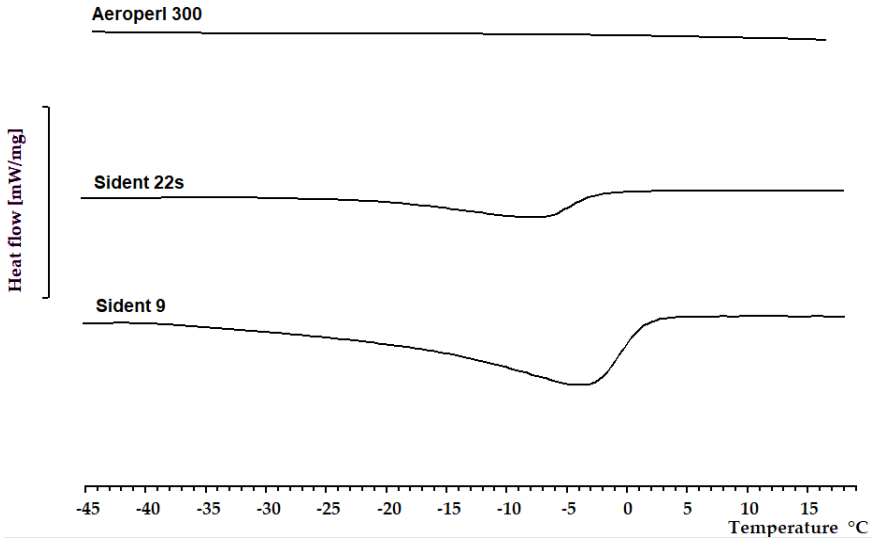

Figure 17. Comparison of DSC curves obtained by flavor-loaded carrier systems with 15% Optamint and Aeroperl 300, Sident 22s or Sident 9

3.1.3.2.2 Loading capacity

When it comes to application, it is important to know the maximum loading capacity of a certain carrier for the active of interest. To assign the load limit, defined as the loading with no crystalline portion present in the carrier system, DSC measurements of Aeroperl 300, Sident 9 and Sident 22s loaded with different amounts of Optamint liquid were performed. Calculated by the point of interception with the x-axes (Figure 18, Figure 19, Figure 20), the loading capacity was determined to be 16.55% for Aeroperl 300, 8.66% for Sident 22s, and 3.43% for Sident 9, respectively. The results were consistent with the different specific surfaces and pore volumes of the carrier systems (3.1.1). Aeroperl 300, which provides both the largest surface area and the largest pore volume among all three silica, is capable of binding the highest amount of flavor in the pores and on the surface. Sident 9, on the other hand, exhibits the smallest surface and the smallest pore volume, thus correlating with the lowest loading capacity.

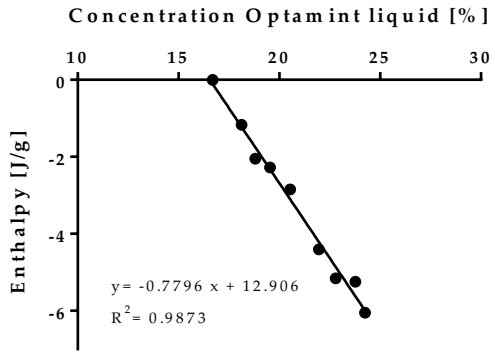

Figure 18. Concentration depended enthalpy of melting peaks of Optamint liquid loaded into Aeroperl 300

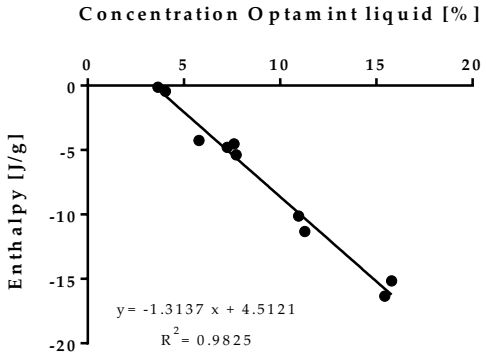

Figure 19. Concentration depended enthalpy of melting peaks of Optamint liquid loaded into Sident 9

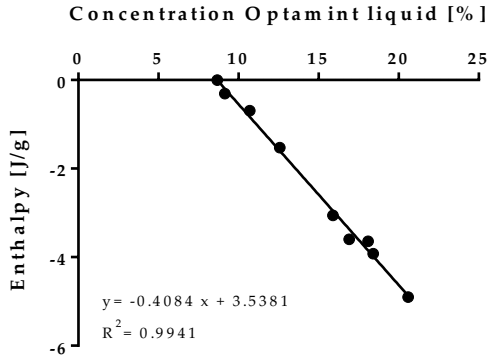

Figure 20. Concentration depended enthalpy of melting peaks of Optamint liquid loaded into Sident 22s

3.1.3.2.3 Flavor release from silica carrier systems

The release profiles of Optamint liquid from the three silica are shown in Figure 21. The flavor was released rapidly from all carrier systems. Complete release was already reached after less than 2 min. This rapid release could be the reason why, the dissolution profiles for the three silica were comparable, although the three silica materials differ in terms of surface area and pore diameter (3.1.2), allowing for a different release behavior. Noticeably, the amount of Optamint liquid is decreasing during the dissolution experiment. This can be attributed to the water vapor volatility of the released flavor.

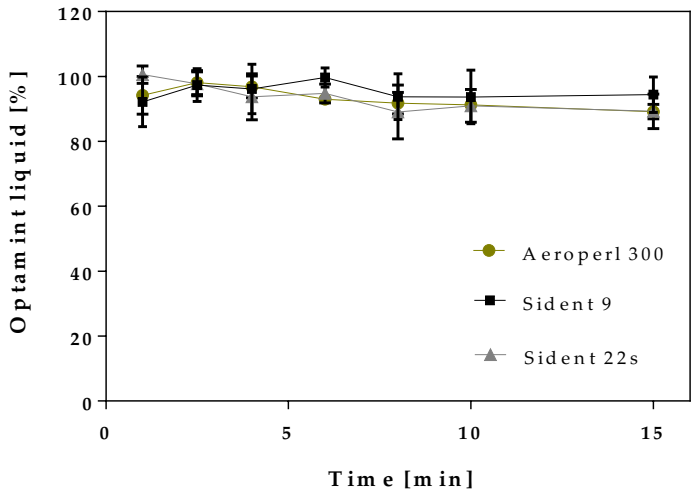

Figure 21. Dissolution profile of Optamint liquid from carrier systems with Aeroperl 300, Sident 9 and Sident 22s

The impact of the dissolution medium on the active's release is described in the literature [95]. To achieve the most realistic simulation of the in vivo conditions, the release in artificial saliva was investigated as the carrier systems are intended to be used in the oral cavity. From Figure 22 it can be seen that there is obviously no difference between water and saliva as dissolution medium. Consequently, it can be assumed that artificial saliva had no influence on the flavor release from the carrier systems.

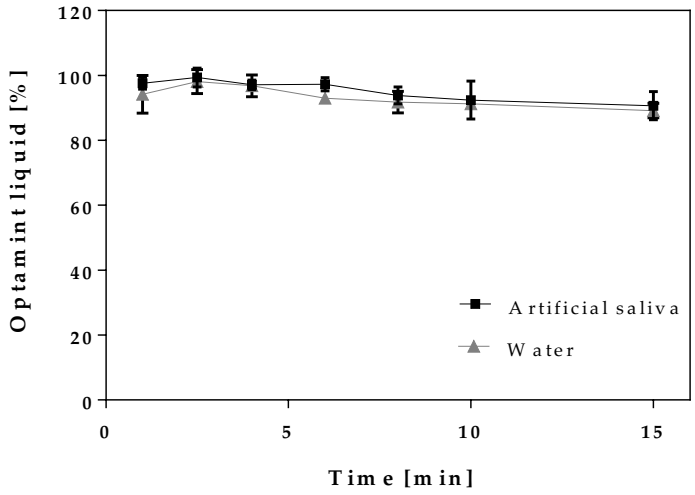

Figure 22. Influence of dissolution medium on release profile of Optamint liquid from Aeroperl 300

3.1.3.2.4 Stability studies of flavor-loaded carrier systems

The content and the physical state of the flavoring agent were investigated for 6 months storage. Loading values obtained by HPLC (Figure 23, Figure 25, Figure 27) showed no to only marginal decrease over the storage period, implying a stable flavor content for all prepared carrier systems independent of the storage conditions (RT or TC). In addition, no changes in the DSC curves (Figure 24, Figure 26, Figure 28) became obvious. It can be concluded that the silica particles used in this work were able to stabilize the amorphous form during storage.

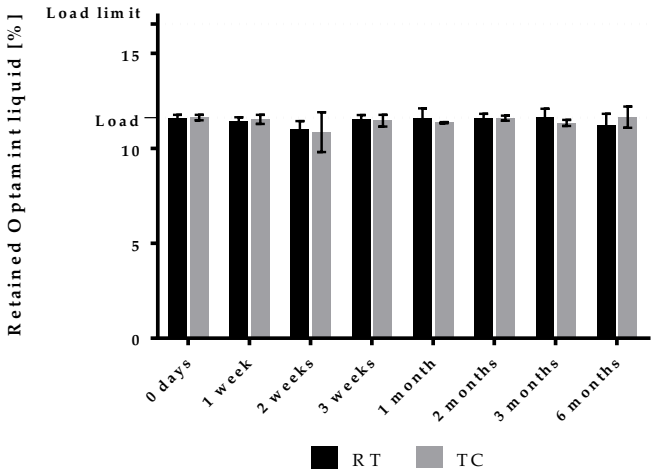

Figure 23. Flavor content of Aeroperl 300 carrier systems loaded with Optamint liquid directly after loading and during storage at RT or TC

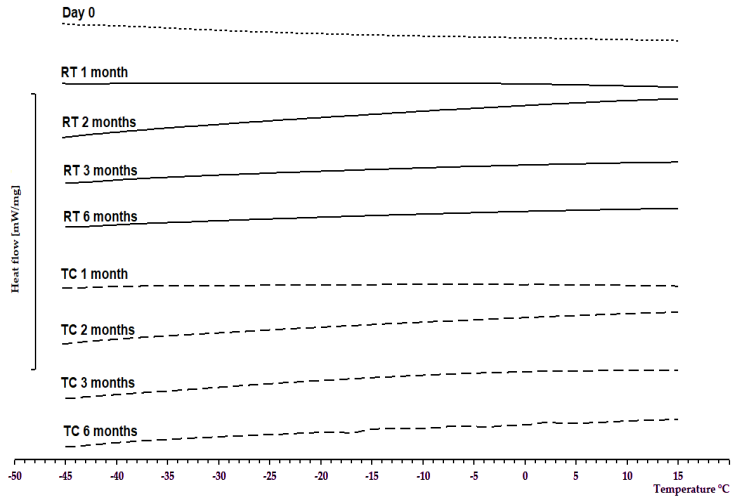

Figure 24. DSC curves of Aeroperl 300 carrier systems loaded with Optamint liquid directly after loading and during storage at RT or TC

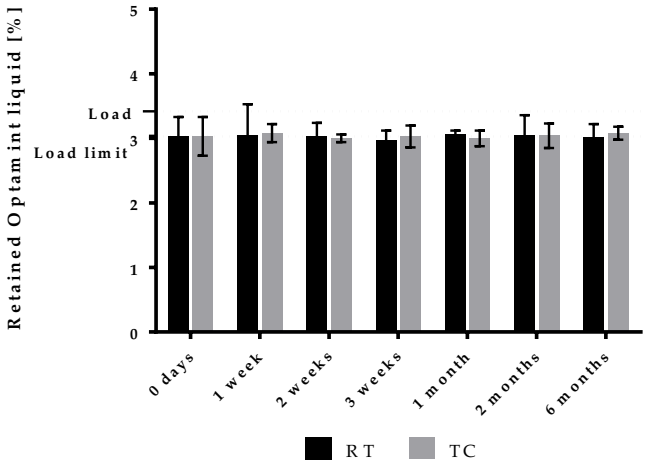

Figure 25. Flavor content of Sident 9 carrier systems loaded with Optamint liquid directly after loading and during storage at RT or TC

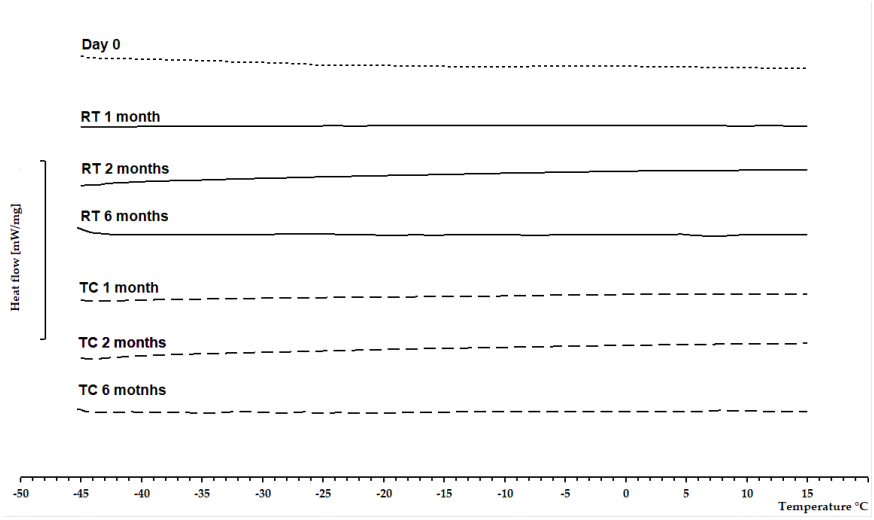

Figure 26. DSC curves of Sident 9 carrier systems loaded with Optamint liquid directly after loading and during storage at RT or TC

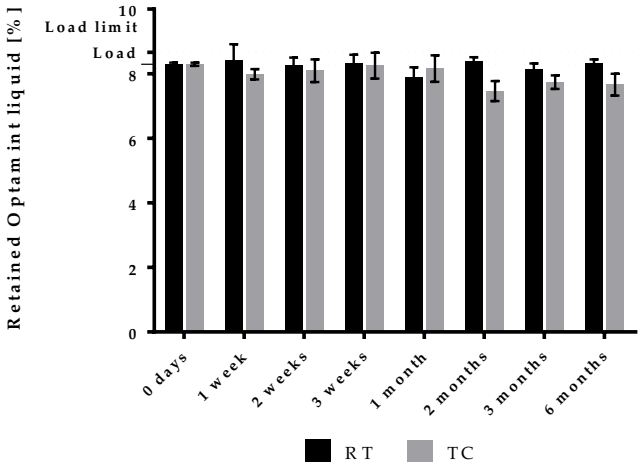

Figure 27. Flavor content of Sident 22s carrier systems loaded with Optamint liquid directly after loading and during storage at RT or TC

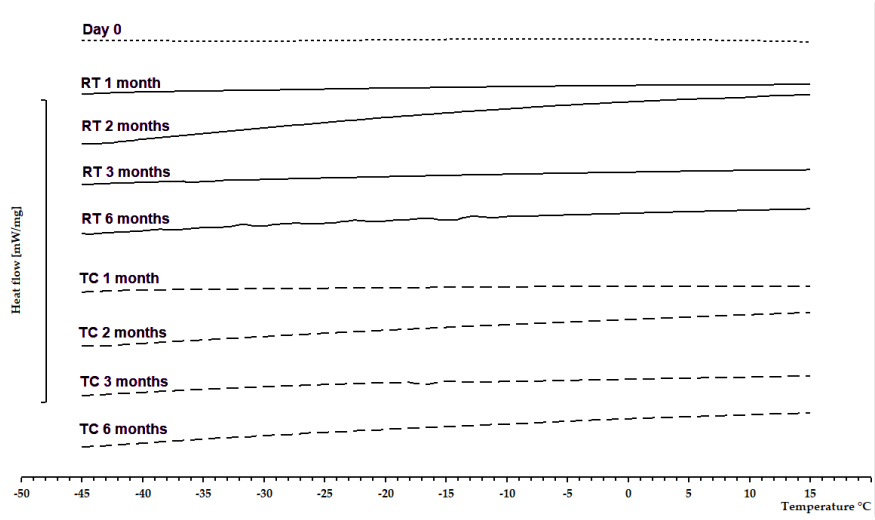

Figure 28. DSC curves of Sident 22s carrier systems loaded with Optamint liquid directly after loading and during storage at RT or TC

Figure 29 and Figure 30 represent the stability results of the carrier system with Sident 9, loaded with Optamint liquid exceeding the maximum loading capacity. The bar plot reveals a decrease in the flavor content, which seems to level off when the load limit is reached. It can be concluded that the crystalline portion of the flavor substance is not bound sufficiently and therefore evaporates over time. This assumption is supported by the thermogram (Figure 30). In the DSC curve from immediately after preparation (day 0) a minor melting peak was visible (Figure 31), which is no longer detectable thereafter. This indicates that the crystalline fraction

which was detected at the beginning disappeared after 1 month storage and remaining flavor was completely amorphous.

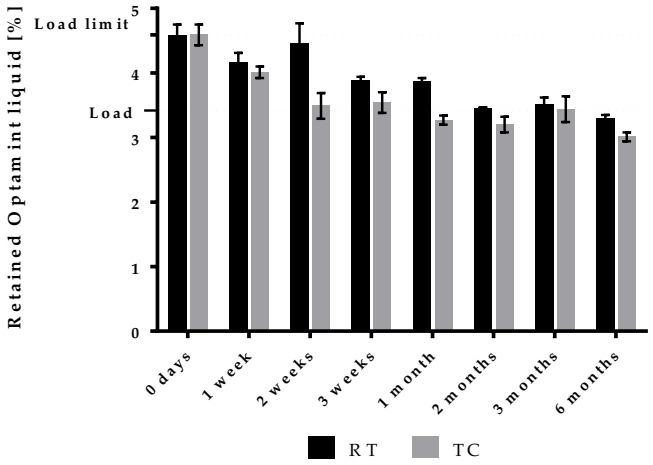

Figure 29. Flavor content of Sident 9 carrier systems loaded with Optamint liquid exceeding the load limit directly after loading and during storage at RT or TC

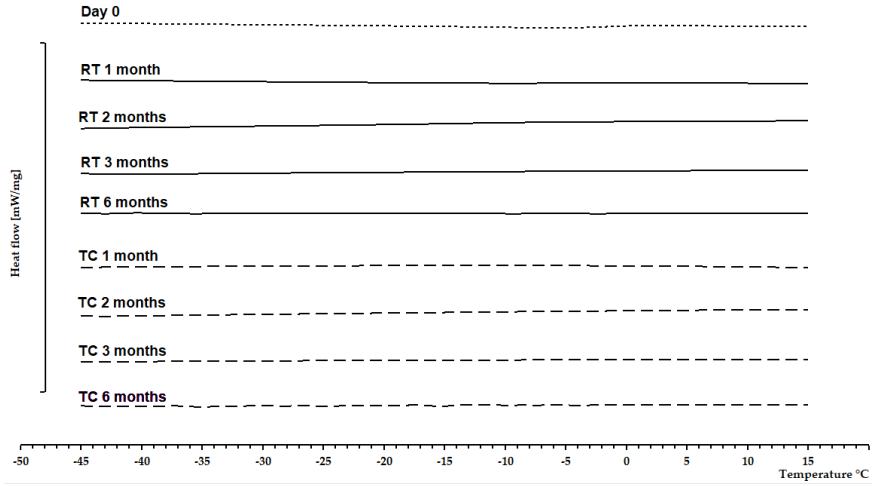

Figure 30. DSC curves of Sident 9 carrier systems loaded with Optamint liquid exceeding the load limit directly after loading and during storage at RT or TC

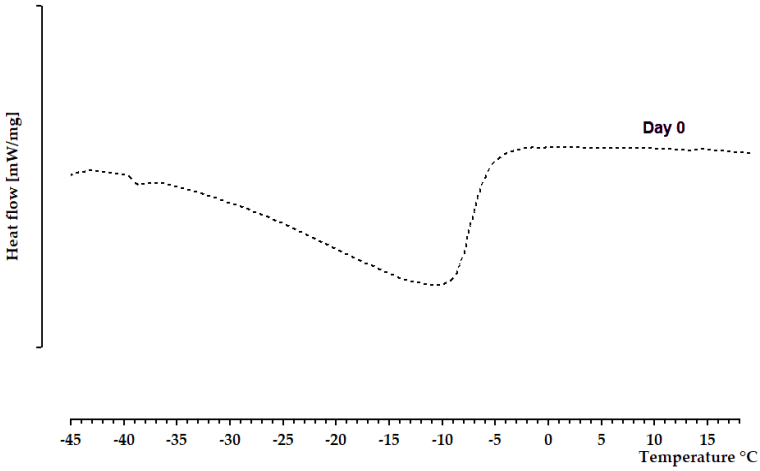

Figure 31. Enlarged display of the DSC curve of flavor loaded Sident 9 carrier system on day 0.

3.1.3.2.5 Mucoadhesion tests of flavor-loaded carrier systems

In a further step, mucoadhesion tests were performed for the carrier systems loaded with Optamint liquid. For this purpose, carrier systems were selected whose flavor content did not exceed the loading capacity of the respective silica carrier (Table 9).

Table 9. Composition of flavor-loaded carrier systems for the mucoadhesion tests

Silica carrier	**Load limit [% (m/m)]**	**Optamint liquid [% (m/m)]**
Aeroperl 300	16.55	12.06
Sident 9	3.43	3.30
Sident 22s	8.66	4.74

For comparison, the behavior of the pure flavoring agent on the mucosa was investigated first. Figure 32 shows the increasing concentration of Optamint liquid, calculated by the analytical marker substance, in the collected saliva samples approximating 100% after 12 min. Consequently, 12 min were selected as the reference value for the following mucoadhesion test. After the stated period of time, 1.83% of Optamint liquid was extracted from the mucosa. Combined with 93.12% in the saliva samples, this results in a recovery rate of 94.95%.

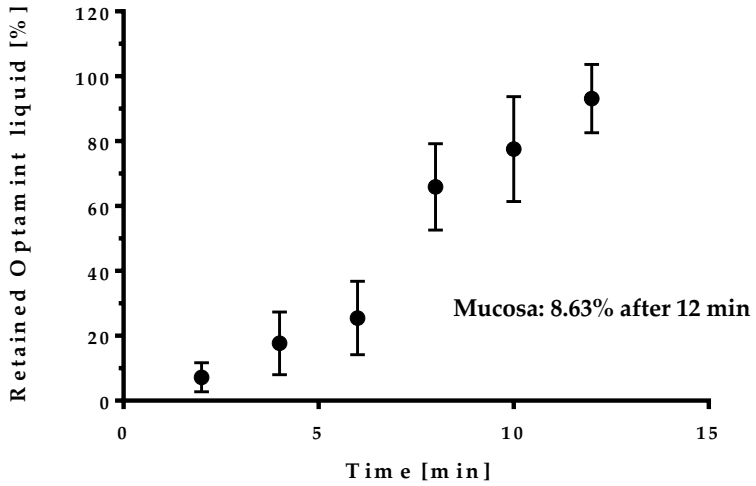

Figure 32. Mucoadhesion test of Optamint liquid: concentration in collected saliva

Loading Optamint liquid into the pores of Aeroperl 300 reduced the amount of flavor flushed away by the saliva to 89.03% and increased the mucoadhering fraction to 8.63% after 12 min (Figure 33). In comparison to plain Optamint liquid the incorporation into the mesoporous carrier led to an approximately 5-fold increase in mucoadhesion. Due to its surface characteristics, the silica carrier enables enhanced interaction with the mucin layer of the mucosa and thus prolongs the retention time of the incorporated flavor. However, the fast release of the flavor from the carrier system into the saliva prevents a more pronounced effect.

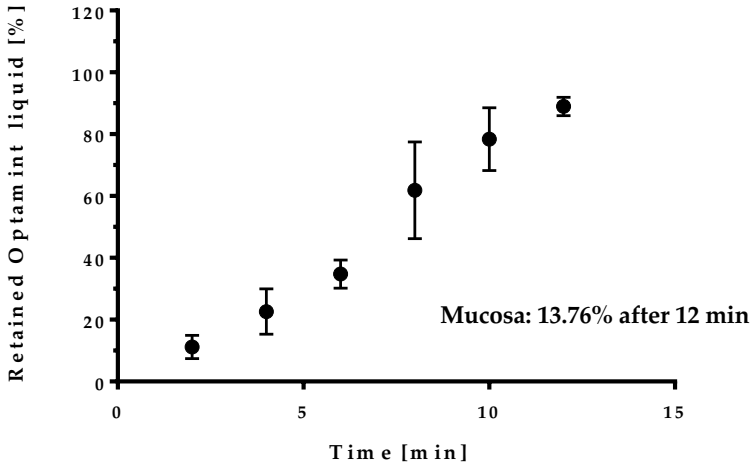

Figure 33. Mucoadhesion test of Optamint liquid loaded into Aeroperl 300: concentration in collected saliva

Comparing the performance of all three carrier systems (Figure 34), Sident 9 showed best mucoadhesion. After 12 min testing time 13.76% Optamint liquid remained on the mucosa. The carrier system with Sident 22s exhibited a substantially lower mucoadhesion (3.61%), whereas with Aeroperl 300 an intermediate result (8.63%) was achieved. (Detailed overview of the percentages on the mucosa and in the saliva see Figure 112)

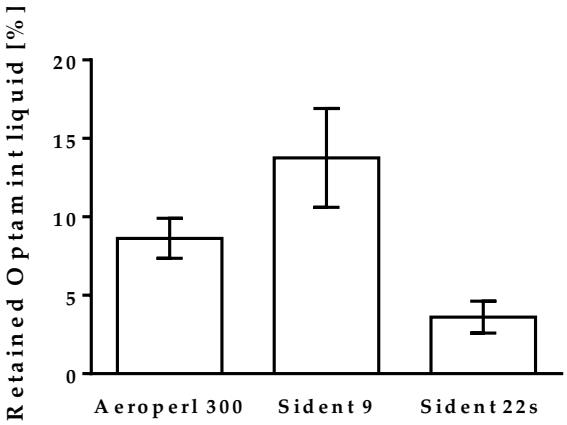

Figure 34. Mucoadhesion of carrier systems with Optamint loaded into Aeroperl 300, Sident 9 and Sident 22s

Mucoadhesion studies over an extended period of up to 60 min revealed that the increased effect of Sident 9 compared to Aeroperl 300 diminished after 30 min (Table 10). Approximately 6% flavor remained on the mucosa for Aeroperl 300 carriers, while only about 1% remained with Sident 9 as carrier. Only a marginal amount of Optamint liquid was detectable on the mucosa after 30 min for Optamint liquid loaded on Sident 22s. Consequently, Sident 22s was excluded from further experiments.

Table 10. Long term mucoadhesion of carrier systems loaded with Optamint liquid

Mucoadhesion [%]	**Aeroperl 300**	**Sident 9**	**Sident 22s**
Time [min]			
12	8.63 ± 1.28	13.76 ± 3.15	3.61 ± 1.02
30	6.06 ± 0.53	1.41 ± 0.51	0.65 ± 0.12
60	3.67 ± 0.40	-	-

3.1.3.2.6 Comparison of different flavors

To gain further knowledge on the influence of different actives on the behavior of carrier loaded flavors, Optamint solid was used as another model compound. As described before for Optamint liquid and Aeroperl 300, Optamint solid and the prepared carrier systems were examined for loading capacity, stability, release and mucoadhesive properties.

From the integrated melting peaks, a load limit of 16.11% onto Aeroperl 300 was calculated for Optamint solid (Figure 35), which was equivalent to the load limit of Optamint liquid (16.55%). For the further characterization, a carrier system with 11.62% Optamint solid (72 % of max load) was investigated.

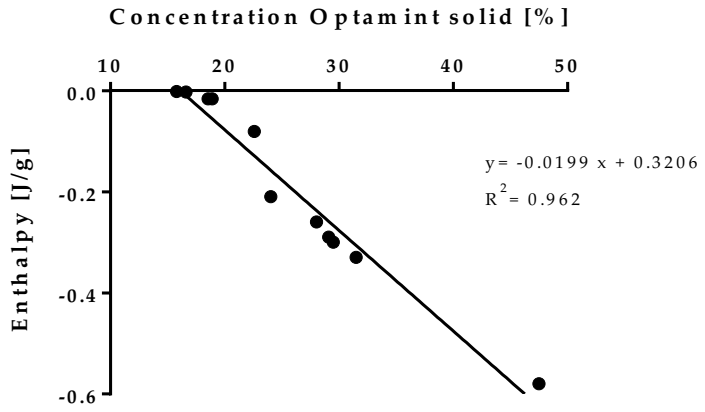

Figure 35. Concentration depended enthalpy of melting peaks of Optamint solid loaded into Aeroperl 300

Both the DSC and HPLC results (Figure 36, Figure 37) confirm that carrier systems with Optamint solid were stable over a period of 6 months in terms of content and physical state of the flavor.

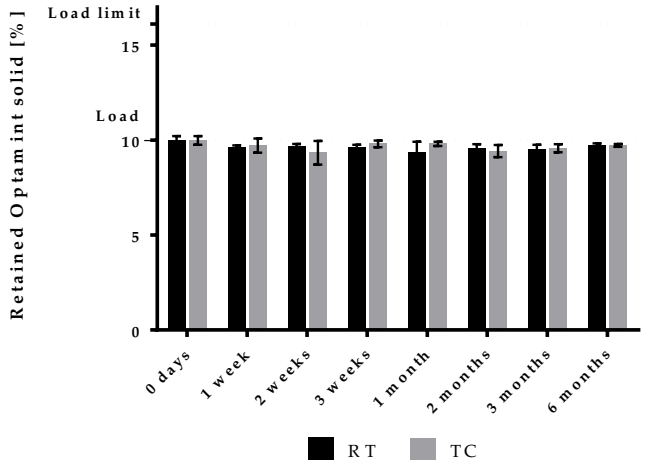

Figure 36. Flavor content of Aeroperl 300 carrier systems loaded with Optamint solid directly after loading and during storage at RT or TC

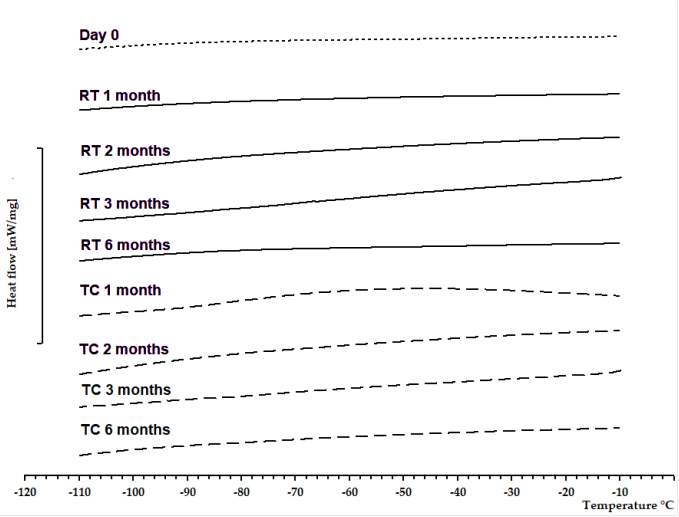

Figure 37. DSC curves of Aeroperl 300 carrier systems loaded with Optamint solid directly after loading and during storage at RT or TC

The dissolution profiles of Optamint solid and Optamint liquid were almost identical, as shown in Figure 38.

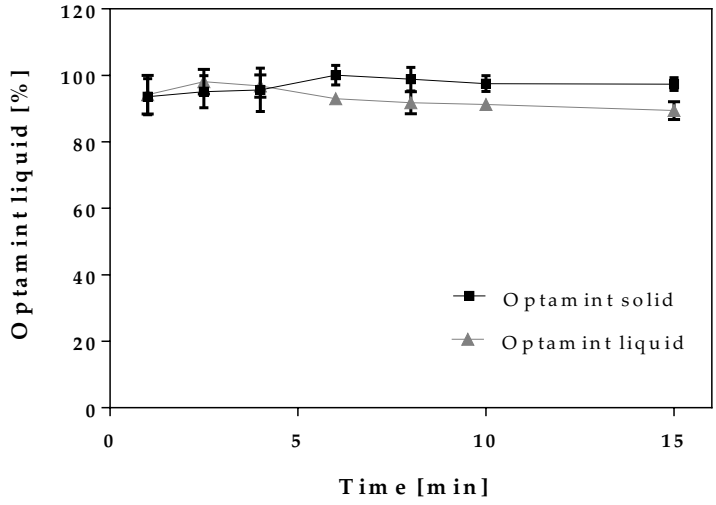

Figure 38. Dissolution profile of Optamint solid compared to Optamint liquid from carrier systems with Aeroperl 300

Figure 39 compares the mucoadhesion of Optamint solid and Optamint liquid when loaded into Aeroperl 300 carrier. After 12 min, approximately 8% of the flavor still adhered to the mucosa for both Optamint products. Consequently, mucoadhesion was not influenced by the composition of the flavoring agent, but by the carrier characteristics and the dissolution kinetic.

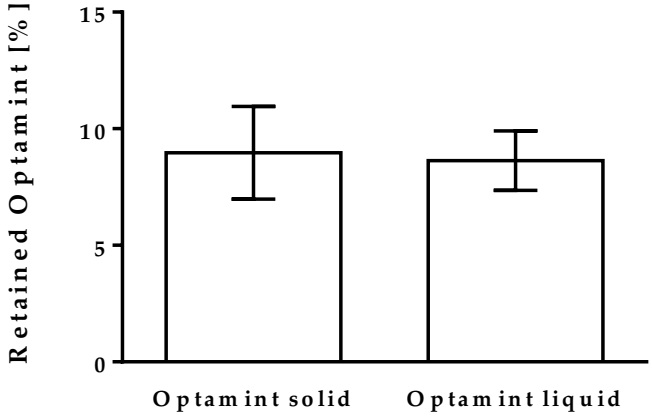

Figure 39. Comparison of mucoadhesion values from Aeroperl 300 carrier systems loaded with Optamint liquid and Optamint solid

3.1.4 Flavor-loaded mucoadhesive carrier systems

3.1.4.1 Development of mucoadhesive carrier systems

For the development of an improved mucoadhesive carrier system, Aeroperl 300 was selected as a mesoporous carrier, Optamint liquid as the flavoring agent, and non-ionic HPMC as a proven mucoadhesive polymer. The polymer was introduced by coating the carrier with a solution or suspension of HPMC and water (formulation 1, 2), or respectively glycerol (formulation 3), sunflower oil (formulation 4), triacetin (formulation 5) or the flavoring agent itself (formulation 6) (2.2.3.1). A further approach was binding the polymer to the carrier by means of high shear mixing (formulation 7) (2.2.3.2). Alternatively, HPMC and a low-melting polymer, e.g., PEG 1000, were added to the flavor loaded silica (formulation 8) (2.2.3.3). A detailed overview with regards to the exact composition of the mucoadhesive carrier systems is reported in Table 11 and Table 28.

Table 11. Composition of flavor-loaded mucoadhesive carrier systems with Aeroperl 300 and HPMC

Formulation	**Aeroperl 300 [%]**	**Optamint liquid [%]**	**HPMC [%]**	**Solvent / Dispersion medium [%]**	
1	50.76	3.51	3.18	Water	37.02
2	23.74	3.12	-	Optamint liquid	-
	34.16	-	4.16	Water	33.86
3	52.84	3.41	2.97	Glycerol	35.10
4	52.13	7.63	4.24	Sunflower oil	34.41
5	54.60	6.10	3.83	Triacetin	35.47
6	84.82	11.79	3.39	none	
7	81.18	11.55	3.27	none	
8	71.76	10.61	4.89	PEG 1000	10.74

3.1.4.1.1 Stability studies of mucoadhesive carrier systems

The content of flavoring agent during the stability study was monitored by HPLC over a period of 6 months. In addition, DSC thermograms of the formulations were recorded at predetermined time points to check for possible changes in the physical state of the flavor.

The samples prepared with an aqueous suspension of polymer (formulation 1) revealed a decrease in flavor from 3.55% to 1.49% after 6 months (Figure 40). This flavor loss was more pronounced for the samples stored under temperature cycle, where the samples were exposed to temperatures up to 40 °C. Nevertheless, the percentage of retained Optamint liquid also decreased for samples stored isothermally at room temperature, but after one month a plateau was reached at around 2.60%. Figure 41 displays the corresponding DSC curves. Unfortunately, the thermal transition around 1.5 °C of eucalyptol was hidden in the DSC measurements by phase transitions of water. Therefore, a statement on the physical state of the flavor in the carrier is restricted. However, the peaks in the thermogram showed a change in size over the period of 6 months, indicating flavor and/or water loss.

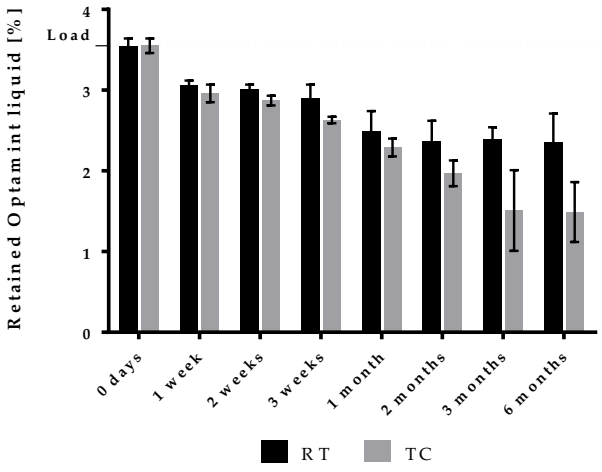

Figure 40. Flavor content of formulation 1 directly after loading and during storage at room temperature or temperature cycle

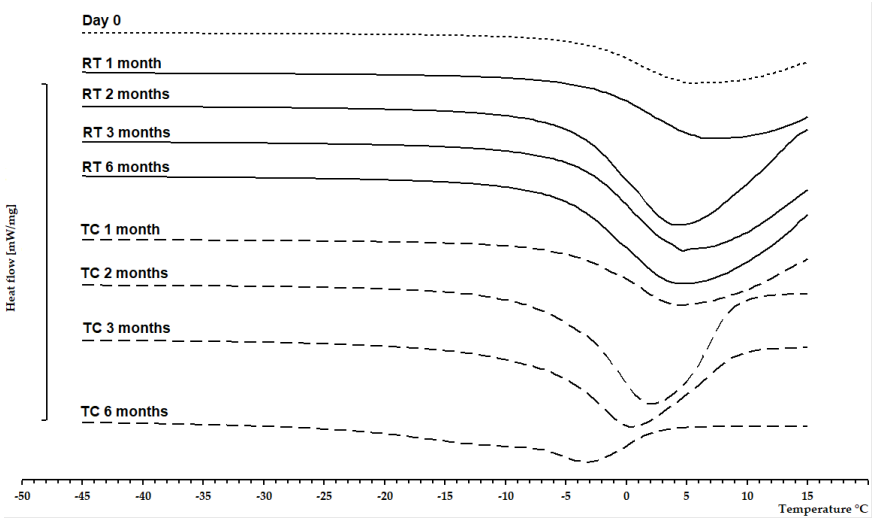

Figure 41. DSC curves of formulation 1 directly after loading and during storage at room temperature or temperature cycle

In difference to formulation 1, in which the flavor-loaded carrier system was coated, in formulation 2 a batch of flavor-free silica was coated with an aqueous polymer suspension and subsequently blended with a batch of flavor-loaded silica. Similar to formulation 1, the physical mixture (formulation 2) showed flavor loss during storage (Figure 42). Although altering melting peaks have been observed in the thermograms, it has to be considered that the peaks may originate from water or a mixture of water and flavor (Figure 43).

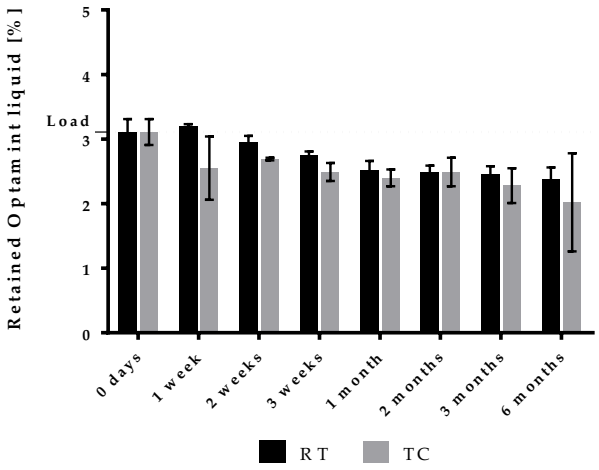

Figure 42. Flavor content of formulation 2 directly after loading and during storage at RT or TC

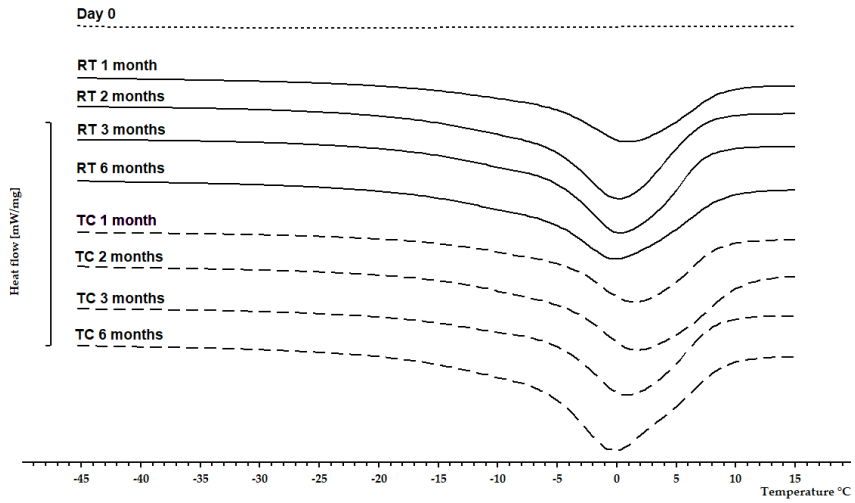

Figure 43. DSC curves of formulation 2 directly after loading and during storage at RT or TC

Concerning formulation 3, which has been prepared using glycerol, the bar plot revealed a loss of Optamint liquid from 3.41% to 2.58% at room temperature and to 1.67% for storage in the temperature cycle (Figure 44). The DSC analysis revealed no changes in the physical state of the flavor in these samples during storage (Figure 45).

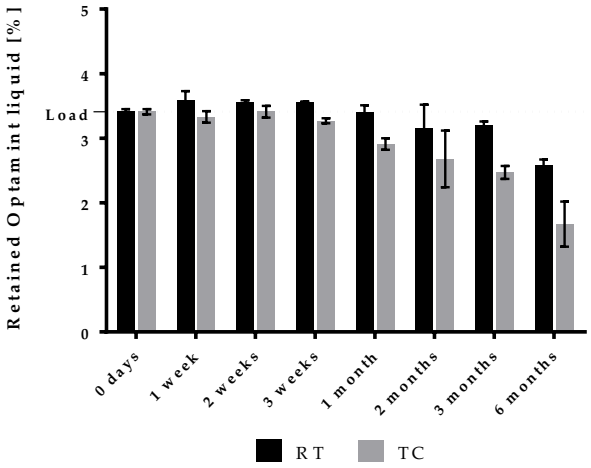

Figure 44. Flavor content of formulation 3 directly after loading and during storage at RT or TC

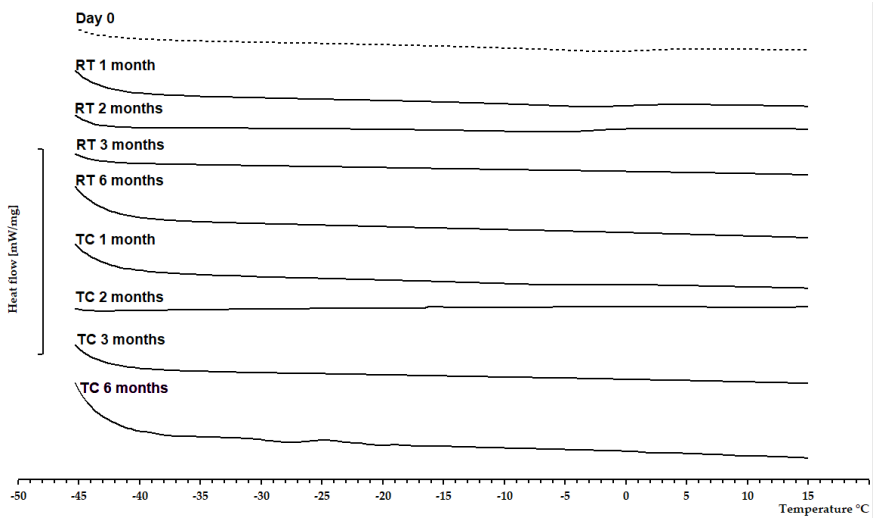

Figure 45. DSC curves of formulation 3 directly after loading and during storage at RT or TC

The addition of water and glycerol caused the flavor to evaporate from the carrier. It can be assumed that the hydrophilic additives displaced the flavor substances from the pores due to their higher affinity to the silica carriers. Due to the observed instability, formulations 1-3 with an aqueous or a glycerol suspension, were excluded from further investigations.

The results for formulation 4, 5, 6, 7 and 8 revealed no to only minor changes in the flavor content (Figure 46, Figure 48, Figure 50, Figure 51, Figure 54) after storage and gave no hints for recrystallization in the DSC thermographs (Figure 47, Figure 49, Figure 51, Figure 53, Figure 55).

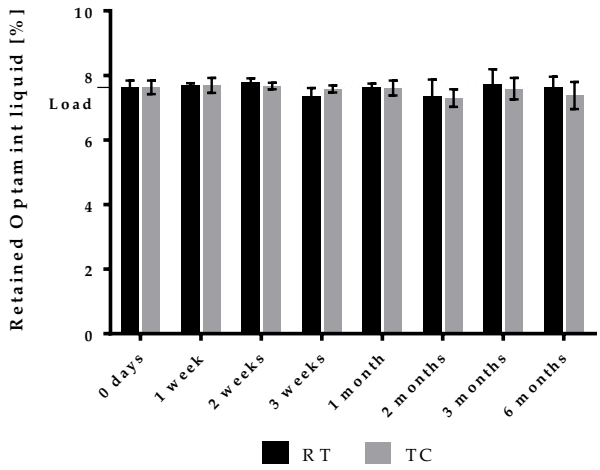

Figure 46. Flavor content of formulation 4 directly after loading and during storage at RT or TC

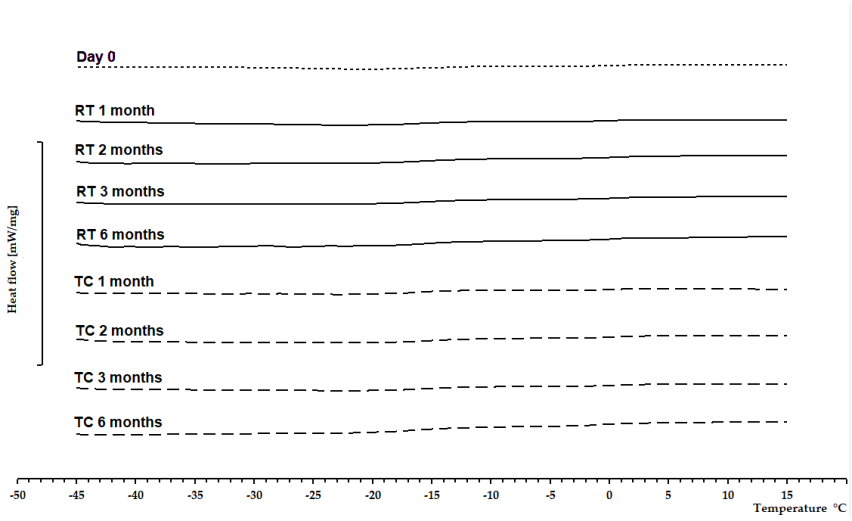

Figure 47. DSC curves of formulation 4 directly after loading and during storage at RT or TC

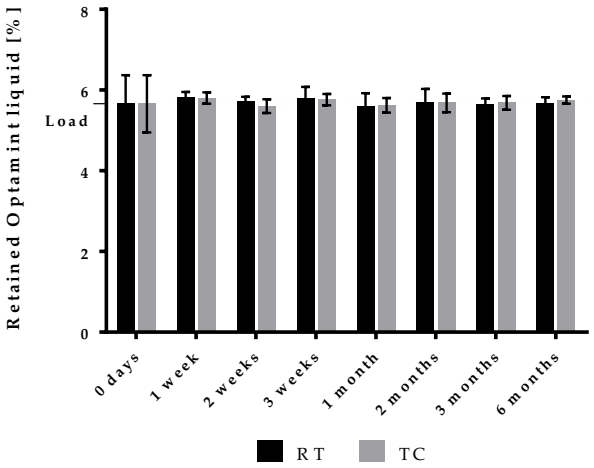

Figure 48. Flavor content of formulation 5 directly after loading and during storage at RT or TC

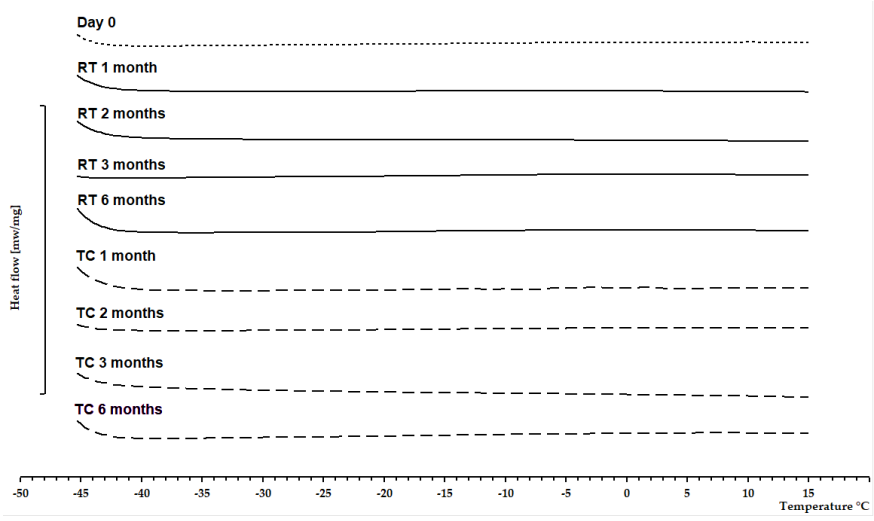

Figure 49. DSC curves of formulation 5 directly after loading and during storage at RT or TC

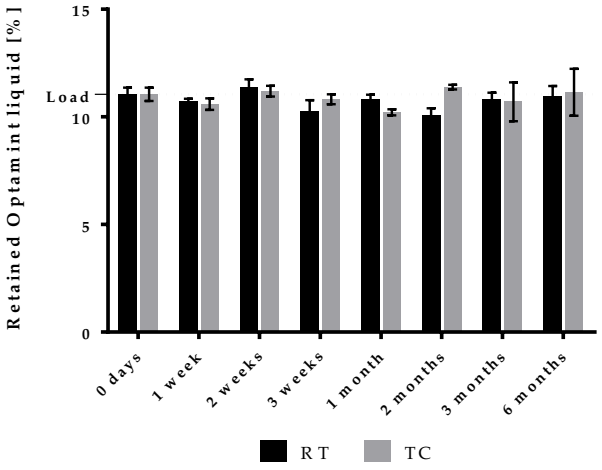

Figure 50. Flavor content of formulation 6 directly after loading and during storage at RT or TC

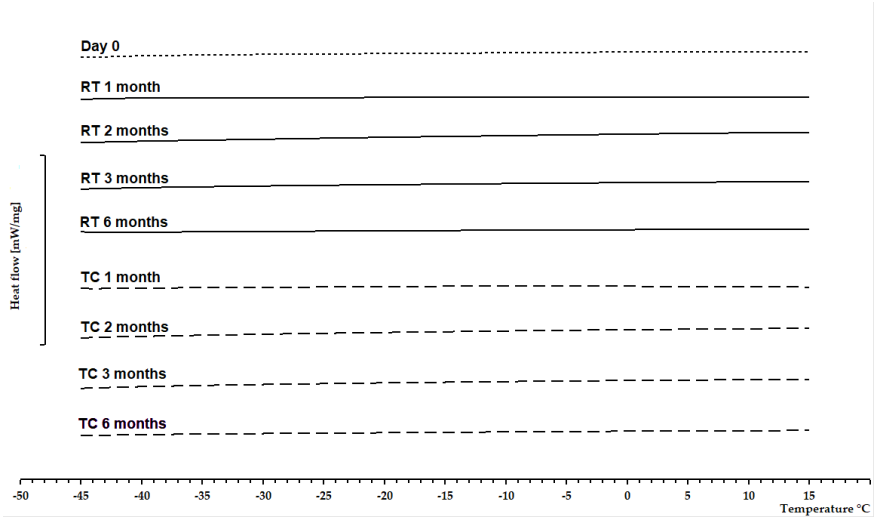

Figure 51. DSC curves of formulation 6 directly after loading and during storage at RT or TC

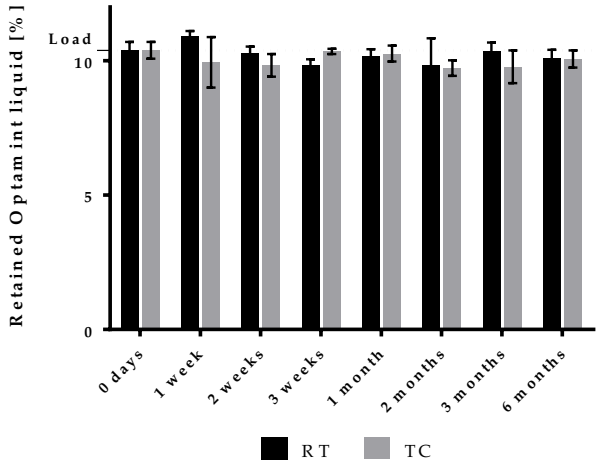

Figure 52. Flavor content of formulation 7 directly after loading and during storage at RT or TC

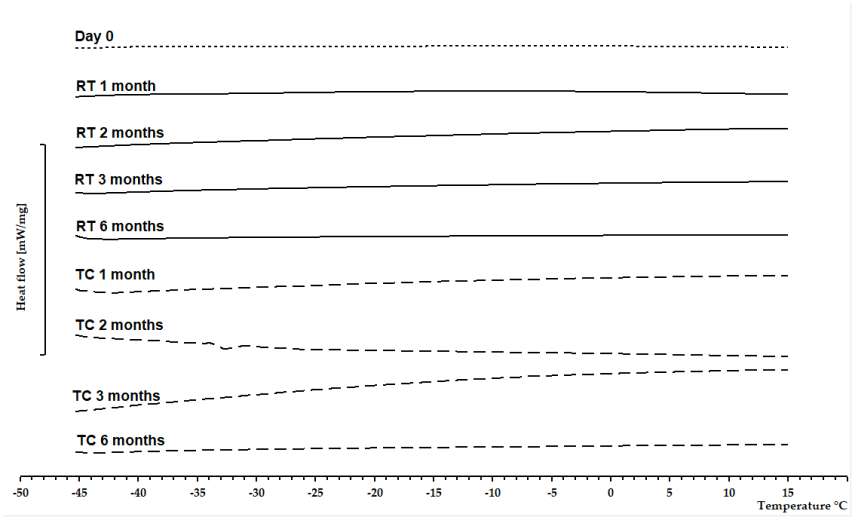

Figure 53. DSC curves of formulation 7 directly after loading and during storage at RT or TC

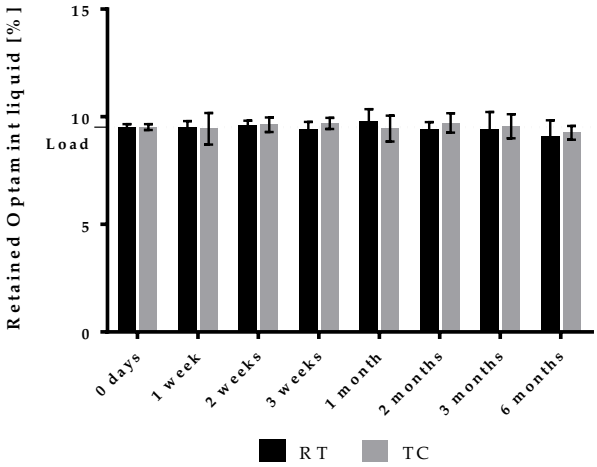

Figure 54. Flavor content of formulation 8 directly after loading and during storage at RT or TC

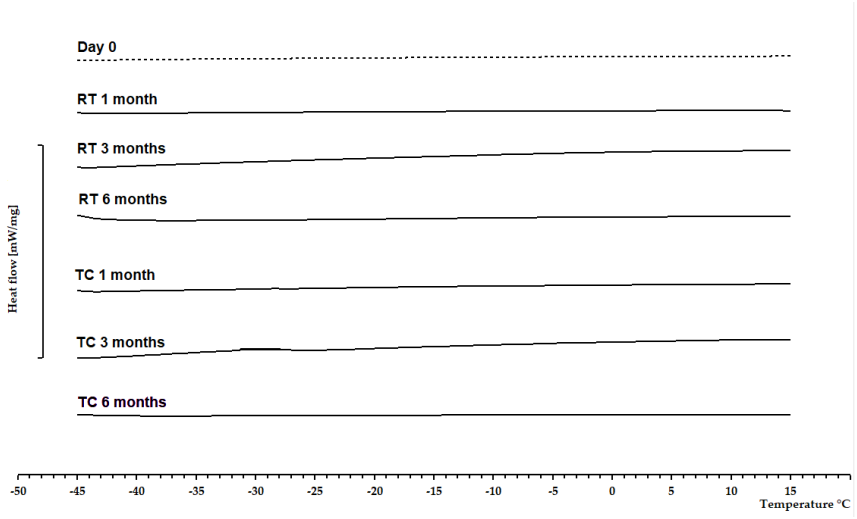

Figure 55. DSC curves of formulation 8 directly after loading and during storage at RT or TC

Based on these results, the conclusion can be drawn that the production method and additives for formulation 4-8 had no negative impact on the stability. The carrier systems were able to preserve the flavoring compounds in their amorphous state for 6 months without any relevant loss.

3.1.4.1.2 Flavor release from mucoadhesive carrier systems

Following the results of the storage stability (3.1.4.1.1), the flavor release from the following five formulations was investigated. The comparison of the dissolution curves of formulation 4-8 with the carrier system consisting solely of Aeroperl 300 loaded with Optamint liquid are

presented in Figure 56 to Figure 60. Due to the similarity of the dissolution rates, it can be assumed, that the preparation and the addition of sunflower oil, triacetin, PEG 1000, plus the mucoadhesive HPMC in the applied concentrations did not affect the flavor release.

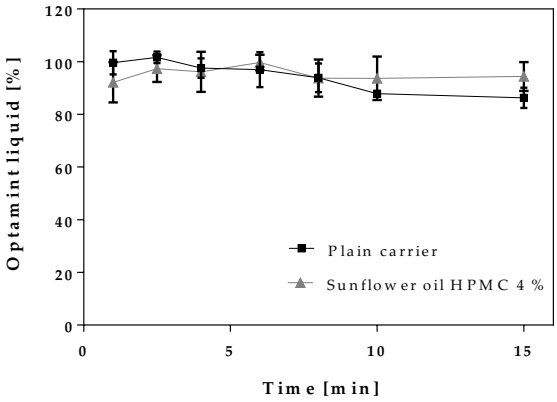

Figure 56. Dissolution profile of carrier system with HPMC suspended in sunflower oil (formulation 4)

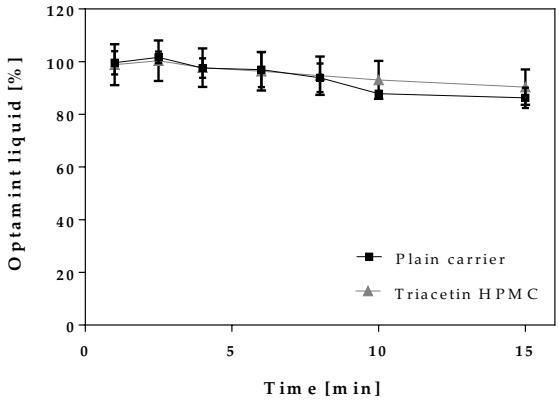

Figure 57. Dissolution profile of carrier system with HPMC suspended in triacetin (formulation 5)

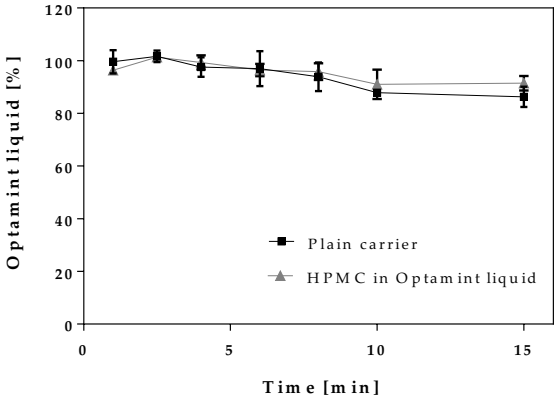

Figure 58. Dissolution profile of carrier system with HPMC suspended in Optamint liquid (formulation 6)

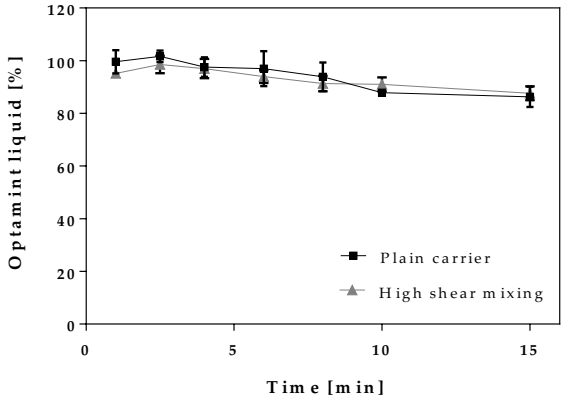

Figure 59. Dissolution profile of carrier system prepared with high shear mixing (formulation 7)

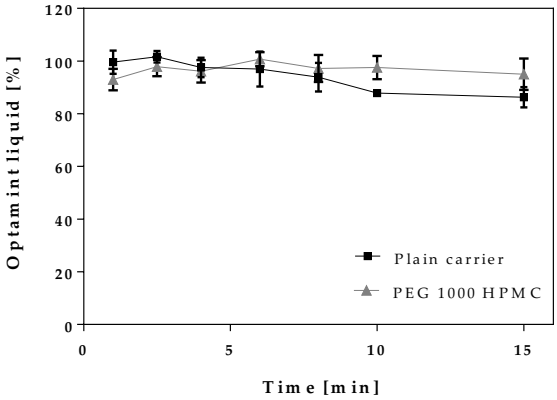

Figure 60. Dissolution profile of carrier system with HPMC and PEG 1000 (formulation 8)

3.1.4.1.3 Mucoadhesion tests of mucoadhesive carrier systems

The stable HPMC coated carrier systems (formulations 4-8) were investigated for their mucoadhesive properties with the results presented in Table 12. Compared to the other formulations, formulation 4 displayed the highest mucoadhesion with 25.28%, followed by 18.58% and 18.18% for formulations 5 and 8. The mucoadhesion of formulations 6 and 7 ranked at values of approximately 8%. The mucoadhesion coefficient underlines that formulation 6 and 7 are not superior in their mucoadhesive properties to the corresponding carrier system without mucoadhesive additives. Concerning formulation 6, this can be attributed to the limited amount of polymer. Due to the otherwise excessively high viscosity, only 3.5% HPMC could be suspended in the given amount of flavoring agent. This HPMC amount seemed to be insufficient for a marked mucoadhesive effect. The low mucoadhesion of formulation 7 may be the result of deficient bonding of the polymer to the flavor loaded carrier material through high shear mixing. In contrast, the adhesion of the formulation with sunflower oil was nearly 3-fold, and that of the formulations with triacetin and PEG 1000 2-fold higher than those of the corresponding polymer-free carrier system. As a consequence of the mucoadhesion test, further investigations were continued only with formulations prepared with PEG 1000, triacetin and sunflower oil.

Table 12. Mucoadhesion results after 12 min mucoadhesion test of formulations 4-7

	Formulation	Mucoadhesion [%]	Mucoadhesion coefficient
4	Sunflower oil	25.28 ± 1.34	2.93
5	Triacetin	18.58 ± 3.05	2.15
6	HPMC in Optamint	8.21 ± 0.76	0.95
7	High shear mixing	7.93 ± 0.48	0.92
8	PEG 1000	18.18 ± 3.33	2.11
	Reference carrier system (Aeroperl 300 with 12.06% Optamint liquid)	8.63 ± 1.28	1.00

3.1.4.2 Optimization of the formulation

3.1.4.2.1 Optimization of the added HPMC amount

The primary measure to optimize the mucoadhesive performance of the carrier system is to adjust the amount of added HPMC. In case of the preparation with sunflower oil, this is limited by two aspects. Firstly, the maximum oil binding capacity of the carrier is limited by the pore volume of the silica. Secondly, the viscosity of the coating suspension. Considering these two factors, the highest quantity of sunflower oil that could be absorbed by Aeroperl 300 was 50% related to the total mass of the final carrier system with a maximum concentration of 10% for HPMC. To determine the optimal composition, mucoadhesion coefficients of Aeroperl 300 carrier systems with varying amounts and concentrations of sunflower oil HPMC suspensions were assessed. The complete composition is outlined in Table 29.

Regarding the results presented in Table 13, increasing the amount of HPMC from 4% to 10% led to a substantial increase in mucoadhesion from 25% to 70%. Addition of 10% polymer resulted in an 8-fold higher mucoadhesion compared to the carrier system without polymer. In accordance with the literature, an increased concentration of mucoadhesive polymer leads to a higher number of functional groups that are available for bonds with the mucosa enabling an enhanced mucosal adhesion [39]. However, this correlation only applies up to a certain concentration. Above this optimum concentration, mucoadhesion decreases because the polymer chains interact excessively with each other and the resulting inflexible conformation impairs the interaction with the mucosa [36]. In the present formulation approach, this critical concentration for HPMC was not exceeded due to the viscosity restrictions, and thus the maximum possible concentration of 10% led to the maximum achievable mucoadhesion.

Simultaneously, a higher amount of sunflower oil also exerts a positive influence. Primarily, higher amounts of oil enable the application of a larger amount of polymer. Interestingly, enhanced mucoadhesion was also observed at the same level of HPMC when a higher amount of oil was applied (see Table 29). As a conclusion, a higher proportion of sunflower oil in the carrier system facilitates a more effective coating of the surface and consequently leads to a better distribution of the polymer which improves adhesion.

Table 13. Influence of the concentration of sunflower oil and HPMC on mucoadhesion of flavor-loaded Aeroperl 300 carrier systems

Sunflower oil [%]	HPMC [%]	Mucoadhesion [%]	Mucoadhesion coefficient
35	4	25.28 ± 1.34	2.93
30	8	37.07 ± 4.09	4.30
50	6	52.79 ± 12.42	6.12
45	10	70.71 ± 4.59	8.19
Reference carrier system (Aeroperl 300 with 12.06% Optamint liquid)		8.63 ± 1.28	1.00

Figure 61 shows the release profiles of Aeroperl 300 carrier systems with 4% and 10% HPMC in comparison to the carrier system without added HPMC. While the carrier system with 4% HPMC displayed no substantial difference in the release compared to the flavor-loaded carrier system without HPMC, the initial release is significantly delayed when 10% were added. Polymer swelling and polymer dissolution are two factors controlling the release of substances from HPMC matrices. These factors are among others affected by the concentration of the polymer [96]. Therefore, the increased concentration of HPMC resulted in a lower release rate of Optamint liquid from the carrier system.

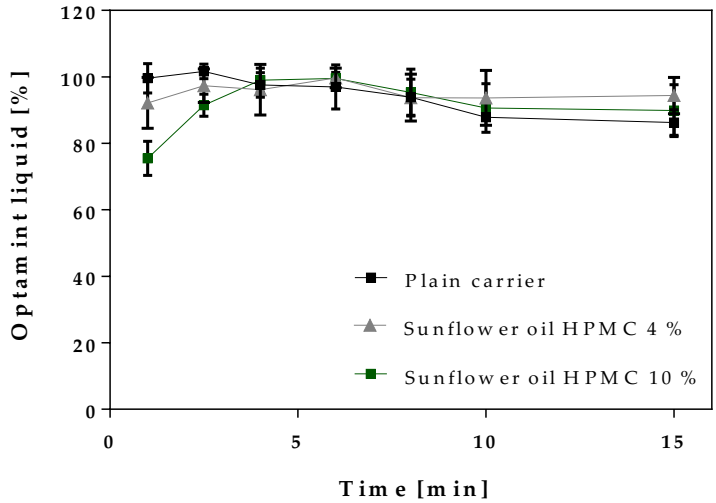

Figure 61. Dissolution profile of carrier systems with 4% and 10% HPMC suspended in sunflower oil compared to a carrier system without polymer

Triacetin as a suspension medium showed the same limitations in terms of the added polymer quantity as sunflower oil. Table 14 displays the mucoadhesion coefficients of Aeroperl 300 carrier systems with varying concentrations of triacetin and HPMC. The complete composition of the respective carrier systems is listed in Table 30. Concerning the trend, these mucoadhesion values are in good agreement with those obtained from the test series with sunflower oil. In both cases, a higher concentration of HPMC and a higher concentration of oil proved to be beneficial for the strength of the mucoadhesive effect. As for sunflower oil, in the series of experiments with triacetin, the carrier system with 10% HPMC and 45% suspension medium was superior to the other compositions.

By direct comparison between the two suspension mediums, it can be stated that sunflower oil was advantageous in terms of the obtained mucoadhesion values compared to triacetin. An explanation for this effect could be that triacetin is a good solvent for the Optamint liquid and at the same time partially miscible with artificial saliva. This allows to partly dissolve Optamint liquid in the saliva and to wash it away. The solubility of triacetin in water at a temperature of 24.5 °C is given as 52.130 mg/L, whereas sunflower oil is practical insoluble [97].

Table 14. Influence of the concentration of triacetin and HPMC on mucoadhesion of flavor-loaded Aeroperl 300 carrier systems

Triacetin [%]	**HPMC [%]**	**Mucoadhesion [%]**	**Mucoadhesion coefficient**
35	4	18.58 ± 3.05	2.15
30	8	25.13 ± 1.39	2.91
50	6	30.52 ± 2.71	3.54
45	10	37.13 ± 1.08	4.30
Reference carrier system (Aeroperl 300 with 12.06% Optamint liquid)		8.63 ± 1.28	1.00

The preparation of carrier systems with PEG 1000 is not restricted by the aforementioned limitations for the incorporation of HPMC. Table 15 displays the influence of the amount of PEG 1000 and HPMC on the mucoadhesive properties. The complete composition of the mucoadhesive carrier systems is reported in Table 31. With 36.35% flavor remaining on the mucosa after 12 min, the carrier system with the composition of 10% PEG 1000 and 10% HPMC provided comparatively the highest adhesion. It is noteworthy that this system did not represent the carrier system with the highest amount of polymer in the study. The comparison of the mucoadhesion coefficients shows that in this case the mucoadhesion was strongly

affected by the quantity of PEG 1000. Carrier systems with a reduced proportion of PEG 1000 exhibited higher mucoadhesion coefficients than carrier systems with 20% PEG 1000, although they contained more HPMC in comparison.

Table 15. Influence of the concentration of PEG 1000 and HPMC on mucoadhesion

PEG 1000 [%]	**HPMC [%]**	**Mucoadhesion [%]**	**Mucoadhesion coefficient**
10	5	18.18 ± 3.33	2.11
20	6	14.88 ± 4.22	1.72
10	10	36.35 ± 1.97	4.21
20	20	25.97 ± 7.25	3.01
Reference carrier system (Aeroperl 300 with 12.06% Optamint liquid)		8.63 ± 1.28	1.00

This effect can be explained by the fact, that with increasing addition of PEG a higher amount is deposited on the outer surface of the carrier. Thus, PEG 1000 would shield HPMC from the mucosa, leading to a decrease in mucoadhesion. Due to its chemical structure PEG 1000 is not able to interact with the mucosa as effectively as HPMC. Low molecular weight types such as PEG 1000, tend to be classified in the literature as mucopenetrating or mucoinert rather than mucoadhesive [20, 45]. The thermogram of the carrier systems (Figure 62) reaffirms the shielding effect of a high proportion of PEG 1000. The curves for flavor loaded carrier systems with 10% PEG 1000 revealed no thermal events. In contrast, the carrier system with 20% PEG 1000 displayed a melting peak indicating that not the entire amount of PEG 1000 was absorbed into the carrier's pores, but on its outer surface. The slight shift towards lower temperatures of the melting peak compared to the bulk material is the result of interactions of PEG 1000 with the other components of the carrier system [98]. Furthermore, PEG 1000 is known to interact with HPMC via hydrogen bonds between the ether oxygen and the hydroxyl groups, which results in reduced interaction of HPMC with the mucosa [99, 100].

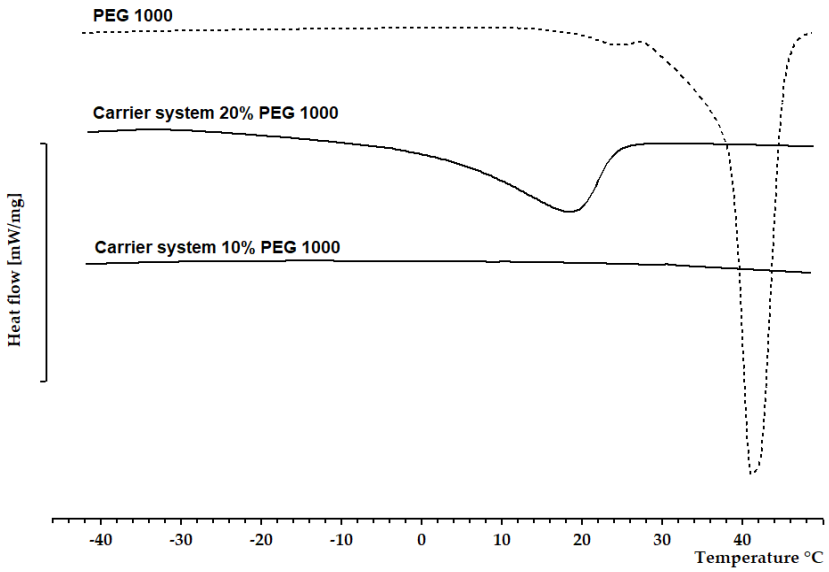

Figure 62. DSC measurements of flavor-loaded carrier systems with different amount of PEG 1000

3.1.4.2.2 Deployment of other mucoadhesive polymers

To further improve the mucoadhesive properties of the carrier systems, the influence of alternative mucoadhesive polymers was investigated. With chitosan, HPMC and carbomer the mucoadhesive performances of a cationic, a non-ionic and an anionic polymer were evaluated. All three polymers are characterized by low toxicity and high biocompatibility and are therefore ideal candidates for the use in buccal drug delivery systems [16, 40].

In order to achieve optimal mucoadhesion, the applied quantity of the mucoadhesive polymer should be as high as possible. However, chitosan possesses a higher viscosity when suspended in sunflower oil compared to HPMC, hence the highest possible amount of chitosan was 6% related to the total mass. Therefore, the comparison was made with the corresponding carrier systems using also 6 %HPMC. For carbomer-containing carrier systems, on the other hand, 10% polymer could be realized and thus these systems were compared with 10% HPMC (composition of the mucoadhesive carrier systems see Table 32). Under these prerequisites, carrier systems with chitosan exhibited an inferior mucoadhesive effect with 17.5% compared to 52.8% mucoadhesion from the corresponding systems with HPMC whereas carbomer was able to increase the retained fraction of flavoring agent to 82.4% (Table 16). Considering the mucoadhesion coefficients, the following ranking results for the mucoadhesive strength of the carrier systems: carbomer > HPMC >> chitosan.

Table 16. Comparison of mucoadhesive performance of different polymers incorporated in Aeroperl 300 carrier systems with sunflower oil

Carrier system	Mucoadhesion [%]	Mucoadhesion coefficient
HPMC 6%	52.79 ± 12.42	6.12
Chitosan 6%	17.53 ± 5.16	2.03
HPMC 10%	70.71 ± 4.95	8.19
Carbomer 10%	82.43 ± 2.63	9.55
Reference carrier system (Aeroperl 300 with 12.06% Optamint liquid)	8.63 ± 1.28	1.00

These differences in mucosal adhesion also became evident when comparing images of the mucosa 12 min after the application and subsequent rinse with artificial saliva (Figure 63). While carbomer and HPMC showed obvious residues of the carrier system, chitosan caused only a small amount to remain on the mucosa.

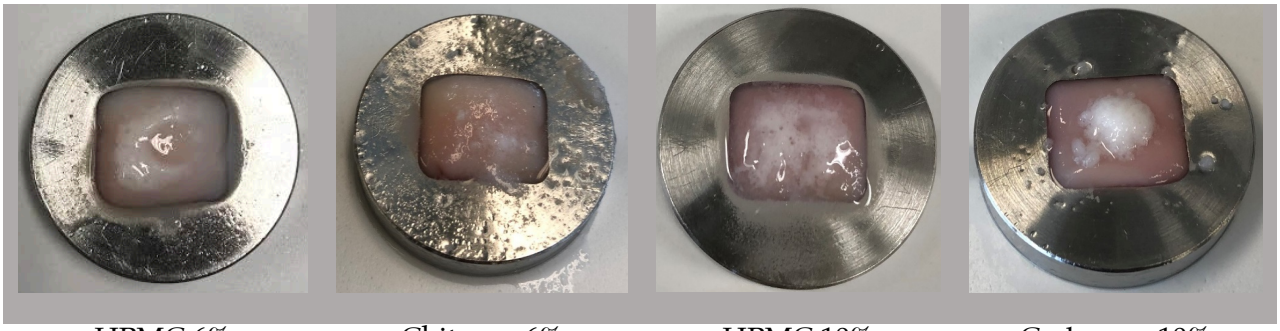

HPMC 6% Chitosan 6% HPMC 10% Carbomer 10%

Figure 63. Comparison of mucosa after 12 min of mucoadhesion testing of mucoadhesive carrier systems with HPMC, chitosan and carbomer

Figure 64 shows that the release of Optamint liquid from the mucoadhesive carrier systems was delayed compared to a carrier system without any mucoadhesive polymer. This slower dissolution rate can be attributed to the swelling of the polymers. As opposed to chitosan and carbomer, the Optamint liquid release from HPMC-containing carrier systems is only slightly impaired. This is indicative of a comparatively less pronounced swelling in an aqueous medium. The more reduced dissolution rate from carrier systems with chitosan and carbomer points to a more enhanced swelling of these polymers. Overall, the results for HPMC and carbomer of the dissolution test were consistent with the visual impression of the mucosa after the mucoadhesion test (Figure 63). The carrier system with carbomer appeared strongly swollen on the mucosa, whereas the swelling was visually less distinct with HPMC. In terms

of mucoadhesion, swelling of the polymer is required to induce mobility in the polymer chains, necessary for enhanced interpenetration between polymer and mucin [36]. Increased polymer swelling permits a mechanical entanglement with the mucus network [39]. Therefore, the strong swelling behavior of carbomer may attribute to the high mucoadhesive values obtained in the experiments. For chitosan, swelling behavior was evident in dissolution test and mucosa imaging (Figure 63). However, this swelling behavior seems to be ineffective for the interaction of the carrier system with the mucosa, as the mucoadhesion results obtained were significantly lower than for the other two polymers. Even the image shows that the swollen parts of the sample were not located on the mucosa, but rather aside on top of the holder.

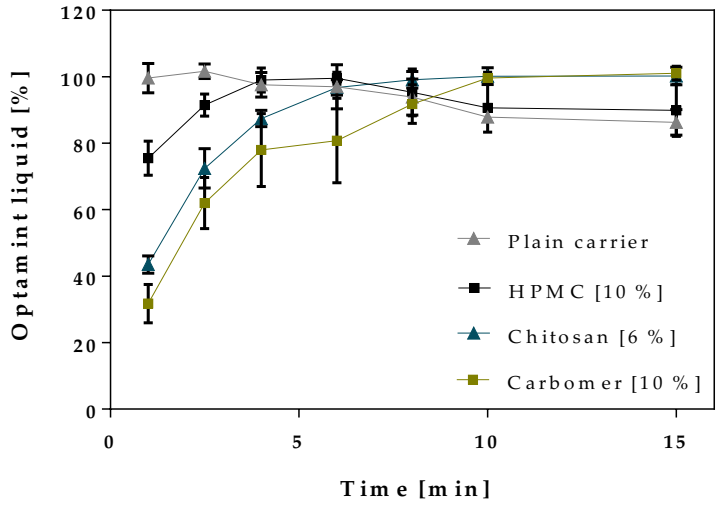

Figure 64. Comparison of dissolution profiles of carrier system without polymer, 10% HPMC suspended in sunflower oil, with 6% chitosan suspended in sunflower and 10% carbomer suspended in sunflower oil

Apart from the differences in the chemical structure of the mucoadhesive additives, their particle size could also affect the mucoadhesive performance. Microscopic images of the polymer particles (Figure 65) clearly reveal that the particle size of the polymers differed significantly. Carbomer comparatively had the finest particles among the polymers in combination with a narrow particle size distribution, followed by HPMC. In the microscopic images of chitosan, particles of the same order of magnitude to those of HPMC were visible, as well as numerous substantially larger ones. Smaller particles can penetrate deeper into the mucin network owing to their smaller diameter and are consequently less susceptible to dislodging stresses [28, 101]. Therefore, the large chitosan particles were only able to slightly increase the mucoadhesive performance, whereas the very fine carbomer revealed the best mucoadhesion.

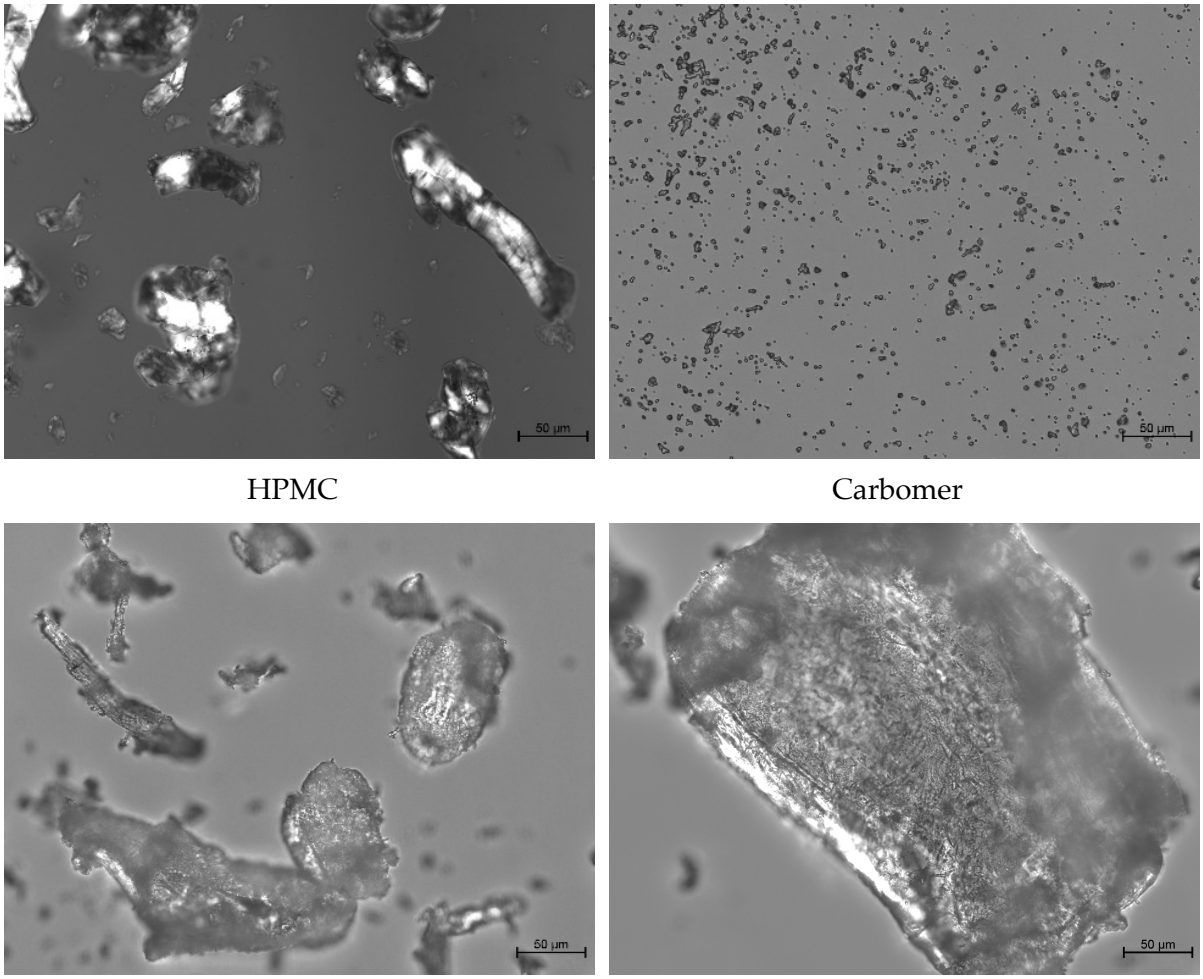

HPMC Carbomer

Chitosan

Figure 65. Microscopic images of HPMC, carbomer and chitosan (40x magnification)

Various test systems are reported in literature to quantify the mucoadhesive effect of polymers, which impedes a reliable comparison of different polymers. However, the overall obtained mucoadhesion values are in good agreement with the reported properties of the used polymers. Carbomer is ranked among the strongest mucoadhesive polymers, while HPMC is known as a moderately mucoadhesive polymer [23, 102]. The comparatively weaker retention time of HPMC can be attributed to the absence of carboxyl groups, which serve as proton donors for hydrogen bonds with the mucins [23]. The mucoadhesive properties of chitosan are reported to range from weak and short-lasting [44] to strong [26]. When comparing its effect in this study with carbomer and HPMC, it has to be considered that the applied concentration of chitosan was limited to 6% compared to 10% of the two others.

Due to its intrinsic properties, the particle size and the 10% loading, carbomer proved to be the best mucoadhesive polymer for flavor-loaded carrier systems with sunflower oil. Therefore, carbomer was also investigated as a mucoadhesive polymer for the carrier systems with triacetin as an alternative suspension medium. Equivalent to the mucoadhesion results

of the carrier systems with sunflower oil, carbomer in combination with triacetin was superior to HPMC. For the mucoadhesive carrier system with triacetin and carbomer 62.38% flavor remained on the mucosa after 12 min, whereas for the carrier system with triacetin and HPMC only 37.13% flavor could be retrieved on the mucosa (Table 17). Nevertheless, the direct comparison of sunflower oil and triacetin showed superiority of sunflower oil over triacetin for introducing carbomer to the carrier system.

Table 17. Mucoadhesion and mucoadhesive coefficients of flavor-loaded Aeroperl 300 carrier systems with triacetin and HPMC compared to triacetin and carbomer and direct comparison to flavor-loaded Aeroperl 300 carrier systems with sunflower oil and HPMC and sunflower oil and carbomer

Formulation	**Mucoadhesion [%]**	**Mucoadhesive coefficient**
45% triacetin +10% HPMC	37.13 ± 1.08	4.30
45% triacetin +10% carbomer	62.28 ± 3.41	7.22
45% sunflower oil +10% HPMC	70.71 ± 4.95	8.19
45% sunflower oil +10% carbomer	82.43 ± 2.63	9.55
Reference carrier system (Aeroperl 300 with 12.06% Optamint liquid)	8.63 ± 1.28	1.00

For HPMC, PEG 1000 was found to be a possible alternative to sunflower oil as a dispersant. Therefore, carbomer as the most promising candidate was also processed with PEG 1000 instead of sunflower oil (complete composition see Table 33). The results are shown in Table 18. The mucoadhesion coefficients show that 5% carbomer in PEG 1000, in contrast to 5% HPMC, did not show any mucoadhesive effect. An increase to 10% carbomer resulted in only a negligible small effect with a mucoadhesion coefficient of 1.33. The corresponding carrier system with HPMC, however, achieved a 4-fold increase in mucoadhesion.

Table 18. Mucoadhesive performance of carrier systems prepared with PEG 1000 and carbomer in comparison to PEG 1000 and HPMC

Carrier system		**Mucoadhesion [%]**	**Mucoadhesion coefficient**
HPMC 5%	**PEG 1000 10%**	18.18 ± 3.33	2.11
Carbomer 5%	**PEG 1000 10%**	7.73 ± 1.47	0.90
HPMC 10%	**PEG 1000 10%**	36.35 ± 1.97	4.21
Carbomer 10%	**PEG 1000 10%**	11.48 ± 1.89	1.33
Reference carrier system (Aeroperl 300 with 12.06% Optamint liquid)		8.63 ± 1.28	1.00

The image of the mucosa (Figure 66) visualizes that the carrier system swelled upon contact with saliva but did not adhere to the mucosa. This effect could be attributed to the impairment of the mucoadhesive performance of carbomer by PEG 1000. The interaction between polycarboxylic acids and polymeric hydrogen bond acceptors as polyoxyethylen has been described in literature [103]. This interpolymer complexation reduces the ability of interaction with the porcine mucosa [100]. Due to the structural conditions, the tendency for interactions between PEG 1000 and the mucoadhesive polymer seems to be larger for carbomer than for HPMC. Therefore, the mucoadhesive effect is markedly less pronounced in carrier systems with carbomer.

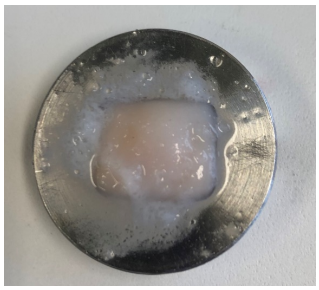

Figure 66. Mucosa after 12 min of mucoadhesion testing of carrier system with 10% PEG 1000 and 10% carbomer

Due to the insufficient results obtained by the mucoadhesive carrier systems with chitosan and sunflower oil, the combination of chitosan and triacetin and chitosan and PEG 1000 were not investigated.

3.1.4.3 Mucoadhesive carrier systems with Sident 9

In analogy to the systems with Aeroperl 300, carrier systems with Sident 9 were prepared (composition see Table 35). The maximum oil binding capacity of Sident 9 is lower than that of Aeroperl 300, as described previously in chapter 3.1.2.1. For the preparation of mucoadhesive carrier systems, Sident 9 allows for a maximum uptake of 30% sunflower oil or triacetin related to the total mass of the final formulation and consequently the possibility to incorporate 8% polymer. Therefore, these carriers were compared to the corresponding carrier systems with Aeroperl 300 containing 8% polymer.

Stability studies were conducted for the Sident 9 carrier systems with triacetin as the suspension medium and HPMC or carbomer as polymers. Both the content of flavoring agent and the physical state of the Optamint liquid showed no changes for 6 months storage (Figure 67 to Figure 70), suggesting the stability of the carrier systems.

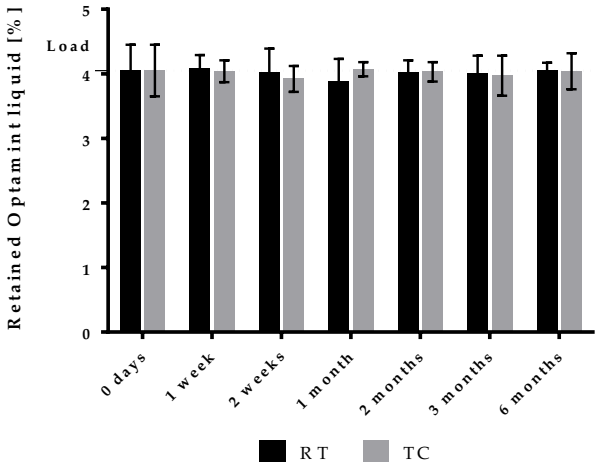

Figure 67. Flavor content of Sident 9 carrier systems loaded with Optamint liquid, triacetin and HPMC directly after loading and during storage at RT or TC

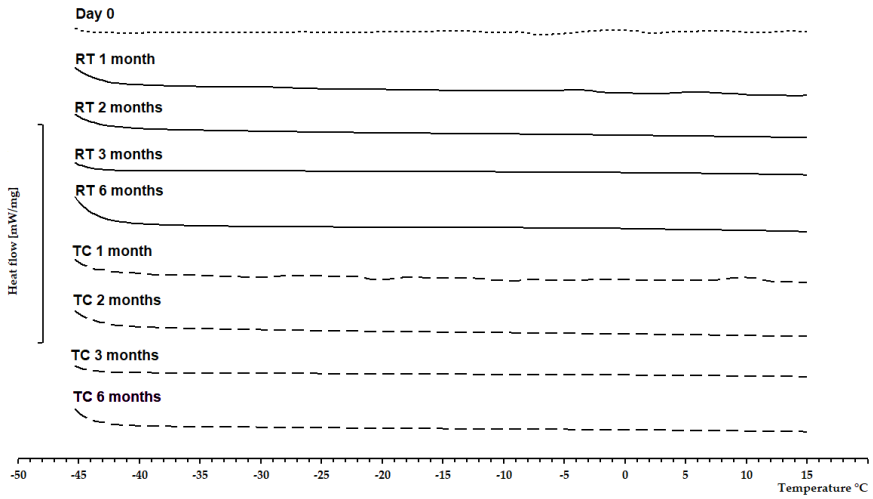

Figure 68. DSC curves of Sident 9 carrier systems loaded with Optamint liquid, triacetin and HPMC directly after loading and during storage at RT or TC

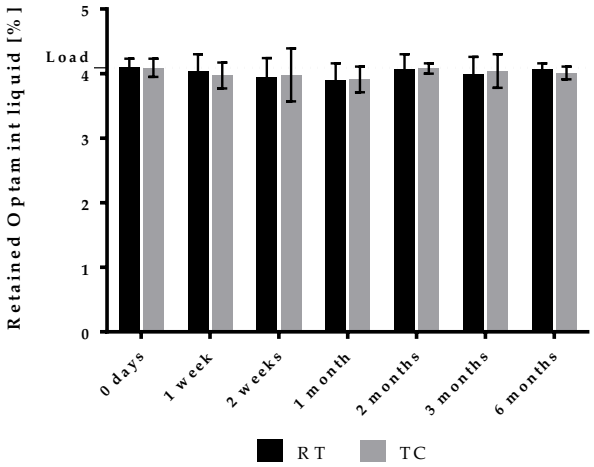

Figure 69. Flavor content of Sident 9 carrier systems loaded with Optamint liquid, triacetin and carbomer directly after loading and during storage at RT or TC

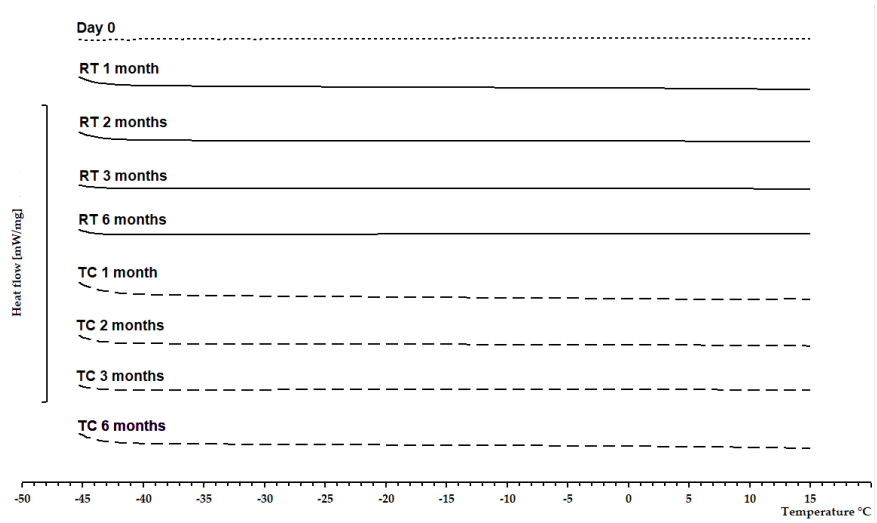

Figure 70. DSC curves of Sident 9 carrier systems loaded with Optamint liquid, triacetin and carbomer directly after loading and during storage at RT or TC

Table 19 lists the mucoadhesion values of the mucoadhesive carrier systems consisting of flavor-loaded Sident 9 fomulated with sunflower oil or triacetin as the suspension medium and HPMC or carbomer as the mucoadhesive polymer. The carrier system with the combination of sunflower oil and carbomer showed the highest value with 50% mucoadhesion. With a mucoadhesion value of approximately 30%, the combinations of sunflower oil and HPMC as well as triacetin and carbomer achieved comparable results The lowest mucoadhesion with 25% flavor remaining on the mucosa was obtained for the carrier system with triacetin and HPMC. Compared to the corresponding result with Aeroperl 300 (Table 17), it can be seen that with both silica types a similar rank order of the different formulation approaches is observed. Carrier systems with carbomer were superior to HPMC and the preparation with triacetin led to lower mucoadhesion values than the corresponding systems with sunflower oil.

Table 19. Mucoadhesion and mucoadhesive coefficients of flavor-loaded Sident 9 carrier system with triacetin and sunflower oil as suspension medium and HPMC and carbomer as polymers

Carrier	**Formulation**	**Mucoadhesion [%]**	**Mucoadhesive coefficient**
Sident 9	30% sunflower oil + 8% HPMC	32.05 ± 5.27	2.33
Sident 9	30% sunflower oil + 8% carbomer	50.19 ± 7.62	3.65
Sident 9	30% triacetin + 8% HPMC	25.66 ± 2.78	1.86
Sident 9	30% triacetin + 8% carbomer	33.54 ± 2.23	2.44
Sident 9	Reference carrier system (3.43% Optamint liquid)	13.76 ± 3.15	1.00

Table 20 shows the results of the mucoadhesion testing from the direct comparison between the carrier system with Sident 9, sunflower oil and 8% HPMC or 8% carbomer and the equally composed mucoadhesive carrier system with Aeroperl 300. In absolute numbers, Aeroperl 300 carriers performed better than the corresponding systems based on Sident 9. In direct comparison, the carrier systems with Aeroperl 300 revealed a nearly 2-fold higher mucoadhesion than the corresponding formulations with Sident 9. Aeroperl 300 seems to be able to bind the mucoadhesive polymer and the flavoring agent more effectively thus contributing to an extended residence time of the flavor on the mucosa.

Table 20. Mucoadhesion and mucoadhesive coefficients of flavor-loaded mucoadhesive carrier systems with Sident 9 compared to carrier systems with Aeroperl 300

Carrier	**Formulation**	**Mucoadhesion [%]**	**Mucoadhesive coefficient**
Aeroperl 300	30% sunflower oil + 8% HPMC	37.07 ± 4.01	4.30
Sident 9	30% sunflower oil + 8% HPMC	32.05 ± 5.27	2.33
Aeroperl 300	30% sunflower oil + 8% carbomer	62.19 ± 2.61	7.21
Sident 9	30% sunflower oil + 8% carbomer	50.19 ± 7.62	3.65
Aeroperl 300	Reference carrier system (12.06% Optamint liquid)	8.63 ± 1.28	1.00
Sident 9	Reference carrier system (3.43% Optamint liquid)	13.76 ± 3.15	1.00

The comparison of carrier systems produced with PEG 1000 as the binder also reveals a clear superiority of carrier systems with Aeroperl 300 (Table 21). The mucoadhesive effect of the carrier system with Sident 9 proved to be extremely weak. The DSC thermogram (Figure 71) reveals that PEG 1000 molecules were partially located on the outer surface of the Sident 9 carrier material, when using 10% PEG 1000. As already discussed in chapter 3.1.4.1.3, this leads to a significant reduction of the mucoadhesion of HPMC. As opposed to Sident 9, carrier systems with Aeroperl 300 displayed no melting peak of PEG 1000 at an applied concentration of 10%. Aeroperl 300 features a higher absorption capacity (3.1.2.1) and is able to bind more PEG 1000 within the carrier system compared to Sident 9. Consequently, Aeroperl 300 yielded superior mucoadhesion values for the formulation approach with PEG 1000.

Table 21. Mucoadhesion of carrier system with Aeroperl 300, 10% HPMC and 10% PEG 1000 compared to Sident 9, 10% HPMC and 10% PEG 1000

Formulation	**Carrier**	**Mucoadhesion [%]**	**Mucoadhesive coefficient**
10% HPMC + 10% PEG 1000	Aeroperl 300	36.35 ± 1.97	4.21
	Sident 9	18.29 ± 3.99	1.32
Reference carrier system (12.06% Optamint liquid)	Aeroperl 300	8.63 ± 1.28	1.00
Reference carrier system (3.43% Optamint liquid)	Sident 9	13.76 ± 3.15	1.00

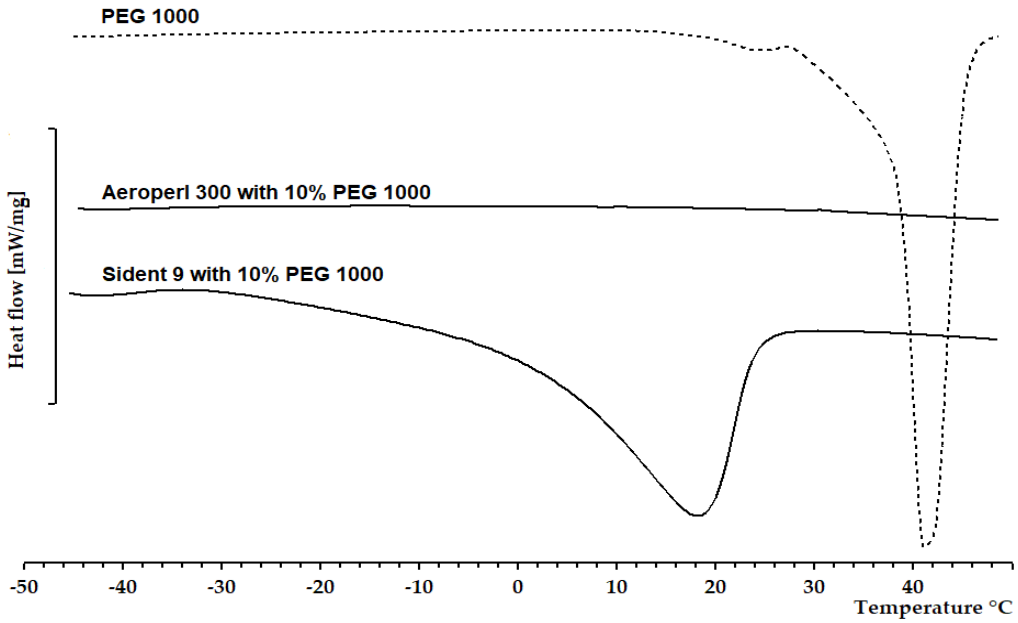

Figure 71. DSC curve of PEG 1000 compared to DSC curve of carrier systems with Aeroperl 300, 10% HPMC and 10% PEG 1000 and Sident 9, 10% HPMC and 10% PEG 1000

3.1.4.4 Influence of the type of flavoring agent on mucoadhesion

Carrier systems consisting of Aeroperl 300, sunflower oil, carbomer and two different flavoring agents, namely Optamint solid and Optamint liquid, were prepared and characterized with respect to their mucoadhesive properties (composition see Table 33 and Table 36). The result is displayed in Figure 72. It is evident that the type of flavoring agent did not affect the mucoadhesive performance.

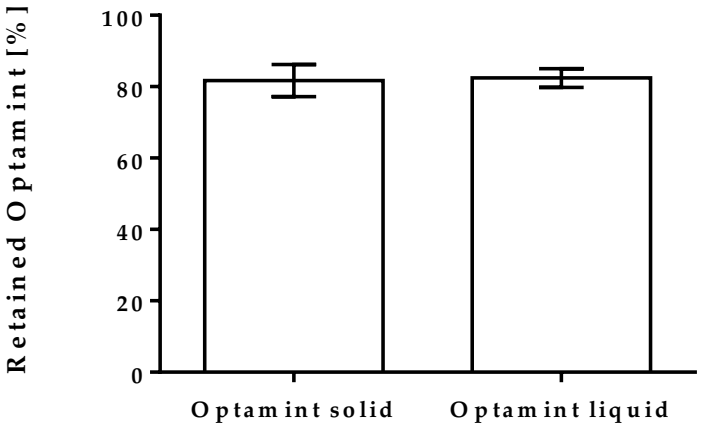

Figure 72. Comparison of mucoadhesion values of Aeroperl 300 carrier system with 10% carbomer suspended in sunflower oil using Optamint liquid or Optamint solid as flavoring agent

3.1.4.5 Mucoadhesion kinetic

For the estimation of the mucoadhesion kinetic, the mucoadhesion test was extended to 60 min. Sampling was done at 12, 30, and 60 min. As shown in Figure 73, carbomer was able to yield not only a high but also a long lasting mucoadhesive effect. After 60 min, approximately 70% of the applied dose of Optamint liquid remained on the mucosa. Even though the mucoadhesive properties of carrier systems with HPMC declined more rapidly compared to those with carbomer in an almost linear decrease, they still showed a high mucoadhesion value of 50% after 30 min and a moderate value of 20% after 60 min.

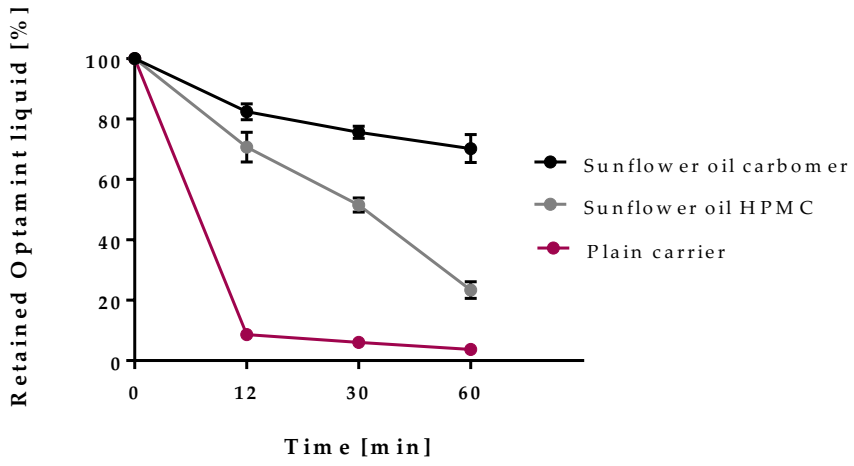

Figure 73. Long-term mucoadhesion of flavor-loaded Aeroperl 300 carrier systems with 10% polymer suspended in sunflower oil compared to flavor-loaded Aeroperl 300 carrier system without polymer

Similar results were found for carrier systems with triacetin as suspension liquid (Figure 74). Systems with carbomer as mucoadhesive additive showed the best performance. With carbomer, 40% of flavor remained on the mucosa after 60 min. HPMC, however, could not substantially enhance the mucoadhesive efficiency compared to the carrier system without polymer.

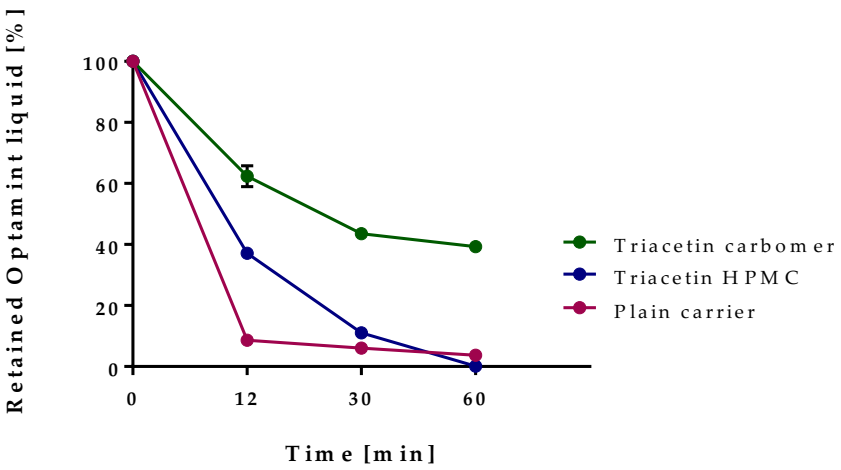

Figure 74. Long-term mucoadhesion of flavor-loaded Aeroperl 300 carrier system with 10% polymer suspended in triacetin compared to flavor-loaded Aeroperl 300 carrier system without polymer

In an overall comparison of all mucoadhesive carrier systems (Figure 75) it is evident that only formulations with carbomer and with the combination of sunflower oil and HPMC possessed good long-term effects. The effect was most pronounced for the carrier system with sunflower oil and carbomer, followed by sunflower oil and HPMC and carbomer suspended in triacetin. Flavor retention of carrier systems with a combination of HPMC and PEG 1000 or HPMC and triacetin was almost negligible already after 30 min and did not exceed the effect of the carrier system without any mucoadhesive additive. The results show that the interactions of carbomer with the mucosa are not only stronger than those of HPMC, but also persist over a longer period. Furthermore, it is demonstrated that triacetin and PEG 1000, in comparison to sunflower oil, are hindering a long-lasting mucosal adhesion effect.

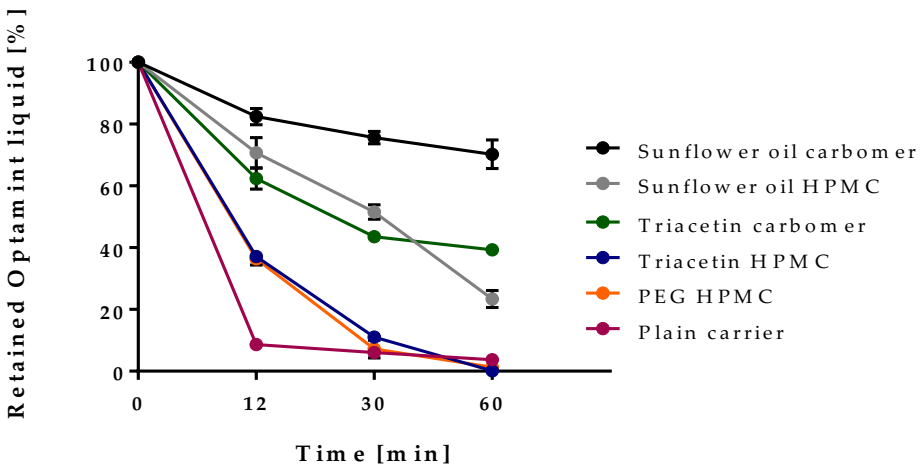

Figure 75. Long-term mucoadhesion of all prepared flavor-loaded Aeroperl 300 carrier system with 10% polymer compared to flavor-loaded Aeroperl 300 carrier system without polymer

Figure 76 shows the long-term mucoadhesion values of Aeroperl 300 and Sident 9 carrier systems with carbomer and sunflower oil. To ensure comparability, an Aeroperl 300 carrier system was tested with a polymer content of 8%, which corresponds to the maximum amount of carbomer in the Sident 9 carrier system. Both carrier systems showed a similar profile with a well sustained mucoadhesion during the whole measuring period of 60 min. In terms of the absolute amount of flavor remaining on the mucosa however, the carrier system with Aeroperl 300 was superior to that with Sident 9.

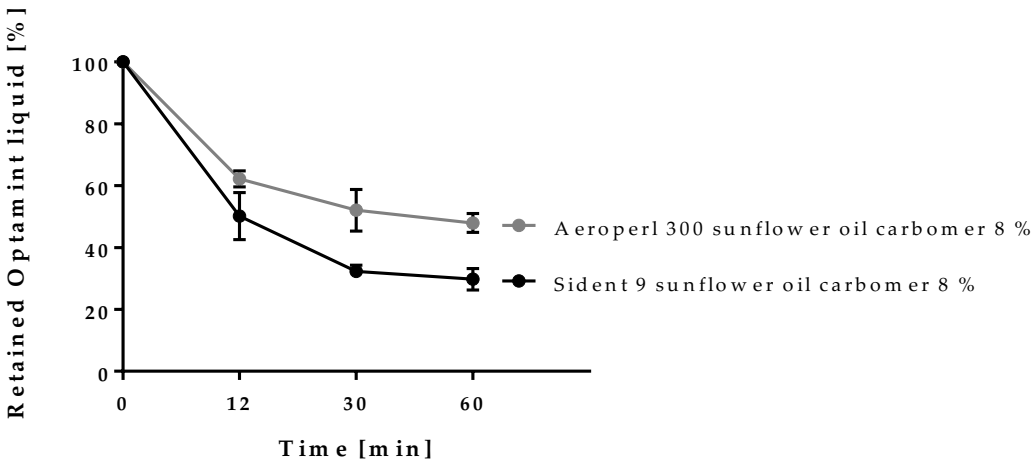

Figure 76. Long-term mucoadhesion of flavor-loaded Aeroperl 300 carrier system with sunflower oil and 8% carbomer compared to flavor-loaded Sident 9 carrier system with sunflower oil and 8% carbomer

3.1.4.6 Mucoadhesion after storage of carrier systems

To investigate the stability of the mucoadhesive properties of the carrier systems, the mucoadhesion tests were repeated after 6 months storage at room temperature. The mucoadhesive qualities were re-assessed and compared with the performance of freshly prepared carriers (Figure 77). Apart from the carrier system with Aeroperl 300, sunflower oil and carbomer, there was no substantial difference in mucoadhesion. Thus, except for this carrier, the mucoadhesive properties of the investigated carrier systems are stable over a period of 6 months. Despite the decrease, the carrier system with Aeroperl 300 and carbomer still showed high mucoadhesion of 70% after 6 months.

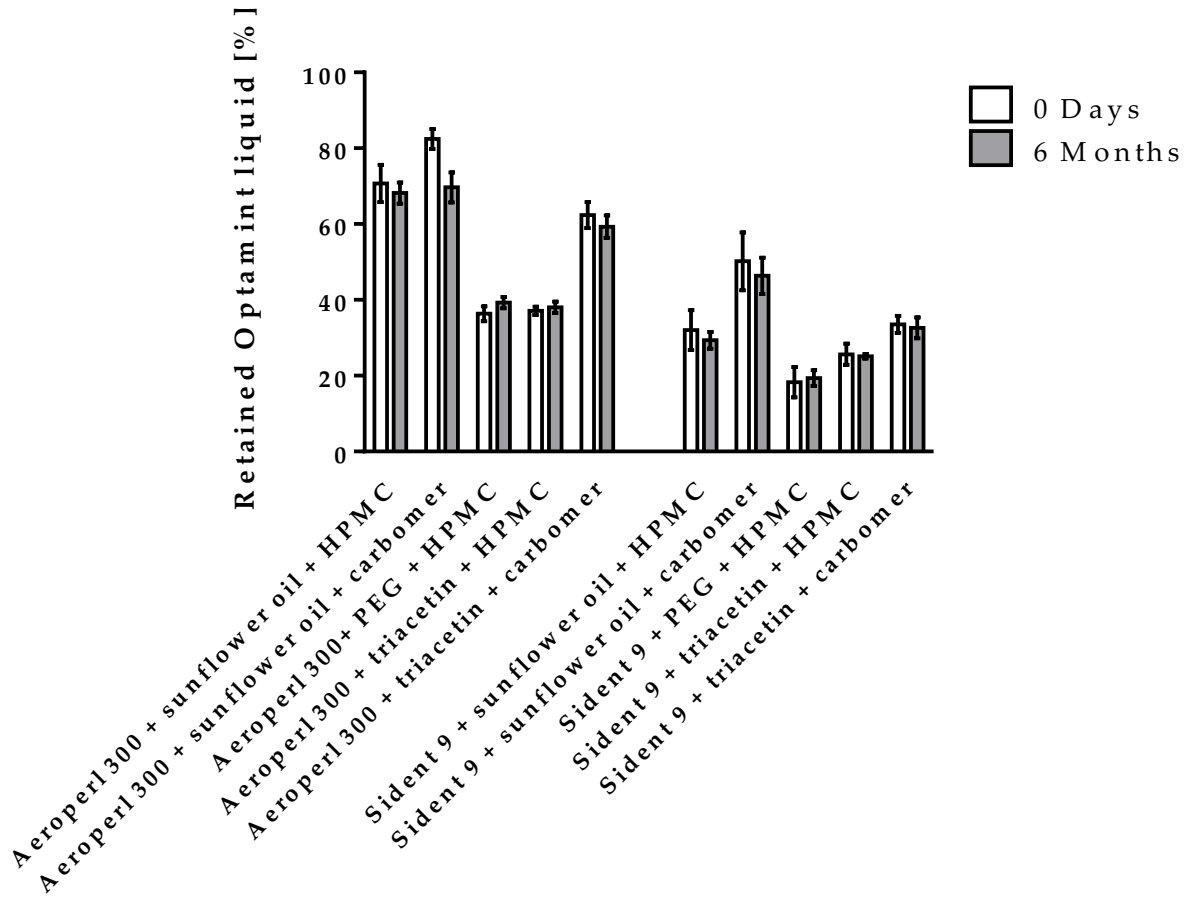

Figure 77. Mucoadhesion of different carriers and polymers directly after prepration and after 6 months storage at RT

3.1.5 Toothpastes

So far, only pure mucoadhesive carrier systems have been investigated. A possible area of application for the mucoadhesive carrier systems is the sector of oral care products, especially in the field of toothpastes. Therefore, the behavior of the mucoadhesive carrier systems in toothpastes was investigated as an application example. In addition to the mucoadhesive properties of the toothpastes, the stability of the formulations as well as the influence of different packaging material was studied. For the preparation of the toothpastes, the most promising mucoadhesive carrier systems were dispersed into a toothpaste base, which was prepared without preservative, flavor, and thickening silica to avoid excessive viscosity after incorporation of carrier loaded flavor. The mucoadhesion of the formulation and stability of the flavor during storage were tested. The incorporation of carrier systems containing carbomer resulted in an unsuitable, crumbly structure, due to the excessive swelling of the carbomer in the presence of the hydrophilic constituents of the toothpastes. For this reason, preparations with carbomer were excluded from further evaluation.

3.1.5.1 Stability studies of toothpastes

The stability studies of the prepared toothpastes in PP vessels (SpeedMixer vessels) showed a drastic loss of Optamint liquid (Figure 78, Figure 79), which was more pronounced for samples exposed to temperature cycling. On the one hand, during storage in the PP vessels the flavor substance evaporates into the large residual gas space of the container. By opening the containers for sampling this flavor fraction is released into the ambient air. As sampling was done repeatedly, flavor loss was unavoidable. Moreover, the flavor substance could migrate into the packaging material and permeate into the environment. PP is known to absorb aromatic compounds [104]. To avoid this predictable flavor loss, the stability study was paralleled using aluminum tubes instead of PP vessels as primary packaging material. Figure 80 and Figure 81 confirm that aluminum tubes can prevent the toothpastes from a relevant loss of Optamint liquid over 3 months.

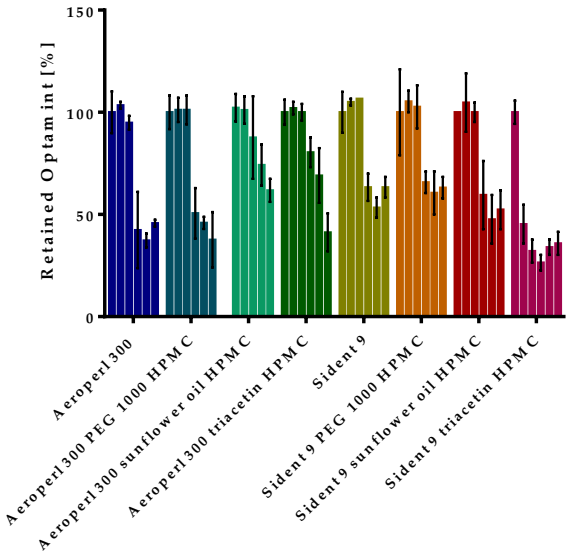

Figure 78. Flavor content of toothpaste stored in SpeedMixer vessels at RT (sampling after 0 days, 1 week, 2 weeks, 4 weeks, 8 weeks, and 12 weeks)

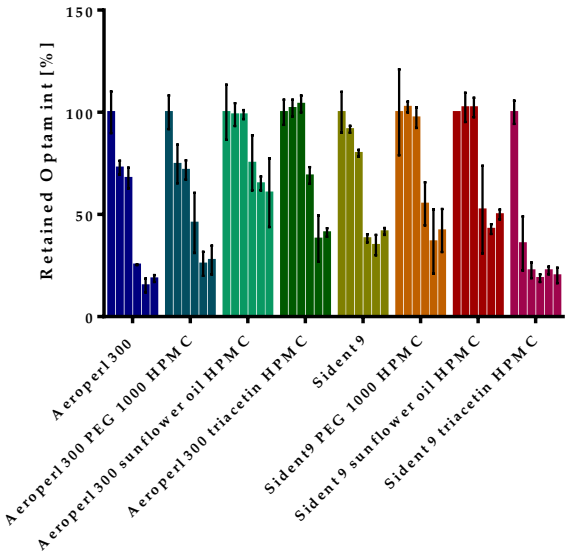

Figure 79. Flavor content of toothpaste stored in SpeedMixer vessels in TC (sampling after 0 days, 1 week, 2 weeks, 4 weeks, 8 weeks, and 12 weeks)

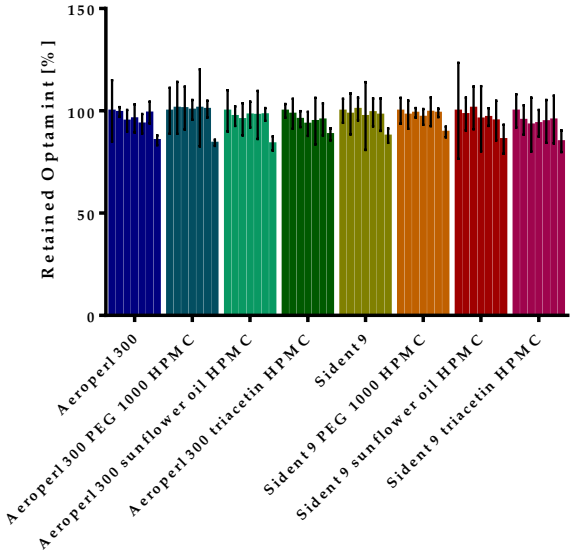

Figure 80. Flavor content of toothpaste stored in aluminum tube at RT (sampling after 0 days, 1 week, 2 weeks, 4 weeks, 8 weeks, and 12 weeks)

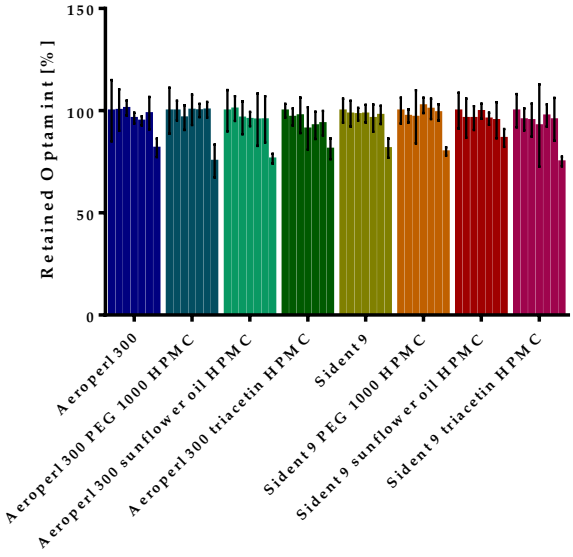

Figure 81. Flavor content of toothpaste stored in aluminum tube in TC (sampling after 0 days, 1 week, 2 weeks, 4 weeks, 8 weeks, and 12 weeks)

3.1.5.2 Mucoadhesion test of toothpastes

Figure 82 shows the mucoadhesion of Optamint liquid from toothpastes, prepared with flavor-loaded mucoadhesive carrier systems (2.2.4). These include toothpastes prepared with Aeroperl 300 carrier systems and HPMC as a mucoadhesive polymer and the corresponding Sident 9 carrier systems. Furthermore, toothpastes with a polymer-free, flavor-loaded Aeroperl 300 carrier systems and the corresponding Sident 9 carrier system, serving as reference toothpastes, were tested. The incorporation of mucoadhesive carrier systems based on Aeroperl 300 yielded increased mucoadhesion values compared to the reference toothpaste. Toothpaste with a carrier system consisting of Aeroperl 300, sunflower oil and HPMC exhibited most pronounced retention of Optamint liquid on the mucosa, followed by toothpaste with Aeroperl 300, triacetin and HPMC. The mucoadhesion values for toothpastes with mucoadhesive carrier systems containing Sident 9 were only marginally higher than the reference, whereby the toothpastes with the combination of sunflower oil and HPMC thereof showed the highest adhesion.

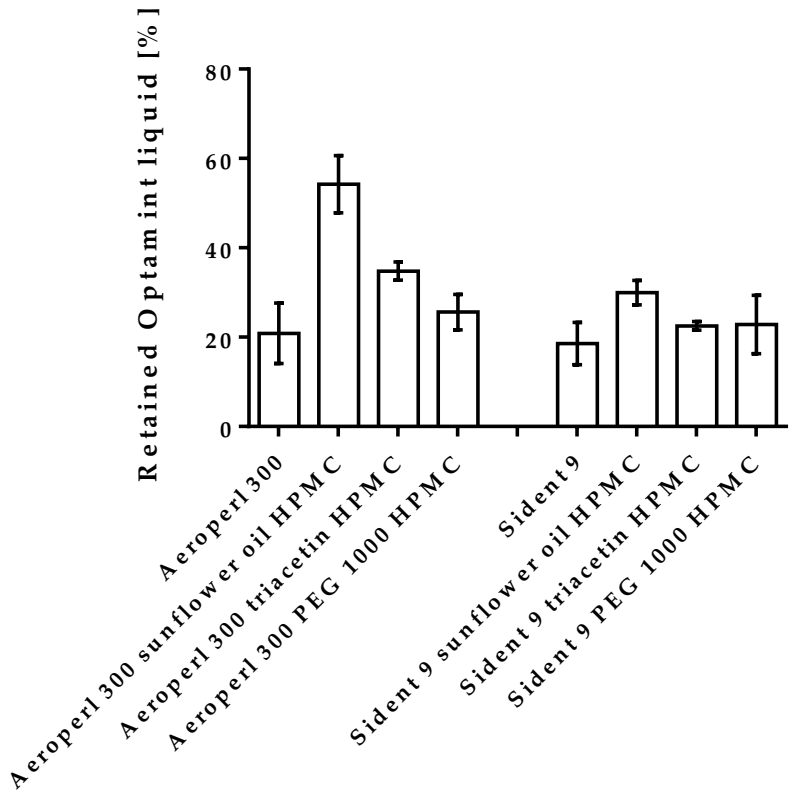

Figure 82. Mucoadhesion of toothpastes including different flavor-loaded silica with or without HPMC

In order to avoid misinterpretation of the mucoadhesion results it has to be considered that the rheological behavior of the different toothpastes varies enormously. This can be seen from

different flow points of the preparations. Regarding the results in Figure 83, toothpastes containing Aeroperl 300 exhibited predominantly a higher flow point than toothpastes with Sident 9. Toothpastes prepared with Aeroperl 300, Aeroperl 300 plus sunflower oil and HPMC and Aeroperl 300, PEG 1000 and HPMC were comparable regarding their flow points. The use of triacetin as dispersion medium for HPMC resulted in significantly low flow point of the toothpaste. For toothpastes with Sident 9 the flow points were within a similar range. The flow point of toothpastes including Sident 9, sunflower oil and HPMC was slightly higher compared to toothpaste with pure Sident 9.

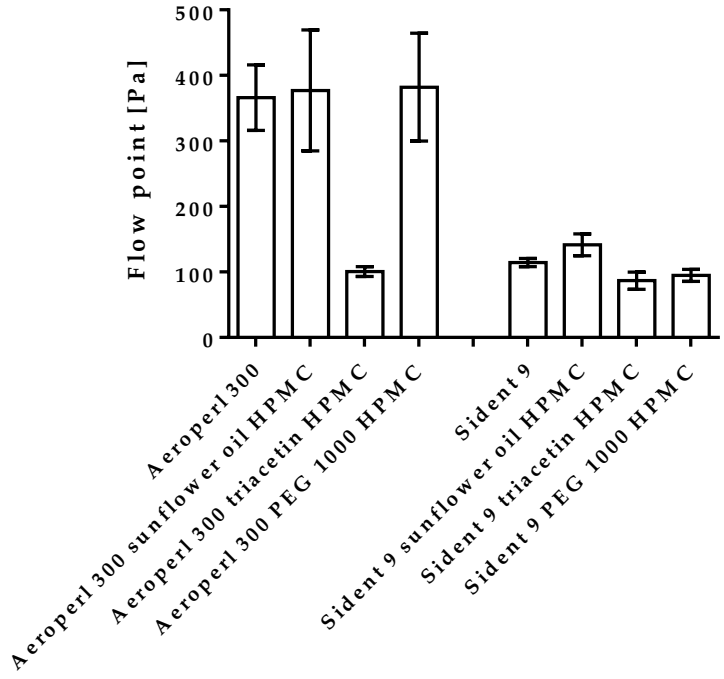

Figure 83. Flow points of toothpastes including different flavor-loaded silica with or without HPMC

Sident 9 is used as an abrasive silica in toothpastes and has only a low thickening effect in liquids [105]. Aeroperl 300 on the contrary is an effective thickening agent. Figure 84 shows the flow points of Aeroperl 300 and Sident 9 suspended in water. A 19.38% suspension of Sident 9 exhibited a comparable flow point as an 8.80% suspension of Aeroperl 300. Meaning that less than half of the concentration of Aeroperl 300 is necessary to obtain a similar viscosity compared to Sident 9. An explanation for the more pronounced viscosity properties of Aeroperl 300 could be a greater external surface area associated with an increased number of silanol groups to form a gel network. Through interparticle hydrogen bonds by the silanol groups on its outer surface, colloidal silica is able to form a three-dimensional particulate network and hence increase the viscosity through gel formation. Hereby the viscosity

increasing effect of Aeroperl 300 in the prepared toothpastes can be explained. Except for the toothpaste containing Aeroperl 300 and triacetin, all toothpastes containing Aeroperl 300 revealed higher flow points than those containing Sident 9. The remarkably low flow point of the toothpaste formulated with Aeroperl 300 and triacetin may be attributable to interference of triacetin with the network structure of Aeroperl 300. Since the formation of a gel network is not as pronounced for Sident 9 as for Aeroperl 300, the effect of triacetin on viscosity is also not as distinctive in the Sident 9 toothpaste.

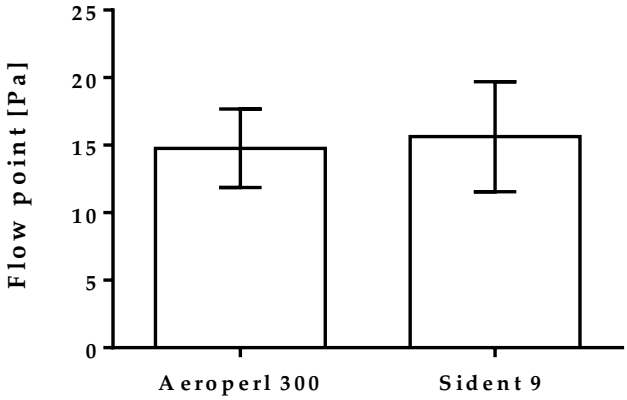

Figure 84. Flow points of 8.80% Aeroperl 300 and 19.38% Sident 9 dispersed in water

Considering the mucoadhesion results in relation to the flow points, the following conclusions can be drawn. The increased mucoadhesion of toothpastes with Aeroperl 300 and HPMC can be clearly attributed to the specific interaction of the polymer with the mucosa. It is not due to an effect on the viscosity, because the flow points of the toothpastes with mucoadhesive carrier system were equivalent or inferior to that of the reference. The enhanced mucoadhesion of toothpastes with Sident 9 and sunflower oil compared to the other Sident 9 formulations might be at least partially attributed to its higher viscosity.

3.1.6 Flavor-loaded carrier systems - Interim conclusion

Based on the results from loading experiments with thymol, the melt method and the incipient wetness method were effective in loading thymol as a model compound into porous silica carriers. By using no or only a limited amount of solvent, the loading methods minimized loss of volatiles during the loading process. For the incipient wetness method, a high initial drug concentration and a low drug-to-carrier ratio was favorable for the loading efficiency. Through the loading process, an amorphous state of the active and a high surface area were generated, which enabled a rapid release from the carrier.

The results obtained with thymol as a model flavor could be transferred to loading with Optamint for the incipient wetness method. For all three investigated silica carriers (Aeroperl 300, Sident 9 and Sident 22s) comparable loading efficiencies of Optamint liquid were achieved. The DSC measurements however revealed that the loading capacity, defined as the maximum amount of flavor that can be deposited in an amorphous state to the silica carrier, was dependent on the type of silica used. The decisive factor for a high loading capacity was a large surface area and pore volume allowing a large amount of flavor to be bound. Therefore, Aeroperl 300, with the largest surface area and the largest pore volume proved to be superior to the other two silica carriers, exhibiting the highest loading capacity. If the respective loading capacity of the silica was not exceeded, the carrier systems loaded with Optamint liquid were stable for 6 months storage, even under temperature cycling in the range of -5 to 40 °C.

The release profiles of the carrier systems and the adhesion of the flavors to the mucosa were evaluated by means of an ex vivo mucoadhesion test system with porcine mucosa. The results of the flavor-loaded silica carriers revealed increased adhesion of the flavor on mucosa compared to the adhesion of pure flavor. Mucoadhesion was even further increased by coating flavor-loaded Aeroperl 300 carrier system with HPMC as a mucoadhesive polymer. Introducing HPMC via a suspension of sunflower oil or triacetin into the flavor-loaded carrier systems proved to be an effective strategy for mucoadhesive carrier systems with stable flavor content for 6 months and a prolonged availability of flavor in the oral cavity. Another approach leading to stable carrier systems and increased mucoadhesion values was the binding of the mucoadhesive polymer to the carrier system using low melting PEG 1000. For all three formulations, an increase in HPMC concentration from 4% to 10% resulted in improved mucoadhesive values. An appropriately high proportion of sunflower oil or triacetin in the carrier systems facilitated an effective coating of the surface and consequently a good distribution of the polymer. For the formulation approach with PEG 1000, the amount of PEG 1000 used was a critical parameter. An excessive amount impaired the mucoadhesion

due to interactions with the mucosa and the mucoadhesive polymer. In a direct comparison of mucoadhesive properties, the formulation with sunflower oil proved superior to the other two formulation approaches. The formulation with sunflower oil was able to achieve an 8-fold increase in mucoadhesion compared to the polymer-free reference carrier system, whereas the formulation with PEG 1000 and triacetin both achieved a 4-fold increase.

When comparing the different polymers studied, chitosan turns out to be unsuitable for achieving a desirable mucoadhesive effect. Also, carbomer seems to be incompatible for the formulation with PEG 1000, as interactions between PEG 1000 and carbomer weakened the mucoadhesion performance. For the formulations with sunflower oil and triacetin, however, carbomer performed as the strongest mucoadhesive polymer. Formulations with sunflower oil and carbomer allowed a 10-fold enhancement of flavor retention on the mucosa compared to the reference carrier and offered the best results out of all mucoadhesive polymers and of all formulation approaches.

The results of the mucoadhesion kinetic studies revealed that mucoadhesive carrier systems prepared with carbomer as the mucoadhesive polymer were superior not only regarding the intensity of mucoadhesion but also with respect to the duration of the effect. Carrier systems composed of Aeroperl 300 and a suspension of carbomer and sunflower oil were able to maintain high mucoadhesion values of over 70% for 60 min. The long-term effect of carrier systems with Aeroperl 300, HPMC and sunflower oil or carbomer and triacetin was moderate, whereas carrier systems produced with a combination of triacetin and HPMC or PEG 1000 and HPMC did not show any substantial mucoadhesive effect over a longer period of time.

The approach of formulating mucoadhesive carrier systems with Sident 9 instead of Aeroperl 300 resulted in flavor-loaded carrier systems with excellent stability behavior for the investigated 6 months period. In terms of mucoadhesion, carrier systems with Aeroperl 300 displayed a clear superiority. This inferiority of the Sident 9 carrier was attributable to its significantly smaller surface area and pore volume, associated with a lower adsorption capacity for the polymer suspension respectively for PEG 1000. An optimal mucoadhesive effect for Sident 9 carrier systems was obtained with the combination of sunflower oil and carbomer, similarly to Aeroperl 300.

In addition to the stability of the flavor content, the mucoadhesive carrier systems also revealed stability in terms of the mucoadhesive performance. All obtained mucosal adhesion values of the formulated carrier systems remained unchanged or in case of the combination of sunflower oil and carbomer only slightly deteriorated over a storage period of 6 months.

The flavoring agent did not appear to have an influence on the performance of the mucoadhesive carrier systems, as the results for carrier systems with Optamint solid were

identical in terms of loading capacity, stability, release and mucoadhesion to those for Optamint liquid.

As an application example, the mucoadhesive carrier systems were incorporated into a toothpaste base. In terms of consistency, carbomer was not suitable as a mucoadhesive additive. Flavor loss from the toothpastes produced with the mucoadhesive carrier systems was highly affected by the primary packing material. In contrast to polypropylene jars, aluminum tubes allowed at least 3 months storage without flavor loss. Toothpastes produced with mucoadhesive carrier systems containing Aeroperl 300 exhibited higher mucoadhesion values in comparison to the reference toothpaste. With up to 3 times higher mucoadhesion than the reference product, the formulation consisting of Aeroperl 300, sunflower oil and HPMC showed the best mucoadhesion value. Among the toothpaste composed of Sident 9 carrier systems, the formulation with sunflower oil and HPMC also achieved the best results in the mucoadhesion test. However, the mucoadhesion values for this formulation were only marginally higher than those of the corresponding reference toothpaste.

Overall, different aspects of preparation and characterization of mucoadhesive carrier systems have been addressed in the experiments and the results proved that the approach of coating flavor-loaded silica with a mucoadhesive polymer is an effective strategy to prolong the residence time of flavor in the oral cavity. In addition to the high and long-lasting mucoadhesion of the flavoring agent on the mucosa, the developed mucoadhesive carrier systems showed excellent storage stability. The transferability of the developed concept to real applications has been verified exemplarily with the incorporation of the mucoadhesive carrier bound Optamint liquid flavor into a toothpaste.

3.2 CBD-loaded carrier systems

3.2.1 CBD loaded silica carrier systems

CBD was used as a model drug to assess whether the formulation approaches of the flavor-loaded mucoadhesive delivery systems can be transferred to API-loaded carrier systems. From the previous results, it was evident that Aeroperl 300 was superior to the two Sident silica grades in terms of loading capacity and mucoadhesion. To this end, the loading of CBD into the mesoporous silica Aeroperl 300 was investigated.

3.2.1.1 Loading of CBD

Based on the results from chapter 3.1.3.1, the incipient wetness method and the melt method were utilized for loading CBD onto Aeroperl 300 (2.2.2.3 Loading of CBD). Figure 85 displays the results for the incipient wetness method. Compared to the theoretical loading amount of CBD, the actual amount obtained by extraction was slightly lower, indicating a minor loss of CBD during the loading process or an incomplete recovery from the carrier. It can be seen in the diagram that the drug to carrier ratio and the concentration of the loading solution do not further reduce this difference between theoretical and actual loading. Thus, the loading efficacy could not be influenced by the variation of the two loading parameters.

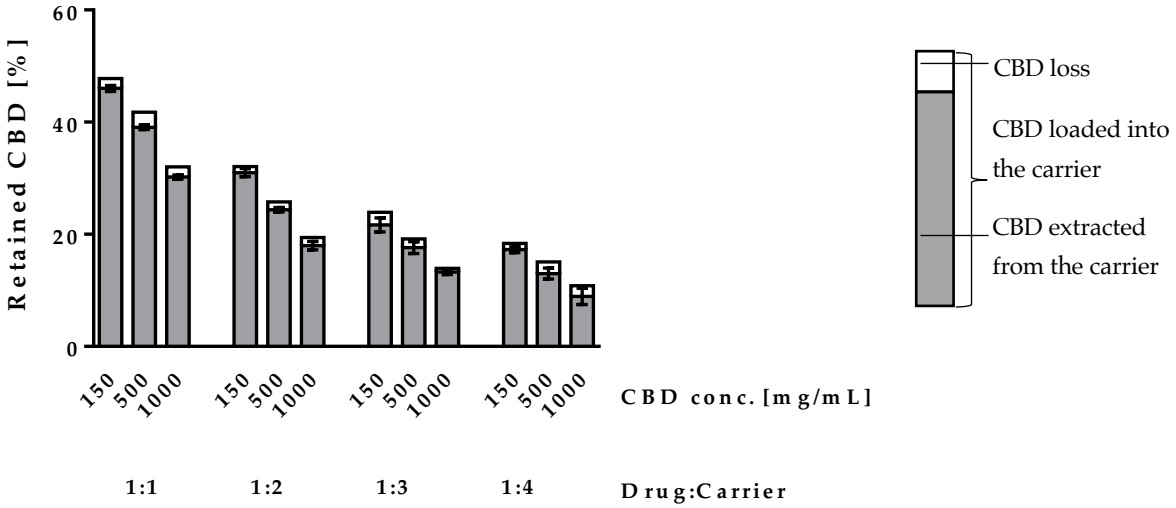

Figure 85. Influence of drug-to-carrier ratio and concentration of the loading solution on loading efficiency of CBD into Aeroperl 300 using the incipient wetness method (The entire bar represents the theoretical amount of CBD loaded into the carrier, the grey bar the actual amount that could be extracted from the loaded carrier and the white bar the loss of drug during the loading)

As with the incipient wetness method, loading by the melt method resulted in a small discrepancy between the theoretical CBD loading and the extracted amount, unaffected by different ratios of CBD to silica (Figure 86).

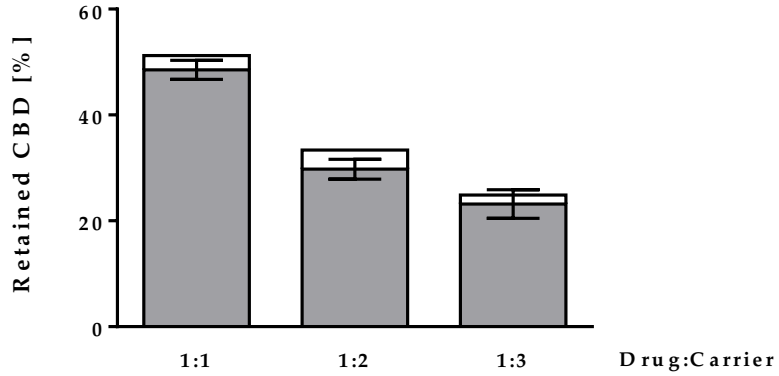

Figure 86. Influence of drug-to-carrier ratio on loading efficiency of CBD into Aeroperl 300 using the melt method

In direct comparison of the two loading methods (Figure 87), both showed comparable results, and none was superior in terms of loading efficiency.

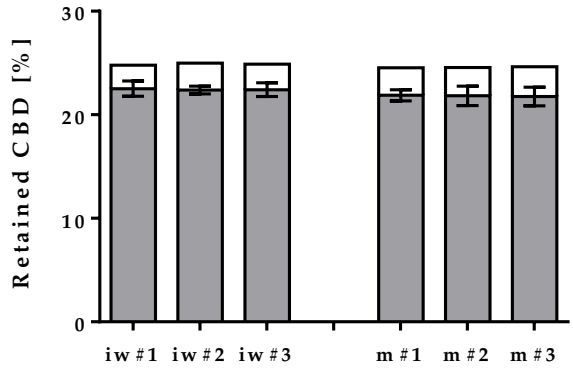

Figure 87. Comparison of different batches prepared by the incipient wetness method (iw) and melt method (m) for loading CBD into Aeroperl 300

3.2.1.2 Loading capacity

The maximum amount of CBD that can be incorporated into the mesoporous silica without crystalline CBD being present in the carrier system was determined by DSC measurements (2.2.7 Differential scanning calorimetry (DSC)) of CBD-loaded silica carrier systems with varying concentrations of CBD. To this end, the measured enthalpies of the melting points were plotted against the concentrations of CBD. and the theoretical loading capacity was calculated by the point of interception with the x-axis. With 27.25% (Figure 88) and 28.77% (Figure 89) loading capacity for the incipient wetness method and the melt method, respectively, both loading methods achieved comparable values. Thus, also with respect to the load limit no substantial difference could be established between the two loading methods. For the following experiments, the incipient wetness method was used for loading CBD owing to its greater convenience.

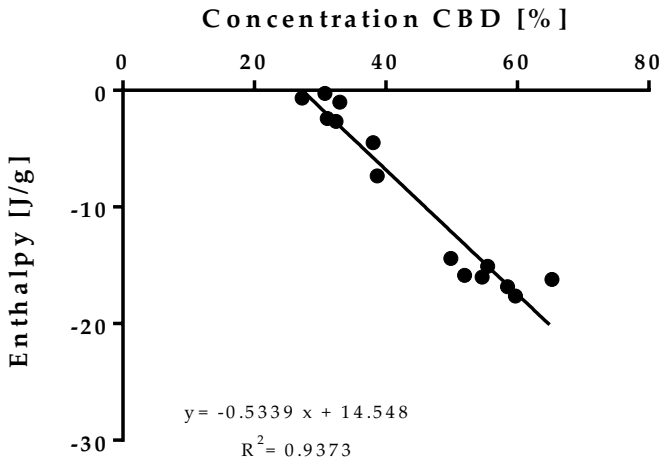

Figure 88. Concentration depended enthalpy of melting peaks of CBD loaded into Aeroperl 300 using incipient wetness method

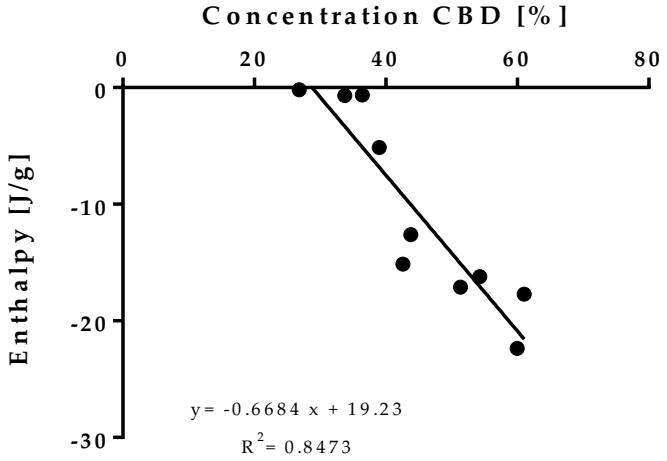

Figure 89. Concentration depended enthalpy of melting peaks of CBD loaded into Aeroperl 300 using melt method

3.2.1.3 CBD release from silica carrier systems

The dissolution profiles from the drug loaded silica carrier and pure CBD is shown in Figure 90. Noticeably, the dissolution rate of CBD from the mesoporous carrier systems was distinctly faster in comparison to the poorly soluble crystalline CBD. For the CBD-loaded silica carrier system 100% release was reached after 60 min. Whereas the poorly soluble crystalline CBD reached a value of only 40% after 120 min. This is in good accordance with the known fact that mesoporous carrier systems have the ability to enhance the dissolution properties of poorly water-soluble substances, as described in chapter 3.1.3.1 (Loading and release of thymol as a model drug).

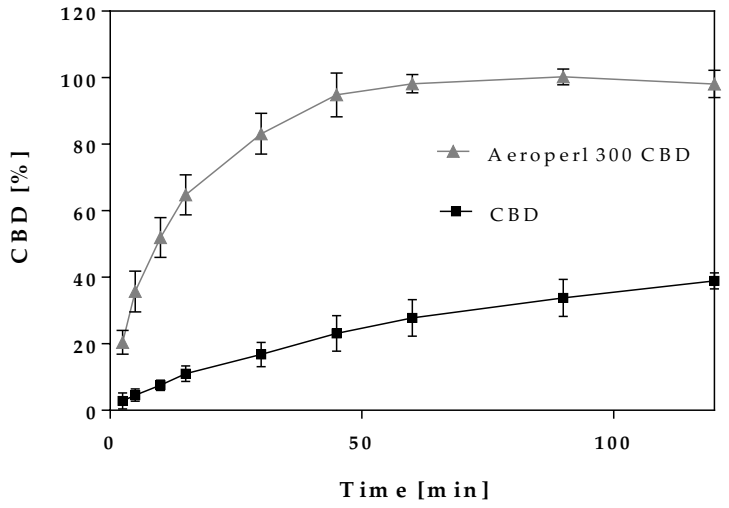

Figure 90. Comparison of dissolution profiles of pure CBD and CBD loaded onto Aeroperl 300 (Aeroperl 300 CBD)

3.2.2 CBD loaded mucoadhesive and mucopenetrating carrier systems

The presence of mucoadhesive polymers is an essential aspect in formulation of buccal drug delivery systems to prolong the residence time of active ingredients at the site of action. As polymers for the development of CBD loaded mucoadhesive delivery systems, HPMC as a nonionic, carbomer as an anionic and chitosan as a cationic mucoadhesive polymer were evaluated. The polymers were introduced into CBD-loaded Aeroperl 300 (2.2.2.3 Loading of CBD) via a suspension of sunflower oil (2.2.3.1 Coating with a polymer suspension). The concentration of the suspension was chosen to yield a final concentration of 10% HPMC or carbomer and 6% chitosan in the mucoadhesive carrier system. The final concentrations were based on the results from chapter 3.1.4.2 (Optimization of the formulation). A detailed overview with regards to the exact composition of the mucoadhesive carrier systems is reported Table 37. In addition to the mucoadhesive properties of the carrier systems, the influence of the polymers on release of CBD from the carrier systems and on penetration of CBD into the mucosa was determined.

3.2.2.1 CBD release from mucoadhesive carrier systems

The drug release profiles in artificial saliva for the mucoadhesive carrier systems compared to pure CBD and to the polymer-free carrier system are shown in Figure 91. The presence of the mucoadhesive polymers appeared to decrease the overall released amount of CBD. None of the mucoadhesive carrier systems was able to reach 100% CBD release within 120 min. Compared to the other carrier systems, the carrier systems containing carbomer exhibited the most pronounced delay with only 45% released after 120 min, followed by the carrier system with HPMC releasing approximately 60% within 120 min. The release profile obtained for the carrier system with chitosan showed a higher dissolution rate within the first 15 min compared to all other carrier systems. However, the release curve flattened rapidly thereafter and after 120 min, only about 85% CBD were released. The observed differences in the release profiles of the mucoadhesive carrier systems can be explained by the different gel-forming ability of the polymers, which slows the release rate of the drug. At the given pH of the artificial saliva (pH 6.9), chitosan possesses very poor gel-forming properties [106], which explains the comparatively higher dissolution rate. The swelling ability of carbomer is superior to those of HPMC, resulting in stronger gel formation and thus CBD encounters greater resistance to diffusion through a thick carbomer gel layer [107].

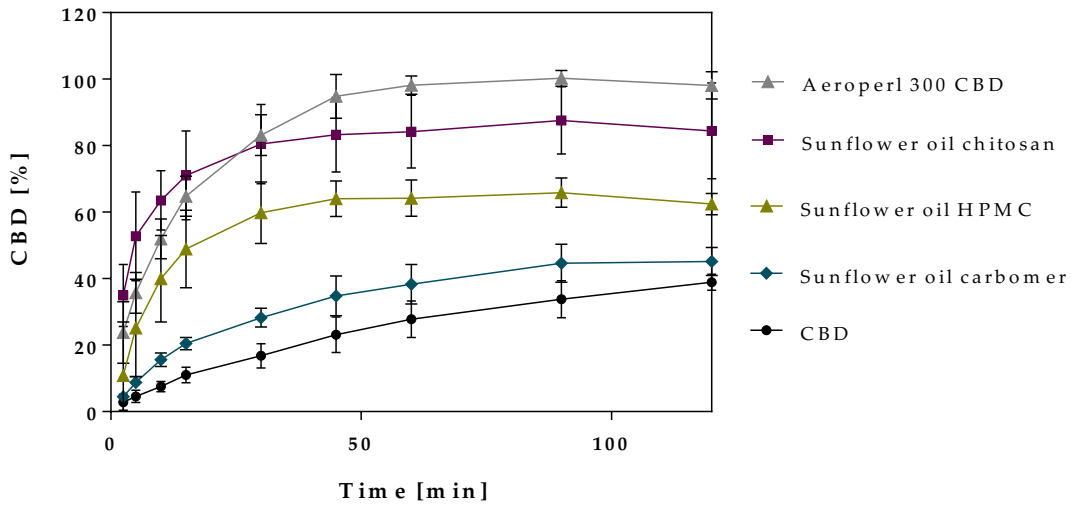

Figure 91. Comparison of dissolution profiles of CBD loaded mucoadhesive carrier systems in comparison to pure CBD and CBD loaded into Aeroperl 300 (Aeroperl 300 CBD)

Figure 92 shows the appearance of the carrier systems after 20 min the dissolution test. The images illustrate the different swelling behavior of the various carrier systems. While the particles in the polymer-free carrier system were very finely dispersed and barely detectable after 20 min, the particles in the carrier system with carbomer were already distinctively swollen. The particles of the carrier system with HPMC were less swollen than those of the carrier system with carbomer but distinctly more swollen than those of the carrier system with chitosan. Thus, the optical impression corresponds closely with the release curves obtained and the data on gel formation from the literature.

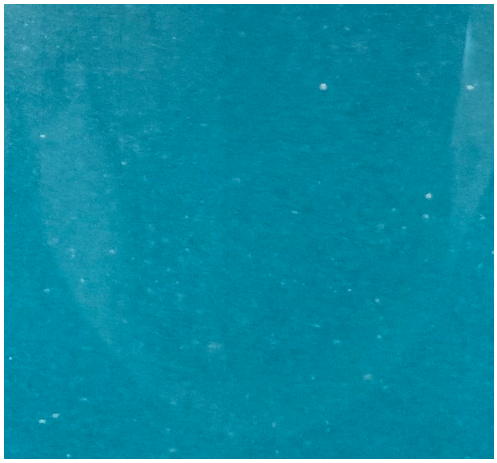

Aeroperl 300 CBD

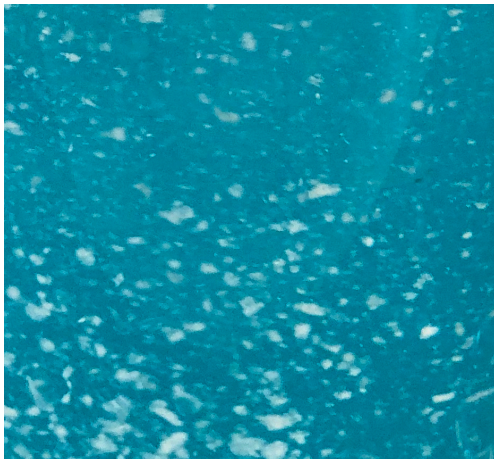

Sunflower oil carbomer

Sunflower oil chitosan

Sunflower oil HPMC

Figure 92. Representative images of CBD-loaded carrier systems after 20 min dissolution test

3.2.2.2 Mucoadhesion tests of CBD loaded mucoadhesive carrier systems

The mucoadhesion potential of the carrier systems was determined and compared with those of pure CBD and CBD incorporated in Aeroperl 300 as references. The results are shown in Table 22. Among all the carrier systems studied, the highest mucoadhesion value with approximately 80% CBD remaining on the mucosa was observed for carbomer, followed by HPMC with ca. 70% mucoadhesion and chitosan with approximately 30%. Overall, all carrier systems with a polymer addition showed considerably increased mucoadhesion compared to pure CBD. It was also shown that incorporation of CBD into Aeroperl 300, even without the addition of a mucoadhesive polymer, already resulted in an increase in the adherent fraction of CBD by more than 5-fold.

Table 22. Mucoadhesion and mucoadhesion coefficient after 12 min mucoadhesion test of

Formulation	**Mucoadhesion [%]**	**Mucoadhesion coefficient**
CBD	3.94 ± 0.85	-
Aeroperl 300 CBD (reference carrier system)	22.31 ± 1.98	1.00
Sunflower oil HPMC	62.87 ± 3.76	2.82
Sunflower oil carbomer	77.65 ± 1.10	3.48
Sunflower oil chitosan	32.82 ± 7.09	1.47

The overall obtained mucoadhesion values are in good agreement with the results for the flavor-loaded mucoadhesive carrier systems from chapter 3.1.4. Due to its intrinsic properties and the 10% loading, carbomer also proved to be the best mucoadhesive polymer for CBD loaded silica carriers.

3.2.2.2.1 Mucoadhesion kinetic

In order to study the mucoadhesion kinetic, the mucoadhesion test was extended to 60 min. The results (Figure 93) revealed that carbomer yielded both high and long-lasting mucoadhesive effects. After 60 min, approximately 70% of the applied dose of CBD remained on the mucosa. The mucoadhesive properties of the carrier systems with HPMC dropped more rapidly compared to those with carbomer, but it nevertheless showed a high mucoadhesion value of 45% after 30 min and a moderate value of 33% after 60 min. Even though the mucoadhesive properties of the carrier system with chitosan were less pronounced than those of the carrier systems with the other two mucoadhesive polymers, the mucoadhesive effect was stable over a period of 60 min. After 60 min, about 20% CBD remained on the mucosa with the carrier system containing chitosan compared to approximately 10% with the carrier system without a mucoadhesive additive. The latter, exhibiting a mucoadhesion of approximately 10% after 60 min, still showed a superior mucoadhesive effect compared to pure CBD, which was almost completely flushed from the mucosa after 30 min.

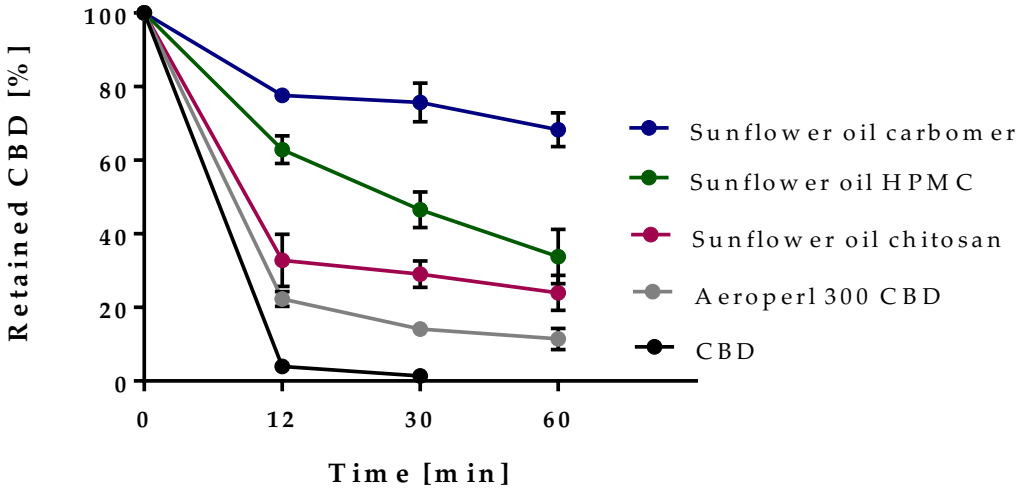

Figure 93. Long-term mucoadhesion test for CBD, CBD incorporated into Aeroperl 300 (Aeroperl 300 CBD) and the CBD-loaded mucoadhesive carrier systems with carbomer, HPMC and chitosan

3.2.2.3 Mucopenetration tests of CBD loaded mucoadhesive carrier systems

Inadequate drug passage through the buccal mucosa can be a major limitation in the administration of transmucosal drug-delivery systems [108]. Therefore, the amount of CBD penetrated the mucosa from the carrier systems during the mucoadhesion test was determined. The total recovery of CBD from the mucoadhesion test and penetration experiments is shown in Figure 113. Figure 94 illustrates the amount of CBD that penetrated from the carrier systems without and with added mucoadhesive polymer in comparison to pure CBD as a reference. It is noteworthy that a prolonged contact time of CBD on the mucosa did not directly lead to an improved penetration. While incorporating CBD into the mesoporous Aeroperl 300 resulted in an increased amount of CBD penetrated compared to pure CBD, the additional incorporation of HPMC and carbomer reduced this effect. In the case of the carrier system with carbomer, the result of the penetration study was even inferior to the reference with pure CBD. Solely the carrier system with chitosan resulted in an increased amount of CBD in the mucosa, indicating that chitosan promotes the mucosal penetration. Compared to pure CBD, the penetrated amount for the chitosan carrier system was increased 3-fold. The increased transmucosal absorption of CBD from the silica carrier systems can be explained by the altered thermodynamic state of CBD in the mesoporous silica, which favors the penetration process [109]. The swelling behavior of the polymers HPMC and carbomer resulted in a hydrophilic gel layer which hinders diffusion of the lipophilic CBD, thus hindering the penetration of CBD into the mucosa. Carbomer forms a stronger gel compared to HPMC [107], as already evident in the release studies, which caused the comparatively lower penetration. The release studies showed that the swelling behavior of chitosan, compared to the other two polymers, did not hinder the release of CBD from the carrier in the first 15 min. On the contrary, the initial release rate is even slightly increased compared to the polymer-free silica carrier system, which may have contributed to the improved penetration.

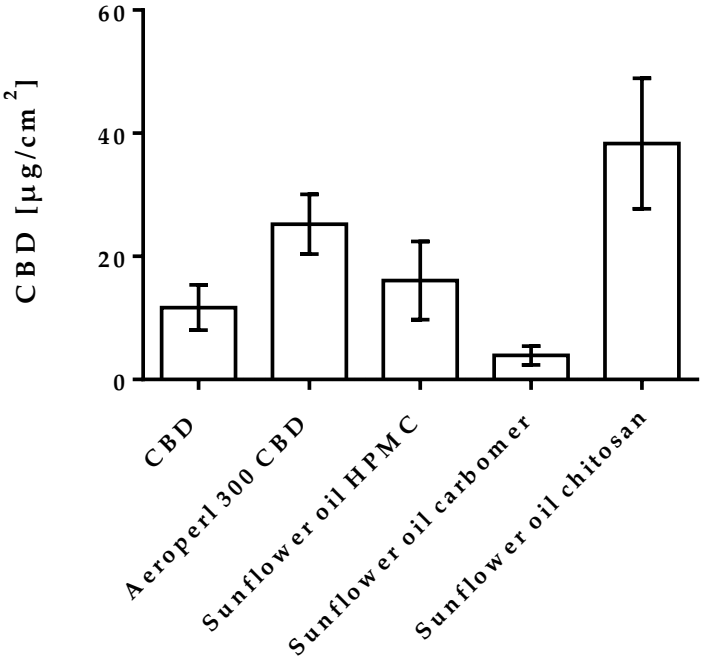

Figure 94. Penetrated amount of CBD from the mucoadhesive CBD-loaded carrier systems with HPMC, carbomer and chitosan and pure CBD and CBD incorporated into Aeroperl 300 (Aeroperl 300 CBD) as references

Figure 95 depicts the amount of CBD penetrated the mucosal tissue from the mucoadhesive carrier systems compared to pure CBD and the polymer-free carrier system as references over a period of 60 min. The results reveal that even with longer contact time of the mucoadhesive carrier systems on the mucosa, the penetrated amount of CBD increases only slightly. The increase in the penetrated amount over time for the polymer-free reference carrier and for pure CBD, on the other hand, was much more pronounced. The gel layer once formed by the polymers appears to shield CBD from the mucosa, thus hindering further penetration into the tissue.

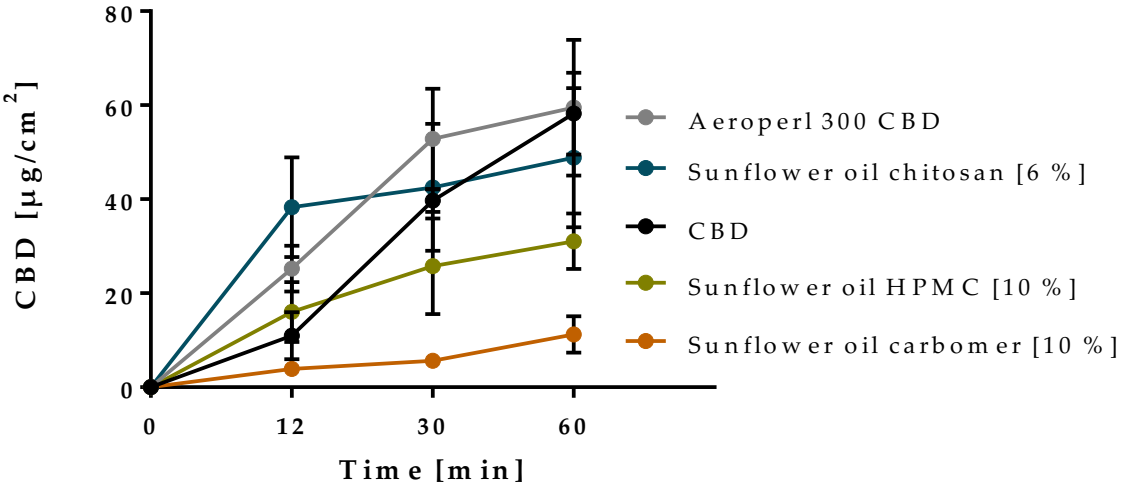

Figure 95. Kinetic of mucopenetration of CBD-loaded mucoadhesive carrier systems compared to pure CBD and to the CBD-loaded silica carrier system (Aeroperl 300 CBD) as references

3.2.2.3.1 Depth profile of CBD penetration

To assess the penetration depth of CBD, the CBD content in different layers of the mucosa was investigated, shown in Figure 96. As the first sample, the outermost layer of mucosa was removed with a section thickness of 100 µm, which corresponds to the approximate thickness of the firm mucus layer of the buccal mucosa [110]. The following samples each contained tissue with a thickness of 500 µm. The overall buccal epithelium thickness is estimated to be 500-600 µm for human mucosa and 500-800 µm for porcine mucosa [57]. Therefore, the second and the third sample comprised the tissue belonging to the epithelium. The subsequent samples consisted of the connective tissue (lamina propria and submucosa) and underlying tissue.

CBD could be extracted from all segmented layers of the mucosa. This demonstrates that CBD was able to pass the main barrier function of the epithelia layer, which is attributed to the outermost 200 µm of the mucosa [52]. The fact that CBD reached the highly vascularized, deeper layers of tissues suggests that the penetration is sufficient for a systemic effect of CBD.

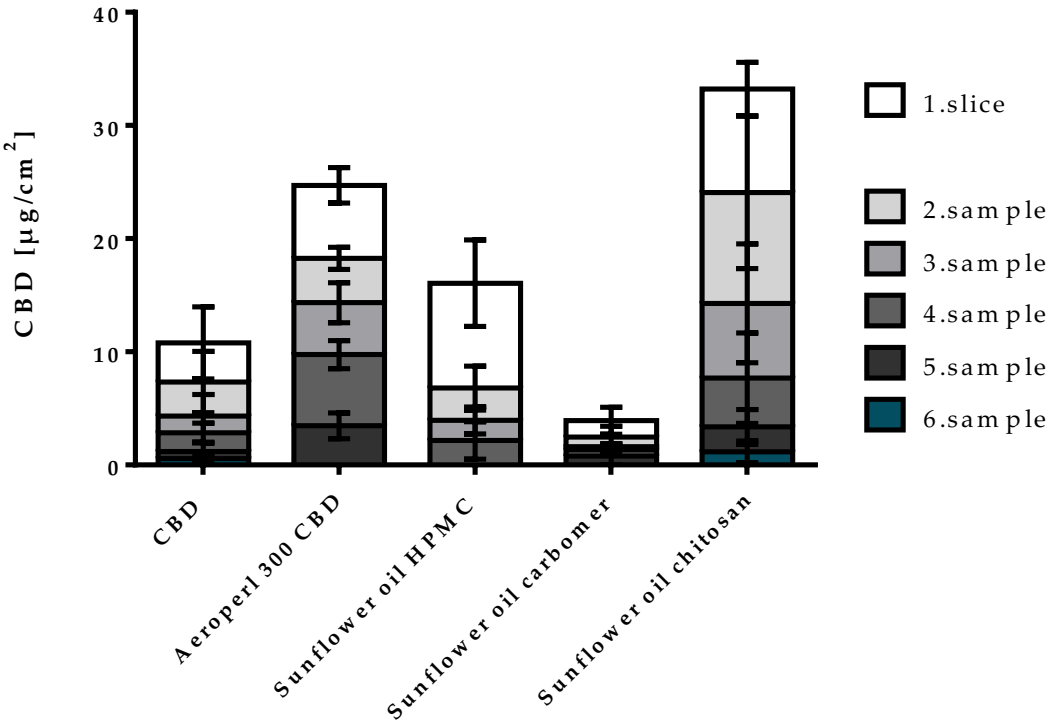

Figure 96. Depth profile of CBD penetration into the mucosa after 12 min from pure CBD, the CBD-loaded silica carrier (Aeroperl 300 CBD) and the mucoadhesive CBD-loaded carrier systems with HPMC, carbomer and chitosan

3.2.3 Mucopenetration enhancer

3.2.3.1 CBD-loaded silica carrier systems with penetration enhancers

To further improve CBD penetration, a variety of chemical substances with penetration enhancing properties were incorporated into CBD-loaded silica carriers (2.2.2.3.1 Preparation of CBD-loaded carrier systems with penetration enhancers). Propylene glycol, SLS and oleic acid were selected as additives, as they have frequently proved to be effective and orally acceptable penetration enhancers. The applied concentrations of enhancers were chosen based on data drawn from the literature [68, 111, 112]. For a detailed composition of the carrier systems, see Table 38. The impact of the enhancers on the release of CBD from the silica carriers and the amount of CBD which penetrated the mucosa was evaluated. In addition to a comparison to the enhancer-free reference carrier system, the properties were also compared to the chitosan-containing carrier system from chapter 3.2.2, as the latter had already proven to promote CBD penetration.

3.2.3.1.1 CBD release from CBD-loaded silica carrier systems with penetration enhancers

Figure 97 compares the release of CBD from the carrier systems with enhancers to the enhancer-free reference system. In the initial phase, all carrier systems with the addition of an enhancer showed a faster release rate than the reference system. Apart from the carrier system containing chitosan, all carrier systems with an enhancer achieved a release rate of 100% after approximately 30 min. Thus, a distinctly faster dissolution was accomplished compared to the enhancer-free reference carrier, where 100% release was reached after 60 min.

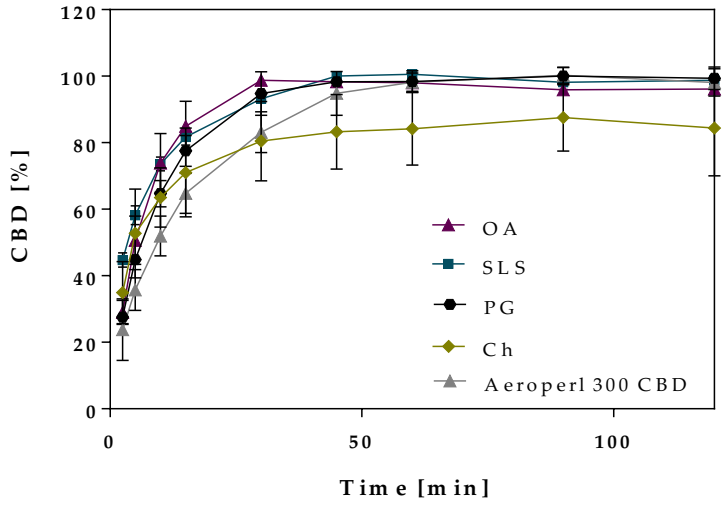

Figure 97. Comparison of dissolution profiles of CBD-loaded carrier system with 6% chitosan (Ch), 5% oleic acid (OA), 1% SLS (SLS) and 10%propylene glycol (PG) as enhancers and the enhancer-free reference carrier system (Aeroperl 300 CBD)

3.2.3.1.2 Mucopenetration test of CBD-loaded silica carrier systems with penetration enhancers

Figure 98 shows the penetrated amount of the CBD-loaded carrier systems with enhancer addition compared to the reference carrier system without enhancer. The corresponding penetration enhancement ratios are shown in Table 23. The selected enhancers increased absorption of CBD compared to the enhancer-free reference carrier system for the concentrations considered. Oleic acid and SLS both exhibited about the same penetration promoting effect with a penetration-enhancement ratio of approximately 4. Chitosan showed increased penetration over the enhancer-free carrier system, as described earlier. However, with a PE of 3, chitosan is slightly inferior to the other enhancing additives. Overall, propylene glycol showed the strongest effect with a penetration enhancement ratio of 6. Therefore, propylene glycol was selected as an enhancer in further experiments.

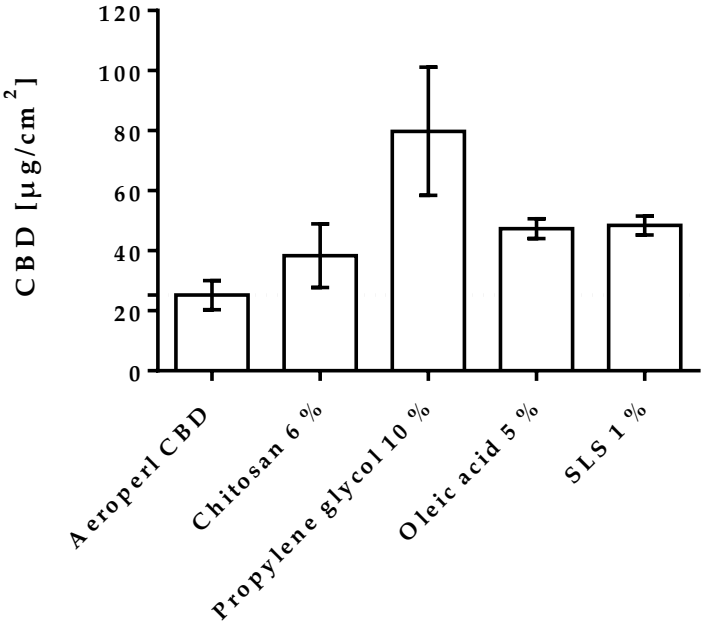

Figure 98. Mucopenetration of CBD-loaded carrier systems with chitosan, propylene glycol, oleic acid and SLS as enhancers compared to pure CBD and the enhancer-free reference carrier system (Aeroperl 300 CBD)

Table 23. Penetrated amount of CBD and PE of CBD-loaded silica carriers with chitosan, propylene glycol, oleic acid and SLS as enhancers compared to pure CBD and the enhancer-free reference carrier system (Aeroperl 300 CBD)

Formulation	**Penetrated CBD [μg/ cm^2]**	**PE**
CBD	11.70 ± 3.70	1.00
Aeroperl 300 CBD	25.23 ± 4.85	2.16
Chitosan 6%	38.31 ± 10.61	3.27
Propylene glycol 10%	77.95 ± 6.44	6.66
Oleic acid 5%	47.32 ± 3.29	4.04
SLS 1%	48.40 ± 3.19	4.14

Penetration is a complex process and, in addition to the diffusion through the epithelial barrier, the state of the drug in the vehicle and its partition from the vehicle into the tissue are important in determining the mechanisms of action [69].

The addition of enhancers notably increased CBD release from the carrier system (3.2.3.1.1) as well as CBD penetration into the mucosa. This prompts the question of whether the effect of the enhancers is a result of an effect on the dosage form rather than an effect on the mucosa. However, the effect of the enhancers on the release rate did not completely coincide with their effect on penetration. In fact, the release of CBD from the carrier system with propylene glycol in the initial phase (corresponding to the 12 min testing time of the mucopenetration experiment) was lower than the release from the carrier systems with SLS and oleic acid. This is not consistent with the distinct higher effect of propylene glycol on the penetrated amount of CBD compared to the other enhancers. In addition, the volume of liquid used in the dissolution experiment, did not reflect the small amount of liquid available during the mucopenetration test. Therefore, an estimation of the penetration behavior based on the results of the dissolution study is restricted.

3.2.3.1.3 CBD loaded silica carrier systems with propylene glycol

To investigate the influence of propylene glycol on penetration, CBD-loaded silica carriers containing 2.5, 5, 10 and 20% propylene glycol relative to the total mass were prepared and assayed. The penetration results are represented in Table 24. The addition of propylene glycol resulted in an increase of the penetrated amount in all carrier systems compared to pure CBD. With 2.5% propylene glycol, the amount of CBD in the mucosa was increased by almost 3-fold compared to pure CBD. This represents only a slight increase compared to the respective CBD-loaded silica carrier without propylene glycol. By increasing the propylene glycol concentration, the penetration-promoting effect was further enhanced. As a result, the carrier system with 5% propylene glycol showed a 6-fold increase in penetration relative to pure CBD, which was also a distinct increase relative to the corresponding silica carrier system without propylene glycol. Similarly, high penetration enhancement ratios of about 6, were observed for the carrier systems with 10% and 20% propylene glycol. This indicates that 5% propylene glycol is almost sufficient for a maximum possible effect and that a further increase in concentration is not recommended.

Table 24. Penetrated amount of CBD and PE of CBD-loaded silica carriers with different amounts of propylene glycol compared to pure CBD and CBD-loaded carrier without propylene glycol (Aeroperl 300 CBD)

Formulation	Penetrated CBD [μg/ cm^2]	PE- ratio
CBD	11.70 ± 3.70	1.00
Aeroperl 300 CBD	25.23 ± 4.85	2.16
Aeroperl 300 CBD 2.5% Propylene glycol	34.01 ± 8.90	2.91
Aeroperl 300 CBD 5% Propylene glycol	70.47 ± 15.63	6.02
Aeroperl 300 CBD 10% Propylene glycol	72.99 ± 11.78	6.24
Aeroperl 300 CBD 20% Propylene glycol	77.95 ± 6.44	6.66

The positive effect of propylene glycol might be attributed to an altered physical state of CBD after loading into the mesoporous silica. Concerning this, different mixtures of CBD and propylene glycol were first dissolved in ethanol and examined microscopically and by DSC after ethanol was evaporated. The mixtures contained propylene glycol and CBD in ratios of 1:4, 1:3; 1:2 and 1:1, corresponding to the ratios of propylene glycol and CBD in the carrier systems studied with 2.5, 5, 10 and 20% propylene glycol. In the microscopic images (Figure 99), crystals of CBD were clearly visible for the mixtures with the lower concentrations of propylene glycol (ratio 1:4, 1:3 and 1:2), indicating that these concentrations of propylene glycol were not sufficient to completely dissolve the respective amount of CBD. At a ratio of 1:1, the entire CBD was dissolved in propylene glycol as no CBD crystals were microscopically detectable. The corresponding DSC thermographs display the melting events of the CBD-propylene glycol mixtures (Figure 100). Pure CBD exhibited a melting range from 66 °C to 67 °C. Comparatively, the melting events of the blends were shifted to lower temperatures, caused by the interaction of CBD with propylene glycol. While at a ratio of 1:4 the endothermic melting peak is still quite large and broad, the detected melting events became smaller as the concentration of propylene glycol increased, indicating that the crystalline fraction of CBD diminishes. The microscopic observation and the DSC measurement confirm that propylene glycol acted as a co-solvent and by increasing the concentration of propylene glycol, the dissolved fraction of CBD could be increased. In the respective carrier systems, however, a further increase in propylene glycol above a concentration of 5% did not result in an enhanced penetration. This suggests that the penetration enhancing effect of propylene glycol is not directly linked to its action as a co-solvent in the carrier system and does not require complete dissolution of CBD. Therefore, it is likely that another effect of propylene glycol besides solubilization came into play and affected mucosal uptake of CBD.

Propylene glycol:CBD(1:4)
corresponding to 2.5% (m/m)
propylene glycol in the carrier system

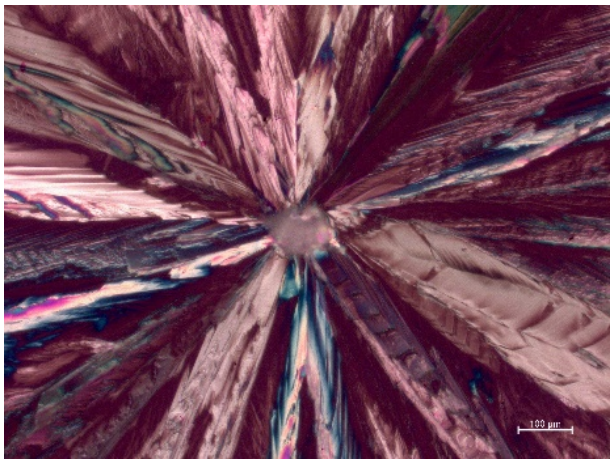

Propylene glycol:CBD (1:3)
corresponding to 5% (m/m)
propylene glycol in the carrier system

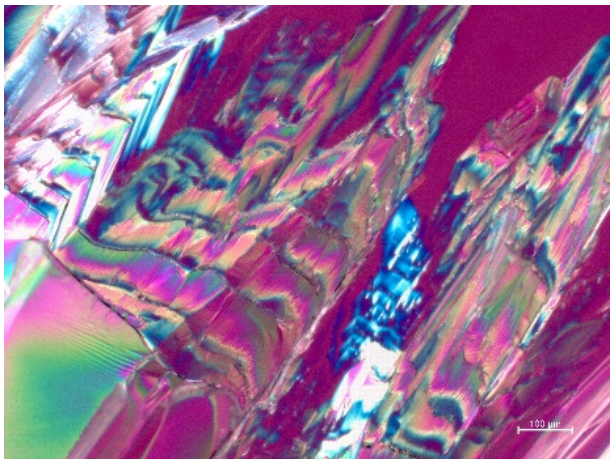

Propylene glycol:CBD (1:2)
corresponding to 10% (m/m)
propylene glycol in the carrier system

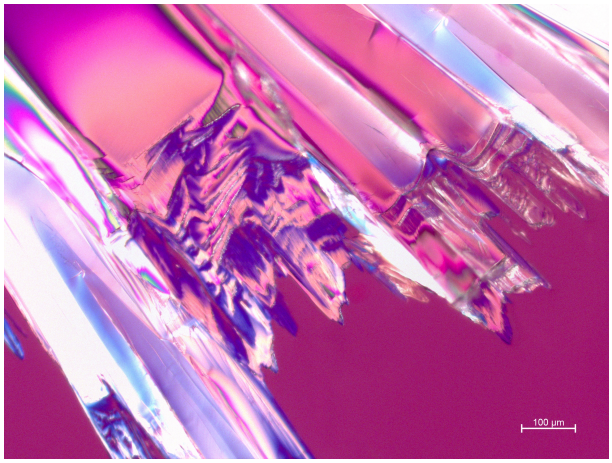

Propylene glycol:CBD (1:1)
corresponding to 20% (m/m)
propylene glycol in the carrier system

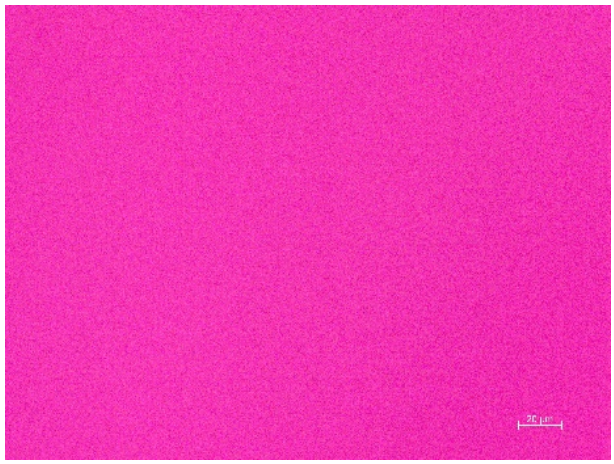

Figure 99. Microscopic images of mixtures of propylene glycol and CBD with the ratio of 1:1, 1:2, 1:3 and 1:4

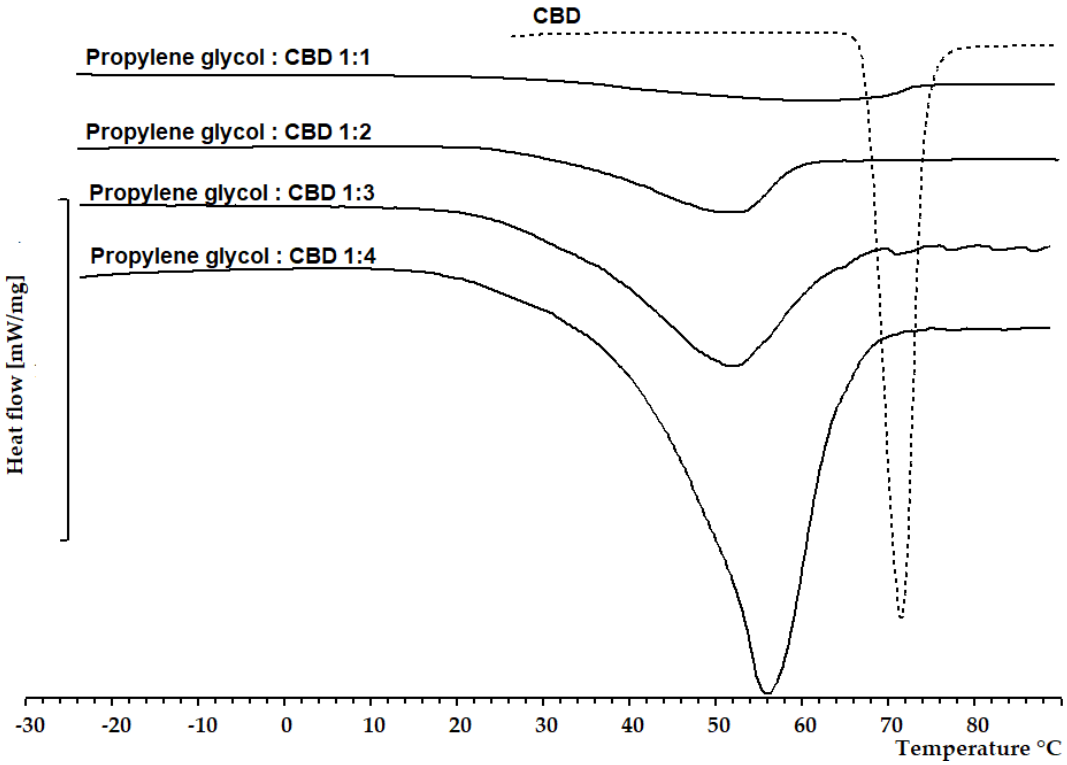

Figure 100. Comparison of DSC curves obtained by the mixture of propylene glycol and CBD with the ratio of 1:1, 1:2, 1:3 and 1:4 CBD and pure CBD

3.2.3.2 CBD loaded mucoadhesive carrier systems with propylene glycol

Mucoadhesive carrier systems were prepared with 5% propylene (Table 39) glycol to assess whether the addition of propylene glycol also has a penetration enhancing effect in the carrier systems containing a mucoadhesive polymer. Furthermore, the influence of propylene glycol on CBD release from the carrier systems and their mucoadhesive performance was investigated.

3.2.3.2.1 CBD release from mucoadhesive carrier systems with propylene glycol

The comparison of the dissolution curves between the carrier systems with propylene glycol and those without can be seen in Figure 101, Figure 102 and Figure 103. The carrier systems with HPMC and carbomer displayed a faster and higher release rate of CBD as a result of the propylene glycol addition. For the carrier system with chitosan, on the other hand, the difference between the dissolution profiles obtained with and without propylene glycol was only marginal. While the chitosan-containing carrier system already showed an increased release rate compared to the polymer-free carrier system, no further increase could be achieved by the addition of propylene glycol.

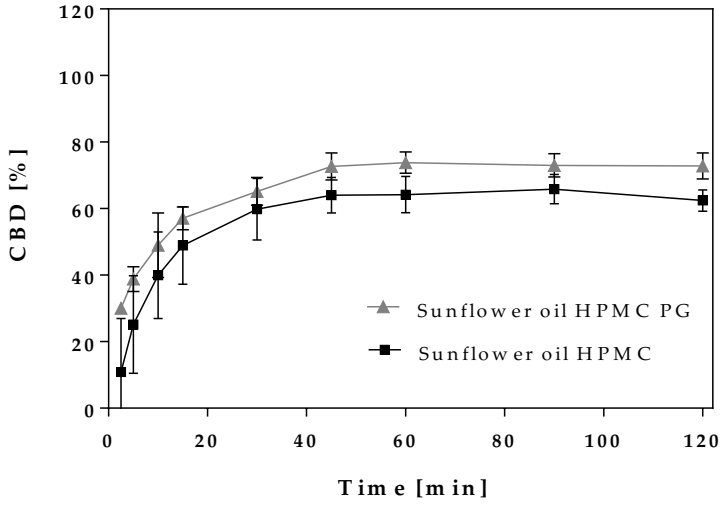

Figure 101. Comparison of the dissolution profile of the CBD-loaded mucoadhesive carrier system containing HPMC with propylene glycol and without propylene glycol

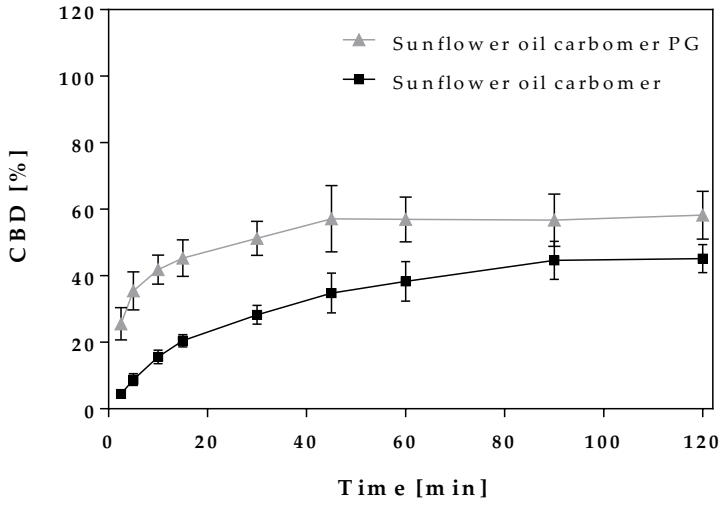

Figure 102. Comparison of the dissolution profile of the CBD-loaded mucoadhesive carrier system containing carbomer with propylene glycol and without propylene glycol

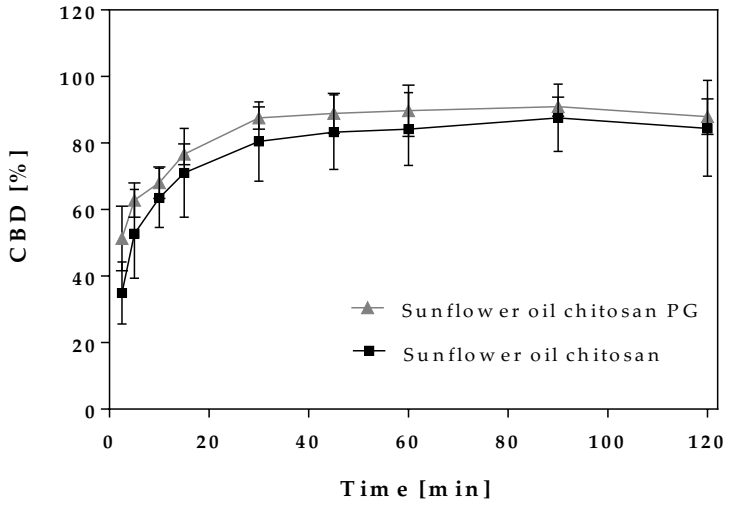

Figure 103 Comparison of the dissolution profile of the CBD-loaded mucoadhesive carrier system containing chitosan with propylene glycol and without propylene glycol

3.2.3.2.2 Mucoadhesion test of CBD loaded mucoadhesive carrier systems with propylene glycol

Figure 104 illustrates the results of the mucoadhesion tests of the carrier systems with propylene glycol (a). By direct comparison with the mucoadhesion values of the carrier systems without propylene glycol (b), it can be clearly seen that comparable values were achieved. The admixture of propylene glycol had no influence on the mucoadhesive properties of the carrier systems.

a)

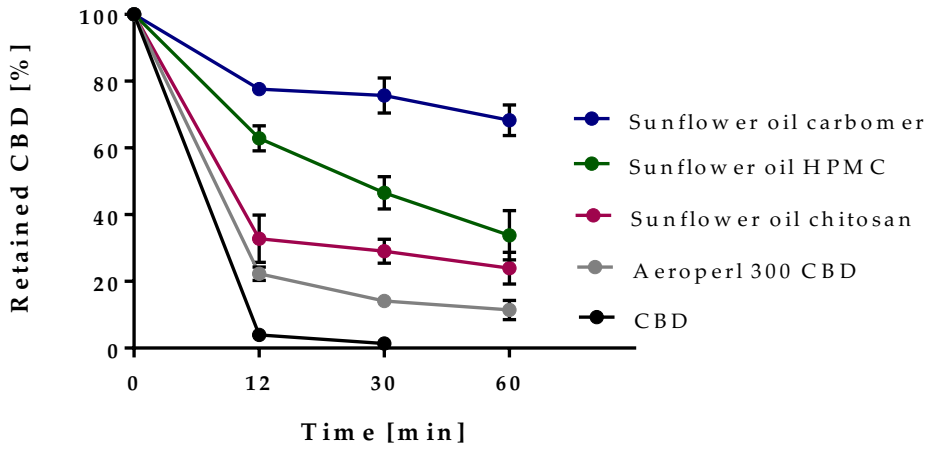

b)

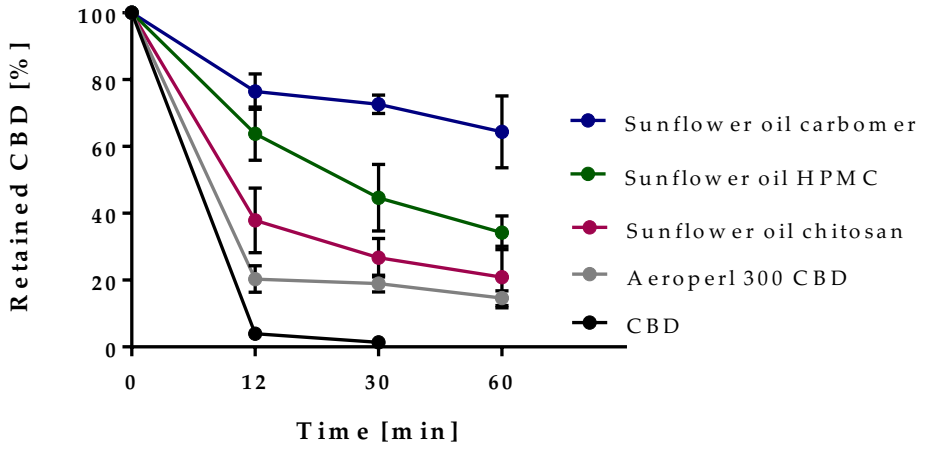

Figure 104. Comparison of long-term mucoadhesion of CBD-loaded mucoadhesive carrier systems with propylene glycol (a) and without propylene glycol (b)

3.2.3.2.3 Mucopenetration test of CBD loaded mucoadhesive carrier systems with propylene glycol

Figure 105 displays the penetrated amount of CBD from the carrier systems with and without propylene glycol. The corresponding penetration enhancement ratios are listed in Table 25. The effect of propylene glycol was most pronounced in the polymer-free carrier system, with a 6-fold increase in mucosal absorption. The addition of propylene glycol also increased penetration from carrier systems with carbomer and HPMC, although comparatively less intense. In terms of the penetration enhancement ratio, the carrier with HPMC achieved a 2-fold higher penetration value compared to pure CBD. The carrier system with carbomer showed a distinctly reduced penetration (PE 0.33) due to the polymer addition, which could be increased again to a value (PE 1.20) comparable to pure CBD by using propylene glycol as enhancer. Consequently, propylene glycol overcompensated the penetration-inhibiting effect of carbomer. However, for the carrier system with chitosan, no effect could be observed by the addition of propylene glycol. Both carrier systems, the one with and the one without propylene glycol, exhibited a penetration enhancement ratio of about 3. This suggests that the penetration enhancing effects of chitosan and propylene glycol are not additive. Moreover, these results indicate that co-solvency plays a minor role in respect to penetration enhancement of CBD.

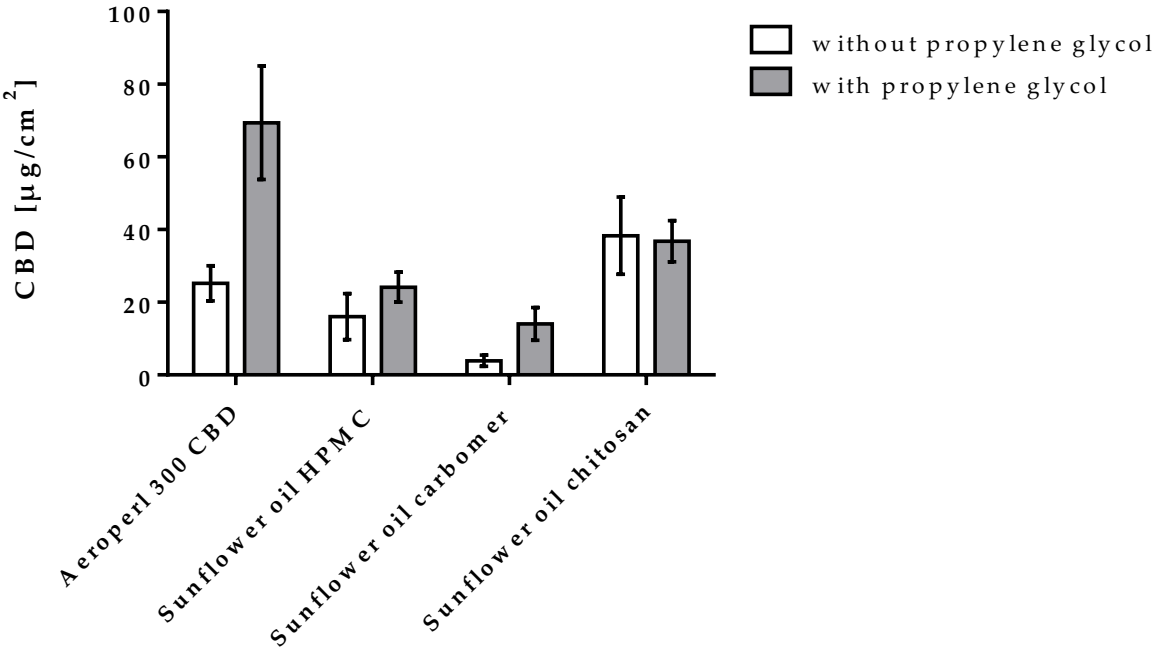

Figure 105. Comparison of the penetrated amount of CBD from CBD-loaded carrier systems with and without propylene glycol

Table 25. Comparison of penetration enhancement ratios of CBD-loaded mucoadhesive carrier systems with and without propylene glycol and pure CBD as a reference

Formulation	**without propylene glycol**		**with propylene glycol**	
	Penetrated CBD [$\mu g / cm^2$]	PE	Penetrated CBD [$\mu g / cm^2$]	PE
CBD	11.70 ± 3.70	1.00	-	-
Aeroperl 300 CBD	25.23 ± 4.85	2.16	70.47 ± 15.63	6.02
Sunflower oil HPMC	16.06 ± 6.35	1.37	24.15 ± 4.14	2.06
Sunflower oil carbomer	3.91 ± 1.54	0.33	14.06 ± 4.52	1.20
Sunflower oil chitosan	38.31 ± 10.81	3.27	36.79 ± 5.67	3.14

3.2.3.2.3.1 Depth profile of CBD penetration from CBD-loaded carrier systems with propylene glycol

Figure 106 presents the penetration of CBD from the carrier systems with propylene glycol into the different layers of the mucosa during the penetration test. For all carrier systems, a relatively uniform distribution of CBD can be observed within all investigated layers up to the last layer. Compared to the depth profile of the carrier systems without propylene glycol (Figure 96), no relevant impact of propylene glycol on the distribution of CBD in the mucosal tissue could be detected.

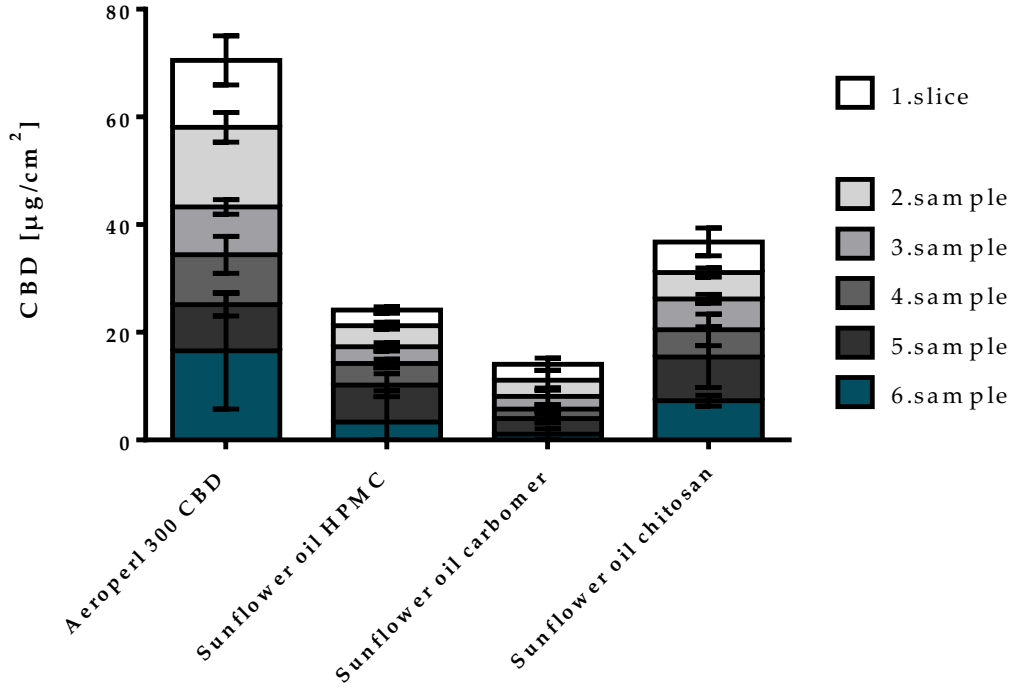

Figure 106. Depth profile of CBD penetration into the mucosa after 12 min from the propylene glycol containing CBD-loaded silica carrier (Aeroperl 300 CBD) and the propylene glycol containing mucoadhesive CBD-loaded carrier systems with HPMC, carbomer and chitosan

3.2.4 CBD-loaded carrier systems - Interim conclusion

The results confirm the transferability of the loading methods applied for flavoring agents in chapter 3 to the loading of CBD into Aeroperl 300 as a carrier system. Supplementing CBD-loaded silica carrier systems with mucoadhesive polymers from a suspension in sunflower oil proved to be an efficient strategy to prolong the residence time of CBD at the buccal mucosa and minimize drug loss due to the washing effect of saliva. Of all tested carrier systems, the one containing carbomer proved to be superior, not only regarding the intensity of mucoadhesion but also with respect to the duration of the effect. Also, HPMC and chitosan were also able to considerably improve mucoadhesion compared to pure CBD.

By loading CBD into the mesoporous silica carrier, a substantially increased penetration into the mucosa was achieved compared to pure CBD due to the altered thermodynamic activity of the active ingredient. The incorporation of the mucoadhesive polymers and the resulting improved contact of the mucoadhesive formulation with the mucosa, however, did not directly lead to improved penetration. HPMC and carbomer strongly swell upon the contact with saliva forming highly viscous hydrogels and thus hinder both the release of lipophilic CBD from the carrier system and subsequently its penetration into the mucosa. By contrast, chitosan, exhibited a penetration enhancing effect and is able to increase the absorbed amount of CBD by about 3 times compared to pure CBD. Therefore, chitosan represents a suitable and biocompatible option for the development of transbuccal delivery systems with sufficient mucoadhesive properties and improved penetration, without relying on the addition of penetration enhancers. Furthermore, the penetration experiments revealed sufficient depth of penetration required for systemic uptake of CBD for all carrier systems studied.

Incorporation of SLS, oleic acid, and propylene glycol as enhancers in CBD-loaded silica carrier systems proved beneficial for increased penetration of CBD. Of the three penetration enhancers studied, propylene glycol, with a PE of 6, attained the best mucosal absorption of CBD. Consequently, propylene glycol was investigated as an enhancer in the mucoadhesive CBD-loaded carrier systems. Except for the carrier systems with chitosan, where the addition of propylene glycol showed no further penetration enhancement, propylene glycol increased the mucosal absorption of CBD in all other carrier systems without affecting the mucoadhesive properties. In the case of the carrier system without a mucoadhesive polymer, 5% propylene glycol improved the penetrated amount by as much as 6-fold. For the carrier system with HPMC, twice the amount of CBD penetrated the buccal mucosa after adding 5% propylene glycol. Regarding the carrier system with carbomer, the addition of propylene glycol compensated the penetration hindering effect of the mucoadhesive polymer and increased the penetrated amount of CBD to a level slightly above the reference value of pure CBD.

The results of the dissolution experiments showed an increased release of CBD from the carrier systems containing the studied enhancer substances. In the case of propylene glycol, it has been demonstrated that it acts as a co-solvent for CBD. This suggests that the enhancers exert an effect on the drug in the carrier system that could contribute to the penetration-promoting effect. However, these results on their own are not sufficient to explain the penetration results obtained. Penetration of drugs into the buccal mucosa is a complex process and further research in this area is required to understand the exact mechanism of action of the enhancers.

Overall, the data obtained confirm that the approach of using CBD-loaded silica carriers and optimizing them with mucoadhesive polymers and penetration enhancers as needed is a promising strategy for the development of buccal drug delivery systems. In this way, the advantages of oromucosal route of administration can be exploited with the potential to enhance the therapeutic effects of CBD.

3.3 Flavor- and CBD-loaded carrier systems

3.3.1 Mucoadhesive carrier systems combining CBD and flavor

Comparing mucoadhesion values obtained by the different formulations of the flavor-loaded carrier systems (3.1.4 Flavor-loaded mucoadhesive carrier systems) with the corresponding CBD-loaded carrier systems (3.2.2 CBD loaded mucoadhesive and mucopenetrating carrier systems), it is noteworthy that both achieved comparable values (Figure 107). The only exceptions were the carrier systems containing chitosan as a mucoadhesive polymer. For the carrier systems with chitosan, comparatively more CBD than Optamint remained on the mucosa than Optamint. The difference may be because a different batch of chitosan was used for the series of tests with CBD than for the tests with Optamint. Nevertheless, the results suggest that the mucoadhesive properties are dependent on the formulation of the mucoadhesive carrier system and are not affected by the active loaded into the silica.

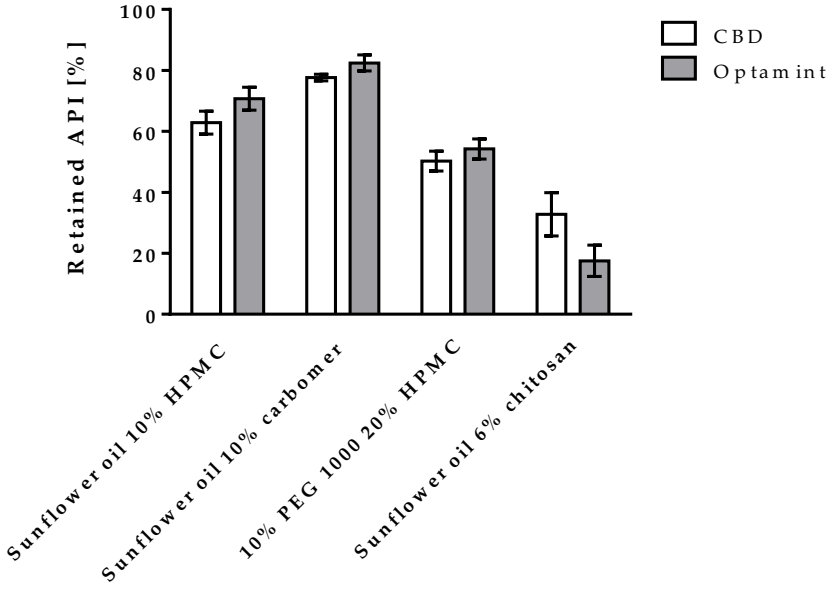

Figure 107. Comparison of the mucoadhesion values after 12 min from mucoadhesive carrier systems loaded with Optamint and CBD

Hence, the question arises whether a carrier system with a combination of flavoring agent and drug, in this case Optamint and CBD, is feasible as well. Potentially, this may be a promising approach to counteract poor-tasting APIs, as this is a critical aspect in patient compliance for oral delivery systems [113]. Therefore, Aeroperl 300 as carrier was loaded with 4% CBD and 12% Optamint as a silica carrier (2.2.2.2, 2.2.2.3) and subsequently coated with a suspension of

sunflower oil and carbomer respectively chitosan (2.2.3.1). The detailed composition of the carrier systems is listed in Table 40. Carbomer and chitosan were selected as mucoadhesive polymers to be combined with the flavored CBD-carrier, as the former achieved the strongest mucoadhesive effect and the latter provided the best combination of mucoadhesion and mucopenetration properties. The DSC curves (Figure 108) of the prepared carrier systems showed no signals indicating a phase transition, which is evidence for the molecularly dispersed state of the flavor and the CBD.

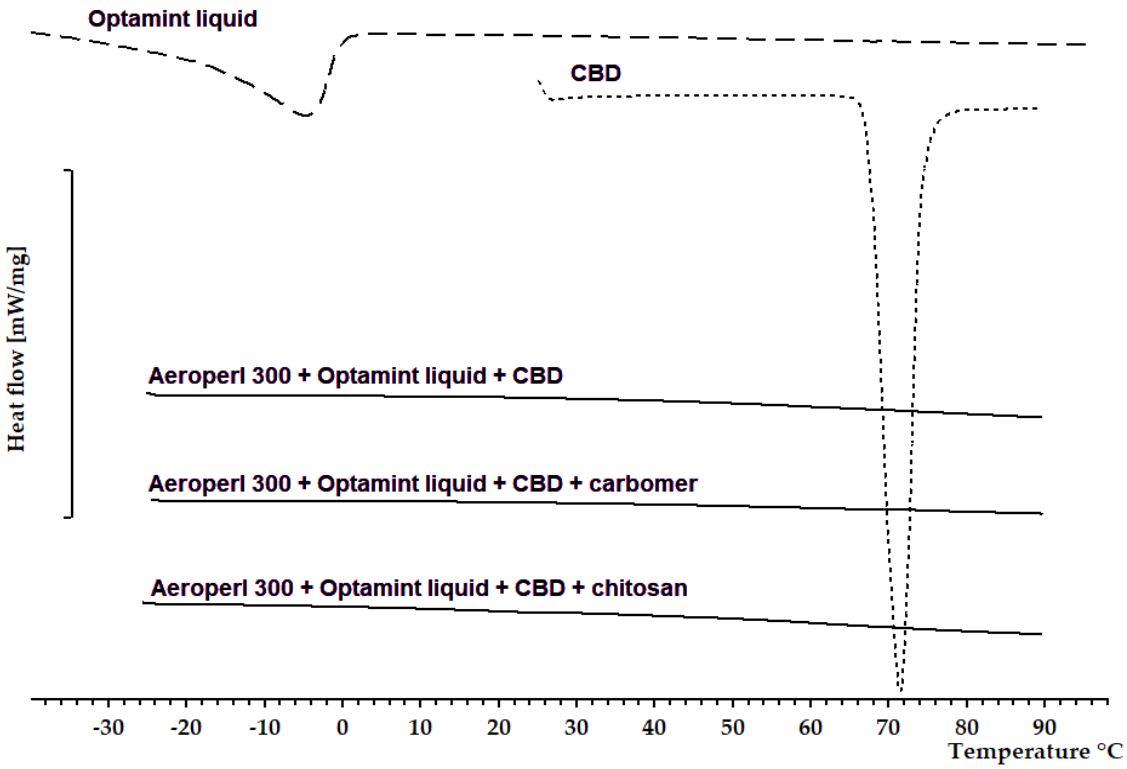

Figure 108. Comparison of DSC curves obtained by flavor-and CBD-loaded carrier systems with pure CBD and pure Optamint liquid

Results from the tests on the mucoadhesive behavior of the carrier systems with Optamint and those with the combination of Optamint and CBD were comparable (Figure 109). Only the values of the carrier systems with chitosan differ somewhat, as already referred to above.

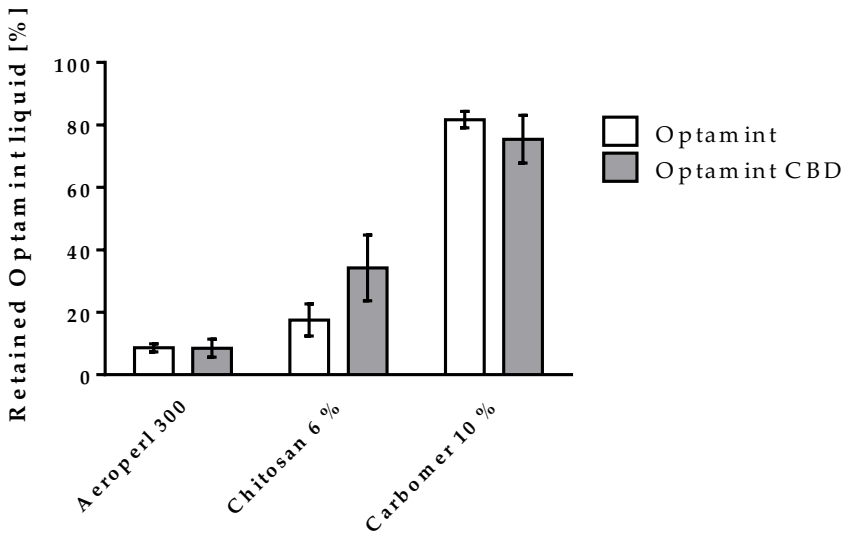

Figure 109. Comparison of the mucoadhesion values after 12 min obtained from carrier systems loaded with Optamint and with the combination of Optamint and CBD

Figure 110 compares the remaining quantity of CBD on the mucosa from the carrier systems loaded with CBD and those loaded with the combination of CBD and Optamint. Both variants of the corresponding carrier systems achieved similar to nearly identical mucoadhesion values. In this case, the mucoadhesion values of the formulations with chitosan showed a smaller difference than in the former comparisons. Since the same batch of chitosan was used for both carrier systems, these results support the assumption that the previous differences for Optamint were batch related.

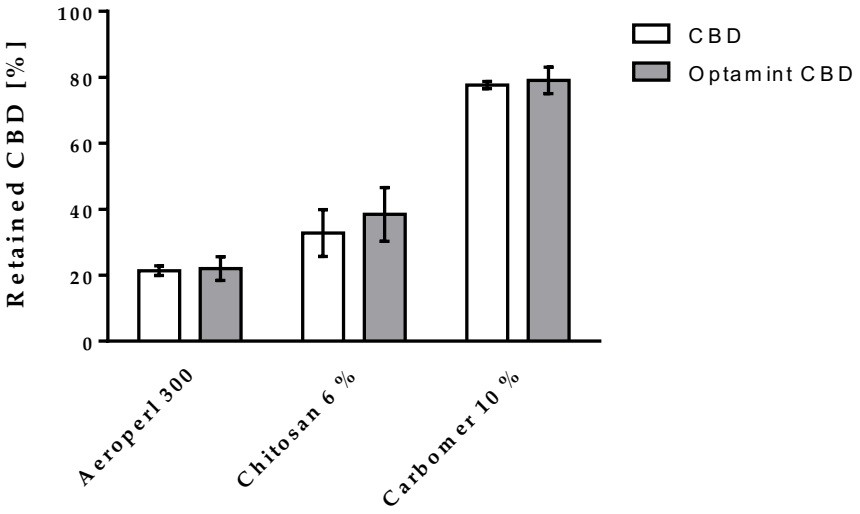

Figure 110. Comparison of the mucoadhesion values after 12 min obtained from carrier systems loaded with CBD and with the combination of Optamint and CBD

Subsequently, the amount of CBD penetrated the mucosa from the carrier systems loaded with the combination of flavor and CBD was examined. In Figure 111, these values are compared with the amount penetrated from the carrier systems loaded with CBD only. For all corresponding carrier systems, similar levels of CBD were obtained. This suggests that Optamint, at the concentration used, had no impact on the penetration of CBD.

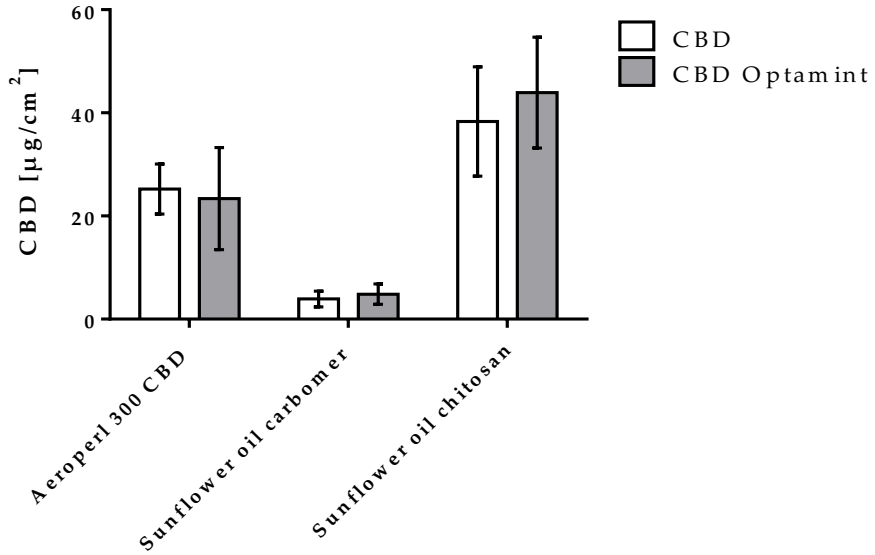

Figure 111. Comparison of the penetrated CBD from carrier systems loaded with CBD and with the combination of Optamint and CBD

3.3.1.1 Flavor- and CBD-loaded carrier system - Interim conclusion

A direct comparison of flavor-loaded mucoadhesive carrier systems with CBD-loaded mucoadhesive carrier systems revealed that similar mucoadhesion was obtained in both. Hence, it can be concluded that the mucoadhesive properties of the carrier systems are independent of the incorporated substance and are only determined by the formulation itself.

Investigation of carrier systems with a combination of CBD and Optamint proved that the combination had no impact on the mucoadhesion of the individual substances, given that both substances were fully incorporated into the carrier. Furthermore, the penetration of CBD into the buccal mucosa remained unaffected by the amount of Optamint used in the combined loaded carrier systems. Thus, this formulation approach with a combination of API and flavor represents a promising opportunity to achieve enhanced compliance in buccal dosage forms by improving the taste of poor-tasting drugs.

4 Summary and conclusion

The buccal mucosa represents an attractive site to realize both local and systemic effects. It is easily accessible and transbuccal drug delivery offers the opportunity to increase bioavailability of drugs by avoiding first-pass metabolism and intestinal drug degradation. But despite numerous advantages, it remains challenging to exploit the full potential of the buccal region. The main limitations derive from the barrier properties of the mucosa and the removal mechanism by the salivary flow in the oral cavity. Therefore, an effective buccal drug delivery formulation requires adequate adhesion and, for systemic effects, additionally sufficient mucosal penetration.

Three objectives were investigated in this work. The first one was to develop carrier systems based on a flavor-loaded porous silica and a mucoadhesive polymer. In addition to stabilizing the volatile flavor, the carrier system was intended to use mucoadhesion to prolong the effects of flavoring agents in the oral cavity. The second part of the work investigated whether the formulation approach can also be transferred to drug-loaded carrier systems. For this purpose, CBD was selected as a model API given its strong need for an alternative administration route based on its poor oral bioavailability. It was hypothesized that the mucoadhesive delivery systems would result in an extended and intimate contact with the mucosa, and thereby favor the absorption of CBD. Finally, regarding taste compliance, it was of interest to clarify whether mucoadhesive carrier systems with a combination of flavoring agent and CBD are feasible.

The results demonstrated that functionalization of flavor-loaded silica carrier systems with mucoadhesive polymers is a promising formulation approach for prolonged availability of flavors in the oral cavity. Stability studies confirmed that the volatile flavors can be stabilized by the formulations in the carrier systems for months. DSC studies revealed that the decisive factor for stability was the physical state of the flavor in the carrier system. The flavor content was stable, when the load limit of the silica was not exceeded, and the flavoring agent was completely deposited in an amorphous state to the silica carrier. The improved adhesion of the flavoring agents to the oral mucosa was evaluated by ex-vivo mucoadhesion studies. Among the tested formulations, the combination of Aeroperl 300 as the carrier material, sunflower oil as a coating medium and carbomer as the mucoadhesive polymer proved to be superior in terms of a strong and long-lasting mucoadhesive effect than other combinations. In summary, a large surface area and large pore volume of the silica proved to be desirable for the loading and coating process. The magnitude of the mucoadhesive effect was determined by the polymer concentration, the ability of the polymer to form bonds with the mucus layer, its particle size and the coating medium applied.

The prepared mucoadhesive carrier systems were successfully incorporated into toothpastes as an application example. The crucial factor here was the compatibility of the polymer with the toothpaste base. With the selection of a suitable packaging material, the toothpastes showed a good storage stability and, depending on the composition, an increased mucoadhesion compared to the reference toothpaste.

The formulation approach was successfully transferred to the development of CBD-loaded mucoadhesive carrier systems. The carrier systems minimized drug loss through salivary flow and ensured a significantly longer residence time of the API at the site of action. Yet, the ex-vivo mucopenetration test carried out with porcine mucosa showed that the improved contact did not directly lead to increased penetration. The absorption of CBD into the mucosal tissue was highly dependent on the swelling behavior of mucoadhesive polymer used. Strong polymer swelling hindered release of CBD from the carrier system and subsequently led to a reduced penetration. The polymers HPMC and carbomer were found to be superior in terms of mucoadhesion strength. However, due to strong swelling, they required the addition of a penetration enhancer, such as propylene glycol, to achieve sufficient penetration of CBD. The polymer chitosan, on the other hand, proved to be both mucoadhesive and penetration enhancing. Thus, chitosan offers the unique characteristic for the development of buccal dosage forms combining both properties necessary for adequate absorption and consequently high bioavailability.

Additionally, the results confirm that mucoadhesive carrier systems with a combination of flavor and CBD were feasible without affecting the mucoadhesive and mucopenetrating properties of the respective substances. The developed carrier systems accordingly provide the possibility to overcome compliance difficulties with poor tasting drugs.

Overall, the results of the thesis demonstrate the successful formulation of a buccal delivery system with the potential to exploit the opportunities of the buccal route for prolonged local effects and improved bioavailability through systemic delivery. Through the selection of polymers, enhancers and the addition of flavors, the characteristics of the carrier systems can be adjusted to meet the requirements for improved adhesion, absorption, and taste.

5 Indices

5.1 List of figures

Figure 1. Classification and localization of the oral mucosa [15] 4
Figure 2. Cross section through the buccal mucosa [16] 5
Figure 3. Mucoadhesion test system, AS: artificial saliva, P: pump, S: sample, Mu: mucosa, M: mucoadhesion cell, W: water bath 36
Figure 4. Temperature profile over time during the temperature cycle 38
Figure 5. SEM images of (1) Aeroperl 300, (2) Sident 9, (3) Sident 22s at different magnifications. Left: 500x magnification, right: 5000x magnification 41
Figure 6. Particle size of Aeroperl 300, Sident 9 and Sident 22s 42
Figure 7. Oil absorption capacity of Aeroperl 300, Sident 9 and Sident 22s for triacetin and sunflower oil 44
Figure 8. Absorption capacity of Aeroperl 300, Sident 9 and Sident 22s for sunflower oil with free-flowing powder as the endpoint 45
Figure 9. Absorption capacity of 100 mg Aeroperl 300, Sident 9, Sident 22s for sunflower oil with free-flowing powder as the endpoint dependent on pore volume and surface area 45
Figure 10. Comparison of loading methods for loading thymol into Aeroperl 300 (The entire bar represents the theoretical amount of thymol loaded into the carrier, the grey bar the actual amount that could be extracted from the loaded carrier and the white bar the loss of drug during the loading). 46
Figure 11. Influence of drug-to-carrier ratio and concentration of the loading solution on loading efficiency of thymol into Aeroperl 300 (The entire bar represents the theoretical amount of thymol loaded into the carrier, the grey bar the actual amount that could be extracted from the loaded carrier and the white bar the loss of drug during the loading) 48
Figure 12. Comparison of DSC curves obtained by Aeroperl 300 carriers loaded with 10, 20 and 30% thymol in contrast to pure thymol 49
Figure 13. Comparison of dissolution profiles of pure thymol and thymol loaded onto Aeroperl 300 (Aeroperl 300 Thymol) 50
Figure 14. Influence of drug-to-carrier ratio on loading efficiency of Optamint liquid into Aeroperl 300 51
Figure 15. Comparison of loading efficiency using different sample size or different machinery for loading 52

Figure 16. Loading of Optamint into different silica carriers (Aeroperl 300, Sident 9 and Sident 22s) 52
Figure 17. Comparison of DSC curves obtained by flavor-loaded carrier systems with 15% Optamint and Aeroperl 300, Sident 22s or Sident 9 53
Figure 18. Concentration depended enthalpy of melting peaks of Optamint liquid loaded into Aeroperl 300 54
Figure 19. Concentration depended enthalpy of melting peaks of Optamint liquid loaded into Sident 9 54
Figure 20. Concentration depended enthalpy of melting peaks of Optamint liquid loaded into Sident 22s 54
Figure 21. Dissolution profile of Optamint liquid from carrier systems with Aeroperl 300, Sident 9 and Sident 22s 55
Figure 22. Influence of dissolution medium on release profile of Optamint liquid from Aeroperl 300 55
Figure 23. Flavor content of Aeroperl 300 carrier systems loaded with Optamint liquid directly after loading and during storage at RT or TC 56
Figure 24. DSC curves of Aeroperl 300 carrier systems loaded with Optamint liquid directly after loading and during storage at RT or TC 56
Figure 25. Flavor content of Sident 9 carrier systems loaded with Optamint liquid directly after loading and during storage at RT or TC 57
Figure 26. DSC curves of Sident 9 carrier systems loaded with Optamint liquid directly after loading and during storage at RT or TC 57
Figure 27. Flavor content of Sident 22s carrier systems loaded with Optamint liquid directly after loading and during storage at RT or TC 58
Figure 28. DSC curves of Sident 22s carrier systems loaded with Optamint liquid directly after loading and during storage at RT or TC 58
Figure 29. Flavor content of Sident 9 carrier systems loaded with Optamint liquid exceeding the load limit directly after loading and during storage at RT or TC 59
Figure 30. DSC curves of Sident 9 carrier systems loaded with Optamint liquid exceeding the load limit directly after loading and during storage at RT or TC 59
Figure 31. Enlarged display of the DSC curve of flavor loaded Sident 9 carrier system on day 0. 60
Figure 32. Mucoadhesion test of Optamint liquid: concentration in collected saliva 61
Figure 33. Mucoadhesion test of Optamint liquid loaded into Aeroperl 300: concentration in collected saliva 61

Figure 34. Mucoadhesion of carrier systems with Optamint loaded into Aeroperl 300, Sident 9 and Sident 22s 62
Figure 35. Concentration depended enthalpy of melting peaks of Optamint solid loaded into Aeroperl 300 63
Figure 36. Flavor content of Aeroperl 300 carrier systems loaded with Optamint solid directly after loading and during storage at RT or TC 64
Figure 37. DSC curves of Aeroperl 300 carrier systems loaded with Optamint solid directly after loading and during storage at RT or TC 64
Figure 38. Dissolution profile of Optamint solid compared to Optamint liquid from carrier systems with Aeroperl 300 65
Figure 39. Comparison of mucoadhesion values from Aeroperl 300 carrier systems loaded with Optamint liquid and Optamint solid 65
Figure 40. Flavor content of formulation 1 directly after loading and during storage at room temperature or temperature cycle 67
Figure 41. DSC curves of formulation 1 directly after loading and during storage at room temperature or temperature cycle 68
Figure 42. Flavor content of formulation 2 directly after loading and during storage at RT or TC 68
Figure 43. DSC curves of formulation 2 directly after loading and during storage at RT or TC 69
Figure 44. Flavor content of formulation 3 directly after loading and during storage at RT or TC 69
Figure 45. DSC curves of formulation 3 directly after loading and during storage at RT or TC 70
Figure 46. Flavor content of formulation 4 directly after loading and during storage at RT or TC 70
Figure 47. DSC curves of formulation 4 directly after loading and during storage at RT or TC 71
Figure 48. Flavor content of formulation 5 directly after loading and during storage at RT or TC 71
Figure 49. DSC curves of formulation 5 directly after loading and during storage at RT or TC 72
Figure 50. Flavor content of formulation 6 directly after loading and during storage at RT or TC 72
Figure 51. DSC curves of formulation 6 directly after loading and during storage at RT or TC 72

Figure 52. Flavor content of formulation 7 directly after loading and during storage at RT or TC 73
Figure 53. DSC curves of formulation 7 directly after loading and during storage at RT or TC 73
Figure 54. Flavor content of formulation 8 directly after loading and during storage at RT or TC 74
Figure 55. DSC curves of formulation 8 directly after loading and during storage at RT or TC 74
Figure 56. Dissolution profile of carrier system with HPMC suspended in sunflower oil (formulation 4) 75
Figure 57. Dissolution profile of carrier system with HPMC suspended in triacetin (formulation 5) 75
Figure 58. Dissolution profile of carrier system with HPMC suspended in Optamint liquid (formulation 6) 75
Figure 59. Dissolution profile of carrier system prepared with high shear mixing (formulation 7) 75
Figure 60. Dissolution profile of carrier system with HPMC and PEG 1000 (formulation 8) 76
Figure 61. Dissolution profile of carrier systems with 4% and 10% HPMC suspended in sunflower oil compared to a carrier system without polymer 79
Figure 62. DSC measurements of flavor-loaded carrier systems with different amount of PEG 1000 82
Figure 63. Comparison of mucosa after 12 min of mucoadhesion testing of mucoadhesive carrier systems with HPMC, chitosan and carbomer 83
Figure 64. Comparison of dissolution profiles of carrier system without polymer, 10% HPMC suspended in sunflower oil, with 6% chitosan suspended in sunflower and 10% carbomer suspended in sunflower oil 84
Figure 65. Microscopic images of HPMC, carbomer and chitosan (40x magnification) 85
Figure 66. Mucosa after 12 min of mucoadhesion testing of carrier system with 10% PEG 1000 and 10% carbomer 87
Figure 67. Flavor content of Sident 9 carrier systems loaded with Optamint liquid, triacetin and HPMC directly after loading and during storage at RT or TC 88
Figure 68. DSC curves of Sident 9 carrier systems loaded with Optamint liquid, triacetin and HPMC directly after loading and during storage at RT or TC 89
Figure 69. Flavor content of Sident 9 carrier systems loaded with Optamint liquid, triacetin and carbomer directly after loading and during storage at RT or TC 89

Figure 70. DSC curves of Sident 9 carrier systems loaded with Optamint liquid, triacetin and carbomer directly after loading and during storage at RT or TC 90
Figure 71. DSC curve of PEG 1000 compared to DSC curve of carrier systems with Aeroperl 300, 10% HPMC and 10% PEG 1000 and Sident 9, 10% HPMC and 10% PEG 1000 93
Figure 72. Comparison of mucoadhesion values of Aeroperl 300 carrier system with 10% carbomer suspended in sunflower oil using Optamint liquid or Optamint solid as flavoring agent 94
Figure 73. Long-term mucoadhesion of flavor-loaded Aeroperl 300 carrier systems with 10% polymer suspended in sunflower oil compared to flavor-loaded Aeroperl 300 carrier system without polymer 95
Figure 74. Long-term mucoadhesion of flavor-loaded Aeroperl 300 carrier system with 10% polymer suspended in triacetin compared to flavor-loaded Aeroperl 300 carrier system without polymer 96
Figure 75. Long-term mucoadhesion of all prepared flavor-loaded Aeroperl 300 carrier system with 10% polymer compared to flavor-loaded Aeroperl 300 carrier system without polymer 97
Figure 76. Long-term mucoadhesion of flavor-loaded Aeroperl 300 carrier system with sunflower oil and 8% carbomer compared to flavor-loaded Sident 9 carrier system with sunflower oil and 8% carbomer 97
Figure 77. Mucoadhesion of different carriers and polymers directly after prepration and after 6 months storage at RT 98
Figure 78. Flavor content of toothpaste stored in SpeedMixer vessels at RT (sampling after 0 days, 1 week, 2 weeks, 4 weeks, 8 weeks, and 12 weeks) . 100
Figure 79. Flavor content of toothpaste stored in SpeedMixer vessels in TC (sampling after 0 days, 1 week, 2 weeks, 4 weeks, 8 weeks, and 12 weeks) . 100
Figure 80. Flavor content of toothpaste stored in aluminum tube at RT (sampling after 0 days, 1 week, 2 weeks, 4 weeks, 8 weeks, and 12 weeks) 100
Figure 81. Flavor content of toothpaste stored in aluminum tube in TC (sampling after 0 days, 1 week, 2 weeks, 4 weeks, 8 weeks, and 12 weeks) 100
Figure 82. Mucoadhesion of toothpastes including different flavor-loaded silica with or without HPMC 101
Figure 83. Flow points of toothpastes including different flavor-loaded silica with or without HPMC 102
Figure 84. Flow points of 8.80% Aeroperl 300 and 19.38% Sident 9 dispersed in water 103

Figure 85. Influence of drug-to-carrier ratio and concentration of the loading solution on loading efficiency of CBD into Aeroperl 300 using the incipient wetness method (The entire bar represents the theoretical amount of CBD loaded into the carrier, the grey bar the actual amount that could be extracted from the loaded carrier and the white bar the loss of drug during the loading)....107
Figure 86. Influence of drug-to-carrier ratio on loading efficiency of CBD into Aeroperl 300 using the melt method....108
Figure 87. Comparison of different batches prepared by the incipient wetness method (iw) and melt method (m) for loading CBD into Aeroperl 300....108
Figure 88. Concentration depended enthalpy of melting peaks of CBD loaded into Aeroperl 300 using incipient wetness method....109
Figure 89. Concentration depended enthalpy of melting peaks of CBD loaded into Aeroperl 300 using melt method....110
Figure 90. Comparison of dissolution profiles of pure CBD and CBD loaded onto Aeroperl 300 (Aeroperl 300 CBD)....111
Figure 91. Comparison of dissolution profiles of CBD loaded mucoadhesive carrier systems in comparison to pure CBD and CBD loaded into Aeroperl 300 (Aeroperl 300 CBD)....113
Figure 92. Representative images of CBD-loaded carrier systems after 20 min dissolution test....114
Figure 93. Long-term mucoadhesion test for CBD, CBD incorporated into Aeroperl 300 (Aeroperl 300 CBD) and the CBD-loaded mucoadhesive carrier systems with carbomer, HPMC and chitosan....116
Figure 94. Penetrated amount of CBD from the mucoadhesive CBD-loaded carrier systems with HPMC, carbomer and chitosan and pure CBD and CBD incorporated into Aeroperl 300 (Aeroperl 300 CBD) as references....118
Figure 95. Kinetic of mucopenetration of CBD-loaded mucoadhesive carrier systems compared to pure CBD and to the CBD-loaded silica carrier system (Aeroperl 300 CBD) as references....119
Figure 96. Depth profile of CBD penetration into the mucosa after 12 min from pure CBD, the CBD-loaded silica carrier (Aeroperl 300 CBD) and the mucoadhesive CBD-loaded carrier systems with HPMC, carbomer and chitosan....120
Figure 97. Comparison of dissolution profiles of CBD-loaded carrier system with 6% chitosan (Ch), 5% oleic acid (OA), 1% SLS (SLS) and 10%propylene glycol

(PG) as enhancers and the enhancer-free reference carrier system (Aeroperl 300 CBD) 122
Figure 98. Mucopenetration of CBD-loaded carrier systems with chitosan, propylene glycol, oleic acid and SLS as enhancers compared to pure CBD and the enhancer-free reference carrier system (Aeroperl 300 CBD) 123
Figure 99. Microscopic images of mixtures of propylene glycol and CBD with the ratio of 1:1, 1:2, 1:3 and 1:4 126
Figure 100. Comparison of DSC curves obtained by the mixture of propylene glycol and CBD with the ratio of 1:1, 1:2, 1:3 and 1:4 CBD and pure CBD 127
Figure 101. Comparison of the dissolution profile of the CBD-loaded mucoadhesive carrier system containing HPMC with propylene glycol and without propylene glycol 128
Figure 102. Comparison of the dissolution profile of the CBD-loaded mucoadhesive carrier system containing carbomer with propylene glycol and without propylene glycol 129
Figure 103 Comparison of the dissolution profile of the CBD-loaded mucoadhesive carrier system containing chitosan with propylene glycol and without propylene glycol 129
Figure 104. Comparison of long-term mucoadhesion of CBD-loaded mucoadhesive carrier systems with propylene glycol (a) and without propylene glycol (b) 130
Figure 105. Comparison of the penetrated amount of CBD from CBD-loaded carrier systems with and without propylene glycol 131
Figure 106. Depth profile of CBD penetration into the mucosa after 12 min from the propylene glycol containing CBD-loaded silica carrier (Aeroperl 300 CBD) and the propylene glycol containing mucoadhesive CBD-loaded carrier systems with HPMC, carbomer and chitosan 133
Figure 107. Comparison of the mucoadhesion values after 12 min from mucoadhesive carrier systems loaded with Optamint and CBD 136
Figure 108. Comparison of DSC curves obtained by flavor-and CBD-loaded carrier systems with pure CBD and pure Optamint liquid 137
Figure 109. Comparison of the mucoadhesion values after 12 min obtained from carrier systems loaded with Optamint and with the combination of Optamint and CBD 138
Figure 110. Comparison of the mucoadhesion values after 12 min obtained from carrier systems loaded with CBD and with the combination of Optamint and CBD 139

Figure 111. Comparison of the penetrated CBD from carrier systems loaded with CBD and with the combination of Optamint and CBD.....139
Figure 112. Recovery of Optamint liquid after 12 min mucoadhesion test of flavor-loaded silica carriers: retained concentrations of Optamint liquid in saliva and from mucosa 162
Figure 113. Recovery of CBD after 12 min from mucoadhesion tests (fraction of CBD on the mucosa and fraction flushed away by saliva) and from mucopenetration test (fraction of CBD penetrated the mucosa); PG: propylene glycol.....162

5.2 List of tables

Table 1. Overview of drug loading techniques [12, 13] 2
Table 2. Examples of oral mucosal drug delivery systems [37, 38] 7
Table 3. Examples of commercially available transbuccal drug delivery systems [37, 38, 66] 14
Table 4. Penetration enhancers used for buccal drug delivery [57] 15
Table 5. Composition of toothpaste base 32
Table 6. Composition of artificial saliva 34
Table 7. Product specification of Aeroperl 300, Sident 9 and Sident 22s (provided by manufacturer Evonik) 42
Table 8. Specific pore volume and pore diameter measured by mercury intrusion porosimetry 43
Table 9. Composition of flavor-loaded carrier systems for the mucoadhesion tests 60
Table 10. Long term mucoadhesion of carrier systems loaded with Optamint liquid ... 62
Table 11. Composition of flavor-loaded mucoadhesive carrier systems with Aeroperl 300 and HPMC 66
Table 12. Mucoadhesion results after 12 min mucoadhesion test of formulations 4-7 ... 77
Table 13. Influence of the concentration of sunflower oil and HPMC on mucoadhesion of flavor-loaded Aeroperl 300 carrier systems 79
Table 14. Influence of the concentration of triacetin and HPMC on mucoadhesion of flavor-loaded Aeroperl 300 carrier systems 80
Table 15. Influence of the concentration of PEG 1000 and HPMC on mucoadhesion 81
Table 13. Comparison of mucoadhesive performance of different polymers incorporated in Aeroperl 300 carrier systems with sunflower oil 83
Table 16. Mucoadhesion and mucoadhesive coefficients of flavor-loaded Aeroperl 300 carrier systems with triacetin and HPMC compared to triacetin and carbomer and direct comparison to flavor-loaded Aeroperl 300 carrier systems with sunflower oil and HPMC and sunflower oil and carbomer 86
Table 17. Mucoadhesive performance of carrier systems prepared with PEG 1000 and carbomer in comparison to PEG 1000 and HPMC 87
Table 18. Mucoadhesion and mucoadhesive coefficients of flavor-loaded Sident 9 carrier system with triacetin and sunflower oil as suspension medium and HPMC and carbomer as polymers 91
Table 19. Mucoadhesion and mucoadhesive coefficients of flavor-loaded mucoadhesive carrier systems with Sident 9 compared to carrier systems with Aeroperl 300 92

Table 20. Mucoadhesion of carrier system with Aeroperl 300, 10% HPMC and 10% PEG 1000 compared to Sident 9, 10% HPMC and 10% PEG 1000 93
Table 21. Mucoadhesion and mucoadhesion coefficient after 12 min mucoadhesion test of 115
Table 22. Penetrated amount of CBD and PE of CBD-loaded silica carriers with chitosan, propylene glycol, oleic acid and SLS as enhancers compared to pure CBD and the enhancer-free reference carrier system (Aeroperl 300 CBD) 123
Table 23. Penetrated amount of CBD and PE of CBD-loaded silica carriers with different amounts of propylene glycol compared to pure CBD and CBD-loaded carrier without propylene glycol (Aeroperl 300 CBD) 125
Table 24. Comparison of penetration enhancement ratios of CBD-loaded mucoadhesive carrier systems with and without propylene glycol and pure CBD as a reference 132
Table 25. HPLC calibration data for carvone and thymol as the reference substances for Optamint liquid and Optamint solid 160
Table 26. HPLC calibration data for CBD 161
Table 27. Composition of formulation 1-7 163
Table 28. Composition of flavor-loaded mucoadhesive carrier systems with Aeroperl 300, sunflower oil and HPMC 164
Table 29. Composition of flavor-loaded mucoadhesive carrier systems with Aeroperl 300, triacetin and HPMC 164
Table 30. Composition of flavor-loaded mucoadhesive carrier systems with Aeroperl 300, PEG 1000 and HPMC 165
Table 31. Composition of flavor-loaded mucoadhesive carrier systems with Aeroperl 300, sunflower oil and carbomer or chitosan 165
Table 32. Composition of flavor-loaded mucoadhesive carrier systems with Aeroperl 300, PEG 1000 and carbomer 166
Table 33. Composition of flavor-loaded mucoadhesive carrier systems with Aeroperl 300, triacetin and HPMC or carbomer 166
Table 34. Composition of flavor-loaded mucoadhesive carrier systems with Sident 9 167
Table 35. Composition of mucoadhesive carrier system with Optamint solid 167
Table 36. Composition of mucoadhesive carrier systems with Aeroperl 300 and CBD 168
Table 37. Composition CBD-loaded Aeroperl 300 carrier systems with enhancer 168
Table 38. Composition of CBD-loaded mucoadhesive carrier systems with 5% propylene glycol (PG) 169
Table 39. Composition of CBD- and flavor-loaded carrier systems 169

5.3 List of equation

Equation 1 Oil absorption capacity 28
Equation 2 Mucoadhesion coefficient (MC) 36
Equation 3 Penetration enhancement ratio (PE) 37

5.4 References

1. Unger, K.K., *Porous silica*. 1979: Elsevier.
2. Prasertsri, S. and N. Rattanasom, *Fumed and precipitated silica reinforced natural rubber composites prepared from latex system: Mechanical and dynamic properties.* Polymer Testing, 2012. **31**(5): p. 593-605.
3. Rahman, I.A. and V. Padavettan, *Synthesis of silica nanoparticles by sol-gel: size-dependent properties, surface modification, and applications in silica-polymer nanocomposites—a review.* Journal of Nanomaterials, 2012.
4. Albert, K., X.-C. Huang, and H.-Y. Hsu, *Bio-templated silica composites for next-generation biomedical applications.* Advances in colloid and interface science, 2017. **249**: p. 272-289.
5. Vraníková, B., et al., *Mechanistic aspects of drug loading in liquisolid systems with hydrophilic lipid-based mixtures.* International Journal of Pharmaceutics, 2020. **578**: p. 119099.
6. Šoltys, M., et al., *Effect of solvent selection on drug loading and amorphisation in mesoporous silica particles.* International journal of pharmaceutics, 2019. **555**: p. 19-27.
7. Chaudhari, S.P. and A. Gupte, *Mesoporous Silica as a Carrier for Amorphous Solid Dispersion.* arXiv preprint arXiv:1707.00036, 2017.
8. Sing, K.S., *Reporting physisorption data for gas/solid systems with special reference to the determination of surface area and porosity (Recommendations 1984).* Pure and applied chemistry, 1985. **57**(4): p. 603-619.
9. Limnell, T., et al., *Drug delivery formulations of ordered and nonordered mesoporous silica: comparison of three drug loading methods.* Journal of pharmaceutical sciences, 2011. **100**(8): p. 3294-3306.
10. Wei, Q., C.M. Keck, and R.H. Müller, *CapsMorph® technology for oral delivery–theory, preparation and characterization.* International journal of pharmaceutics, 2015. **482**(1-2): p. 11-20.
11. Mellaerts, R., et al., *Physical state of poorly water soluble therapeutic molecules loaded into SBA-15 ordered mesoporous silica carriers: a case study with itraconazole and ibuprofen.* Langmuir, 2008. **24**(16): p. 8651-8659.
12. Trzeciak, K., et al., *Mesoporous Silica Particles as Drug Delivery Systems—The State of the Art in Loading Methods and the Recent Progress in Analytical Techniques for Monitoring These Processes.* Pharmaceutics, 2021. **13**(7): p. 950.
13. Seljak, K.B., P. Kocbek, and M. Gašperlin, *Mesoporous silica nanoparticles as delivery carriers: An overview of drug loading techniques.* Journal of Drug Delivery Science and Technology, 2020: p. 101906.
14. Cauda, V., et al., *Tuning drug uptake and release rates through different morphologies and pore diameters of confined mesoporous silica.* Microporous and Mesoporous Materials, 2009. **118**(1-3): p. 435-442.
15. Sarah, L., et al., *Mucoadhesion: A food perspective.* Food hydrocolloids, 2017.
16. Bagan, J., et al., *Mucoadhesive polymers for oral transmucosal drug delivery: a review.* Current pharmaceutical design, 2012. **18**(34): p. 5497-5514.
17. Rathbone, M.J., S. Senel, and I. Pather, *Oral mucosal drug delivery and therapy*. 2015: Springer.
18. Mansuri, S., et al., *Mucoadhesion: A promising approach in drug delivery system.* Reactive and functional polymers, 2016. **100**: p. 151-172.
19. Squier, C. and K. Brogden, *Human oral mucosa: development, structure and function*. 2010: John Wiley & Sons.
20. Punitha, S. and Y. Girish, *Polymers in mucoadhesive buccal drug delivery system–A review.* International Journal of Research in Pharmaceutical Sciences, 2010. **1**(2).
21. Salamat-Miller, N., M. Chittchang, and T.P. Johnston, *The use of mucoadhesive polymers in buccal drug delivery.* Advanced drug delivery reviews, 2005. **57**(11): p. 1666-1691.
22. Jayanthi, V., et al., *Oral submucosal fibrosis--a preventable disease.* Gut, 1992. **33**(1): p. 4.
23. Russo, E., et al., *A focus on mucoadhesive polymers and their application in buccal dosage forms.* Journal of Drug Delivery Science and Technology, 2016. **32**: p. 113-125.

24. Peppas, N.A. and P.A. Buri, *Surface, interfacial and molecular aspects of polymer bioadhesion on soft tissues.* Journal of Controlled Release, 1985. **2**: p. 257-275.
25. Brahmbhatt, D., *Bioadhesive drug delivery systems: Overview and recent advances.* Int. J. Chem. Life Sci, 2017. **6**(3): p. 2016-2024.
26. Khutoryanskiy, V.V., *Advances in mucoadhesion and mucoadhesive polymers.* Macromolecular bioscience, 2011. **11**(6): p. 748-764.
27. Sogias, I.A., A.C. Williams, and V.V. Khutoryanskiy, *Why is chitosan mucoadhesive?* Biomacromolecules, 2008. **9**(7): p. 1837-1842.
28. Smart, J.D., *The basics and underlying mechanisms of mucoadhesion.* Advanced drug delivery reviews, 2005. **57**(11): p. 1556-1568.
29. Yu, T., G.P. Andrews, and D.S. Jones, *Mucoadhesion and characterization of mucoadhesive properties*, in *Mucosal Delivery of Biopharmaceuticals*. 2014, Springer. p. 35-58.
30. Yadav, V.K., et al., *Mucoadhesive polymers: means of improving the mucoadhesive properties of drug delivery system.* J. Chem. Pharm. Res, 2010. **2**(5): p. 418-432.
31. Dawes, C., et al., *The functions of human saliva: A review sponsored by the World Workshop on Oral Medicine VI.* Archives of oral biology, 2015. **60**(6): p. 863-874.
32. Humphrey, S.P. and R.T. Williamson, *A review of saliva: normal composition, flow, and function.* The Journal of prosthetic dentistry, 2001. **85**(2): p. 162-169.
33. Carpenter, G.H., *The secretion, components, and properties of saliva.* Annual review of food science and technology, 2013. **4**: p. 267-276.
34. Mandel, I., *The functions of saliva.* Journal of dental research, 1987. **66**(1_suppl): p. 623-627.
35. Squier, C., *The permeability of oral mucosa.* Critical Reviews in Oral Biology & Medicine, 1991. **2**(1): p. 13-32.
36. Asane, G., et al., *Polymers for mucoadhesive drug delivery system: a current status.* Drug development and industrial pharmacy, 2008. **34**(11): p. 1246-1266.
37. Rathbone, M.J., I. Pather, and S. Şenel, *Overview of oral mucosal delivery*, in *Oral mucosal drug delivery and therapy*. 2015, Springer. p. 17-29.
38. Madhav, N.S., et al., *Orotransmucosal drug delivery systems: a review.* Journal of controlled release, 2009. **140**(1): p. 2-11.
39. Boddupalli, B.M., et al., *Mucoadhesive drug delivery system: An overview.* Journal of advanced pharmaceutical technology & research, 2010. **1**(4): p. 381.
40. Sudheer, P., *Mucoadhesive Polymers: A Review.* Journal of Pharmaceutical Research, 2018. **17**(1): p. 47-55.
41. Madsen, F., K. Eberth, and J.D. Smart, *A rheological assessment of the nature of interactions between mucoadhesive polymers and a homogenised mucus gel.* Biomaterials, 1998. **19**(11-12): p. 1083-1092.
42. Kinloch, A., *The science of adhesion.* Journal of materials science, 1980. **15**(9): p. 2141-2166.
43. Ahagon, A. and A. Gent, *Effect of interfacial bonding on the strength of adhesion.* Journal of Polymer Science: Polymer Physics Edition, 1975. **13**(7): p. 1285-1300.
44. Grabovac, V., D. Guggi, and A. Bernkop-Schnürch, *Comparison of the mucoadhesive properties of various polymers.* Advanced drug delivery reviews, 2005. **57**(11): p. 1713-1723.
45. Schattling, P., et al., *A polymer chemistry point of view on mucoadhesion and mucopenetration.* Macromolecular bioscience, 2017. **17**(9): p. 1700060.
46. Shin, S.-C., J.-Y. Kim, and I.-J. Oh, *Mucoadhesive and physicochemical characterization of carbopol-poloxamer gels containing triamcinolone acetonide.* Drug development and industrial pharmacy, 2000. **26**(3): p. 307-312.
47. Bernkop-Schnurch, A., *Mucoadhesive polymers.* Polymeric biomaterials, 2001: p. 147-164.
48. Banchonglikitkul, C., et al., *An in-vitro evaluation of lectin cytotoxicity using cell lines derived from the ocular surface.* Journal of drug targeting, 2002. **10**(8): p. 601-606.
49. Woertz, C., et al., *Assessment of test methods evaluating mucoadhesive polymers and dosage forms: an overview.* European Journal of Pharmaceutics and Biopharmaceutics, 2013. **85**(3): p. 843-853.

50. Davidovich-Pinhas, M. and H. Bianco-Peled, *Mucoadhesion: a review of characterization techniques.* Expert opinion on drug delivery, 2010. **7**(2): p. 259-271.
51. Pinto, S., M.E. Pintado, and B. Sarmento, *In vivo, ex vivo and in vitro assessment of buccal permeation of drugs from delivery systems.* Expert opinion on drug delivery, 2020. **17**(1): p. 33-48.
52. Shojaei, A.H., *Buccal mucosa as a route for systemic drug delivery: a review.* J Pharm Pharm Sci, 1998. **1**(1): p. 15-30.
53. da Silva, J.B., et al., *A mucosa-mimetic material for the mucoadhesion testing of thermogelling semi-solids.* International journal of pharmaceutics, 2017. **528**(1-2): p. 586-594.
54. Cook, M.T., S.L. Smith, and V.V. Khutoryanskiy, *Novel glycopolymer hydrogels as mucosa-mimetic materials to reduce animal testing.* Chemical Communications, 2015. **51**(77): p. 14447-14450.
55. Cook, M.T. and V.V. Khutoryanskiy, *Mucoadhesion and mucosa-mimetic materials—A mini-review.* International journal of pharmaceutics, 2015. **495**(2): p. 991-998.
56. Sattar, M., O.M. Sayed, and M.E. Lane, *Oral transmucosal drug delivery–current status and future prospects.* International journal of pharmaceutics, 2014. **471**(1-2): p. 498-506.
57. Sohi, H., et al., *Critical evaluation of permeation enhancers for oral mucosal drug delivery.* Drug development and industrial pharmacy, 2010. **36**(3): p. 254-282.
58. Rossi, S., G. Sandri, and C.M. Caramella, *Buccal drug delivery: a challenge already won?* Drug Discovery Today: Technologies, 2005. **2**(1): p. 59-65.
59. Sandri, G., et al., *(Trans) buccal drug delivery.* Nanotechnology for Oral Drug Delivery, 2020: p. 225-250.
60. Şenel, S. and A.A. Hıncal, *Drug permeation enhancement via buccal route: possibilities and limitations.* Journal of Controlled Release, 2001. **72**(1-3): p. 133-144.
61. Caon, T., et al., *Enhancing the buccal mucosal delivery of peptide and protein therapeutics.* Pharmaceutical research, 2015. **32**(1): p. 1-21.
62. Nicolazzo, J.A., B.L. Reed, and B.C. Finnin, *Buccal penetration enhancers—how do they really work?* Journal of controlled release, 2005. **105**(1-2): p. 1-15.
63. Smart, J.D., *Buccal drug delivery.* Expert opinion on drug delivery, 2005. **2**(3): p. 507-517.
64. Patel, V.F., F. Liu, and M.B. Brown, *Advances in oral transmucosal drug delivery.* Journal of controlled release, 2011. **153**(2): p. 106-116.
65. Chinna Reddy, P., K.S. Chaitanya, and Y. Madhusudan Rao, *A review on bioadhesive buccal drug delivery systems: current status of formulation and evaluation methods.* Daru, 2011. **19**(6): p. 385-403.
66. Pather, S.I., M.J. Rathbone, and S. Şenel, *Current status and the future of buccal drug delivery systems.* Expert Opinion on Drug Delivery, 2008. **5**(5): p. 531-542.
67. Şenel, S., et al., *Recent developments in buccal and sublingual delivery systems.* Expert opinion on drug delivery, 2012. **9**(6): p. 615-628.
68. Padula, C., et al., *New insights on the mechanism of fatty acids as buccal permeation enhancers.* Pharmaceutics, 2018. **10**(4): p. 201.
69. Manganaro, A.M. and P.W. Wertz, *The effects of permeabilizers on the in vitro penetration of propranolol through porcine buccal epithelium.* Military medicine, 1996. **161**(11): p. 669-672.
70. Senel, S., et al., *Effect of chitosan in enhancing drug delivery across buccal mucosa.* Advances in chitin science. Potsdam: University of Potsdam, 2000: p. 254-8.
71. Schipper, N.G., et al., *Chitosans as absorption enhancers for poorly absorbable drugs 2: mechanism of absorption enhancement.* Pharmaceutical research, 1997. **14**(7): p. 923-929.
72. Benson, H.A., *Transdermal drug delivery: penetration enhancement techniques.* Current drug delivery, 2005. **2**(1): p. 23-33.
73. Brandl, M. and A. Bauer-Brandl, *Oromucosal drug delivery: Trends in in-vitro biopharmaceutical assessment of new chemical entities and formulations.* European Journal of Pharmaceutical Sciences, 2019. **128**: p. 112-117.
74. Casiraghi, A., et al., *Topical Administration of Cannabidiol: Influence of Vehicle-Related Aspects on Skin Permeation Process.* Pharmaceuticals, 2020. **13**(11): p. 337.

75. Jung, B., et al., *Synthetic Strategies for (−)-Cannabidiol and Its Structural Analogs.* Chemistry–An Asian Journal, 2019. **14**(21): p. 3749-3762.
76. Noreen, N., et al., *Is cannabidiol a promising substance for new drug development? A review of its potential therapeutic applications.* Critical Reviews™ in Eukaryotic Gene Expression, 2018. **28**(1).
77. Matarazzo, A.P., et al., *Mucoadhesive nanostructured lipid carriers as a cannabidiol nasal delivery system for the treatment of neuropathic pain.* European Journal of Pharmaceutical Sciences, 2021. **159**: p. 105698.
78. Abu-Sawwa, R., B. Scutt, and Y. Park, *Emerging use of epidiolex (cannabidiol) in epilepsy.* The Journal of Pediatric Pharmacology and Therapeutics, 2020. **25**(6): p. 485-499.
79. Guy, G.W. and C.G. Stott, *The development of Sativex®—a natural cannabis-based medicine*, in *Cannabinoids as therapeutics*. 2005, Springer. p. 231-263.
80. Itin, C., et al., *Prolonged oral transmucosal delivery of highly lipophilic drug cannabidiol.* International journal of pharmaceutics, 2020. **581**: p. 119276.
81. Millar, S.A., et al., *Towards Better Delivery of Cannabidiol (CBD).* Pharmaceuticals (Basel), 2020. **13**(9).
82. Cherniakov, I., et al., *The effect of Pro NanoLipospheres (PNL) formulation containing natural absorption enhancers on the oral bioavailability of delta-9-tetrahydrocannabinol (THC) and cannabidiol (CBD) in a rat model.* European Journal of Pharmaceutical Sciences, 2017. **109**: p. 21-30.
83. Silmore, L.H., et al., *Food Effects on the Formulation, Dosing, and Administration of Cannabidiol (CBD) in Humans: A Systematic Review of Clinical Studies.* Pharmacotherapy: The Journal of Human Pharmacology and Drug Therapy, 2021.
84. Itin, C., A.J. Domb, and A. Hoffman, *A meta-opinion: cannabinoids delivered to oral mucosa by a spray for systemic absorption are rather ingested into gastro-intestinal tract: the influences of fed/fasting states.* Expert opinion on drug delivery, 2019. **16**(10): p. 1031-1035.
85. Morrison, G., et al., *A phase 1, open-label, pharmacokinetic trial to investigate possible drug-drug interactions between clobazam, stiripentol, or valproate and cannabidiol in healthy subjects.* Clinical pharmacology in drug development, 2019. **8**(8): p. 1009-1031.
86. Bruni, N., et al., *Cannabinoid delivery systems for pain and inflammation treatment.* Molecules, 2018. **23**(10): p. 2478.
87. Glancy, C.W., *Oil Absorption of Pigments*. 2012: ASTM International.
88. Hoffmann, A. and R. Daniels, *A novel test system for the evaluation of oral mucoadhesion of fast disintegrating tablets.* International journal of pharmaceutics, 2018. **551**(1-2): p. 141-147.
89. Bavnhøj, C.G., et al., *The role interplay between mesoporous silica pore volume and surface area and their effect on drug loading capacity.* International journal of pharmaceutics: X, 2019. **1**: p. 100008.
90. Horcajada, P., et al., *Influence of pore size of MCM-41 matrices on drug delivery rate.* Microporous and Mesoporous Materials, 2004. **68**(1-3): p. 105-109.
91. Lai, J., et al., *Investigating the effects of loading factors on the in vitro pharmaceutical performance of mesoporous materials as drug carriers for ibuprofen.* Materials, 2017. **10**(2): p. 150.
92. Riikonen, J., et al., *Determination of the physical state of drug molecules in mesoporous silicon with different surface chemistries.* Langmuir, 2009. **25**(11): p. 6137-6142.
93. Salonen, J., et al., *Mesoporous silicon microparticles for oral drug delivery: loading and release of five model drugs.* Journal of controlled release, 2005. **108**(2-3): p. 362-374.
94. Mellaerts, R., et al., *Aging behavior of pharmaceutical formulations of itraconazole on SBA-15 ordered mesoporous silica carrier material.* Microporous and Mesoporous Materials, 2010. **130**(1-3): p. 154-161.
95. Ali, J., et al., *Application of biorelevant saliva-based dissolution for optimisation of orally disintegrating formulations of felodipine.* International journal of pharmaceutics, 2019. **555**: p. 228-236.

96. Wan, L.S., P.W. Heng, and L.F. Wong, *Relationship between swelling and drug release in a hydrophilic matrix.* Drug development and industrial pharmacy, 1993. **19**(10): p. 1201-1210.
97. He, Y., P. Jain, and S.H. Yalkowsky, *Handbook of aqueous solubility data*. 2010: CRC press.
98. Maloney, T., *Messen der Porengrößenverteilung mittels DSC.* UserCom Mettler Toledo, 2000. **12**: p. 15-17.
99. Sudharsan Reddy, K., et al., *Miscibility studies of hydroxypropyl cellulose/poly (ethylene glycol) in dilute solutions and solid state.* International journal of carbohydrate chemistry, 2012. **2012**.
100. Shojaei, A.H. and X. Li, *Mechanisms of buccal mucoadhesion of novel copolymers of acrylic acid and polyethylene glycol monomethylether monomethacrylate.* Journal of controlled release, 1997. **47**(2): p. 151-161.
101. Lamprecht, A., U. Schäfer, and C.-M. Lehr, *Size-dependent bioadhesion of micro-and nanoparticulate carriers to the inflamed colonic mucosa.* Pharmaceutical research, 2001. **18**(6): p. 788-793.
102. Esim, O., et al., *Effect of polymer type on characteristics of buccal tablets using factorial design.* Saudi Pharmaceutical Journal, 2018. **26**(1): p. 53-63.
103. Bednar, B., H. Morawetz, and J.A. Shafer, *Kinetics of the cooperative complex formation and dissociation of poly (acrylic acid) and poly (oxyethylene).* Macromolecules, 1984. **17**(8): p. 1634-1636.
104. Lebossé, R., V. Ducruet, and A. Feigenbaum, *Interactions between reactive aroma compounds from model citrus juice with polypropylene packaging film.* Journal of Agricultural and Food Chemistry, 1997. **45**(8): p. 2836-2842.
105. Doytcheva, B.K., *Structural Disruption of Toothpastes Under Deformation—An Easy Release of Active Ingredients.* The Canadian Journal of Chemical Engineering, 2003. **81**(2): p. 285-288.
106. Park, S.-H., M.-K. Chun, and H.-K. Choi, *Preparation of an extended-release matrix tablet using chitosan/Carbopol interpolymer complex.* International journal of pharmaceutics, 2008. **347**(1-2): p. 39-44.
107. Esim, O., et al., *Investigation of the mucoadhesivity, swelling, and drug release mechanisms of indomethacin buccal tablets: effect of formulation variables.* Drug Development and Industrial Pharmacy, 2020. **46**(12): p. 1979-1987.
108. Hassan, N., et al., *Chemical permeation enhancers for transbuccal drug delivery.* Expert opinion on drug delivery, 2010. **7**(1): p. 97-112.
109. Moser, K., et al., *Supersaturation: enhancement of skin penetration and permeation of a lipophilic drug.* Pharmaceutical research, 2001. **18**(7): p. 1006-1011.
110. Netsomboon, K. and A. Bernkop-Schnürch, *Mucoadhesive vs. mucopenetrating particulate drug delivery.* European Journal of Pharmaceutics and Biopharmaceutics, 2016. **98**: p. 76-89.
111. Nicolazzo, J.A., B.L. Reed, and B.C. Finnin, *Assessment of the effects of sodium dodecyl sulfate on the buccal permeability of caffeine and estradiol.* Journal of pharmaceutical sciences, 2004. **93**(2): p. 431-440.
112. Rasool, B.K.A. and S.A. Khan, *In vitro evaluation of miconazole mucoadhesive buccal films.* Int. J. Appl. Pharm, 2010. **2**(4): p. 23-26.
113. Sohi, H., Y. Sultana, and R.K. Khar, *Taste masking technologies in oral pharmaceuticals: recent developments and approaches.* Drug development and industrial pharmacy, 2004. **30**(5): p. 429-448.

6 Appendix

6.1 HPLC UV-calibration

Table 26. HPLC calibration data for carvone and thymol as the reference substances for Optamint liquid and Optamint solid

Ethanolic extraction:

Parameters	**Carvone**	**Thymol**
Linearity	0.5 - 50 µg/mL	0.5 - 50 µg/mL
Correlation coefficient	0.9998	0,9999
LOD	0.750 µg/mL	0.99 µg/mL
LOQ	2.273 µg/mL	0.899 µg/mL
Accuracy ± SD	98.22 ± 3.43%	99.91 ± 2.05%
Linearity	20 - 500 µg/mL	20 - 500 µg/mL
Correlation coefficient	0.9997	0.9999
LOD	10.020 µg/mL	6.645 µg/mL
LOQ	30.363 µg/mL	20.136 µg/mL
Accuracy ± SD	99.68 ± 2.86%	100.70 ± 3.64%

Aqueous samples after protein precipitation (2.2.8 Dissolution, 2.2.10 Mucoadhesion test**):**

Parameters	**Carvone**	**Thymol**
Linearity	1 - 100 µg/mL	5 - 150 µg/mL
Correlation coefficient	0.9994	0.9994
LOD	1.980 µg/mL	1.306 µg/mL
LOQ	6.001 µg/mL	4.312 µg/mL
Accuracy ± SD	100.99 ± 3.76%	99.94 ± 3.73%

Table 27. HPLC calibration data for CBD

Ethanolic extraction:

Parameters	**CBD**
Linearity	1 - 100 μg/mL
Correlation coefficient	0.9999
LOD	0.95 μg/mL
LOQ	2.89 μg/mL
Accuracy ± SD	100.25 ± 1.24%
Linearity	0.1 - 1 μg/mL
Correlation coefficient	0.9999
LOD	0.01 μg/mL
LOQ	0.04 μg/mL
Accuracy ± SD	99.54 ± 2.17%

6.2 Mucoadhesion test of flavor-loaded silica carriers

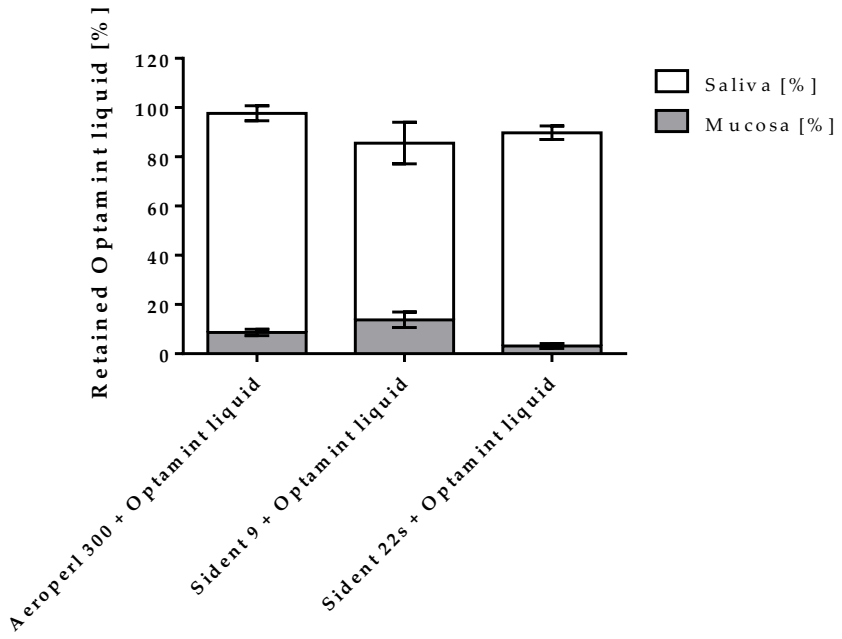

Figure 112. Recovery of Optamint liquid after 12 min mucoadhesion test of flavor-loaded silica carriers: retained concentrations of Optamint liquid in saliva and from mucosa

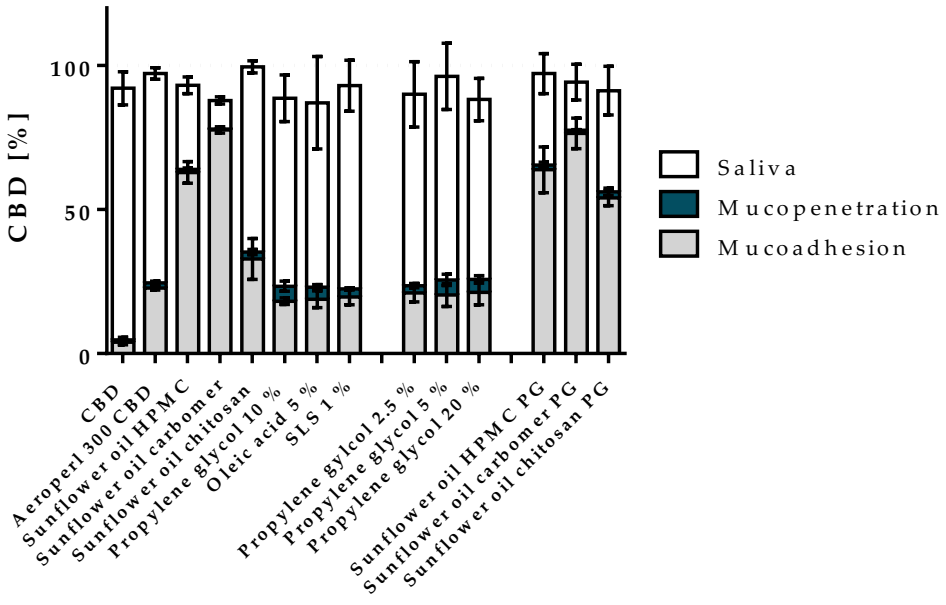

Figure 113. Recovery of CBD after 12 min from mucoadhesion tests (fraction of CBD on the mucosa and fraction flushed away by saliva) and from mucopenetration test (fraction of CBD penetrated the mucosa); PG: propylene glycol

6.3 Composition of mucoadhesive carrier systems

Table 28. Composition of formulation 1-7

Formulation	1		2		3			
	[%]	g	[%]	g	[%]	g	[%]	g
Aeroperl300	56.25	18.04	24.75	8.42	34.13	11.61	58.69	15.69
Optamint liquid	3.51	1.13	3.12	1.06			3.41	0.91
Water	37.02	11.88			33.83	11.51		
Glycerol							35.10	9.41
HPMC	3.18	1.02			4.17	1.42	2.79	0.75

Formulation	4		5		6		7		8	
	[%]	g	[%]	g	[%]	g	[%]	g	[%]	g
Aeroperl 300	53.72	13.46	54.60	13.25	84.82	15.27	85.18	13.29	73.76	13.73
Optamint liquid	7.63	1.91	1.57	6.10	11.79	2.98	11.55	1.81	10.61	1.97
Sunflower oil	34.41	8.62								
Triacetin			35.47	9.12						
PEG 1000									10.74	1.99
HPMC	4.24	1.06	3.83	0.99	3.39	0.64	3.27	0.51	4.89	0.91

Table 29. Composition of flavor-loaded mucoadhesive carrier systems with Aeroperl 300, sunflower oil and HPMC

Formulation:	4% HPMC Sunflower oil		6% HPMC Sunflower oil		8% HPMC Sunflower oil		10% HPMC Sunflower oil	
	[%]	g	[%]	g	[%]	g	[%]	g
Aeroperl300	53.72	13.46	40.41	13.68	53.73	13.75	38.76	13.68
Optamint liquid	7.63	1.91	5.49	1.86	6.80	1.74	4.79	1.69
Sunflower oil	34.41	8.62	48.06	16.27	31.42	8.04	45.17	15.94
HPMC	4.24	1.06	6.06	2.05	8.05	2.06	11.28	3.98

Table 30. Composition of flavor-loaded mucoadhesive carrier systems with Aeroperl 300, triacetin and HPMC

Formulation:	4% HPMC Triacetin		6% HPMC Triacetin		8% HPMC Triacetin		10% HPMC Triacetin	
	[%]	g	[%]	g	[%]	g	[%]	g
Aeroperl 300	54.60	13.25	36.23	12.54	54.61	13.80	37.89	13.53
Optamint liquid	6.10	1.57	6.38	2.21	6.09	1.54	5.15	1.84
Triacetin	35.47	9.12	51.49	17.822	31.46	7.95	46.04	16.44
HPMC	3.83	0.95	5.87	2.030	7.80	1.97	10.92	3.90

Table 31. Composition of flavor-loaded mucoadhesive carrier systems with Aeroperl 300, PEG 1000 and HPMC

Formulation:	**5% HPMC 10% PEG 1000**		**6% HPMC 20% PEG 1000**		**10% HPMC 10% PEG 1000**		**20% HPMC 20% PEG 1000**	
	[%]	**g**	**[%]**	**g**	**[%]**	**g**	**[%]**	**g**
Aeroperl 300	73.76	13.73	67.16	13.50	70.16	13.59	55.25	11.58
Optamint liquid	10.61	1.97	7.41	1.49	8.67	1.68	6.15	1.29
PEG 1000	10.74	1.99	19.35	3.89	10.53	2.04	19.47	4.08
HPMC	4.89	0.91	6.07	1.22	10.64	2.06	19.13	4.01

Table 32. Composition of flavor-loaded mucoadhesive carrier systems with Aeroperl 300, sunflower oil and carbomer or chitosan

Formulation:	**Chitosan 6% Sunflower oil**		**Carbomer 10% Sunflower oil**	
	[%]	**g**	**[%]**	**g**
Aeroperl 300	40.30	13.32	36.95	13.30
Optamint liquid	3.78	1.25	5.25	1.98
Sunflower oil	49.77	16.45	46.21	16.63
Polymer	6.17	2.04	11.34	4.08

Table 33. Composition of flavor-loaded mucoadhesive carrier systems with Aeroperl 300, PEG 1000 and carbomer

Formulation:	5% Carbomer 10% PEG 1000		10% Carbomer 10% PEG 1000	
	[%]	g	[%]	g
Aeroperl 300	67.96	13.06	69.04	13.49
Optamint liquid	10.18	1.96	9.37	1.83
PEG 1000	11.37	2.19	11.21	2.19
Polymer	10.64	2.05	10.39	2.03

Table 34. Composition of flavor-loaded mucoadhesive carrier systems with Aeroperl 300, triacetin and HPMC or carbomer

Formulation:	10% HPMC Triacetin		10% Carbomer Triacetin	
	[%]	g	[%]	g
Aeroperl 300	37.89	13.53	37.86	13.43
Optamint liquid	5.15	1.84	5.30	1.88
Triacetin	46.04	16.44	46.04	16.33
Polymer	10.92	3.90	10.79	3.83

Table 35. Composition of flavor-loaded mucoadhesive carrier systems with Sident 9

Formulation:	8% HPMC Sunflower oil		8% Carbomer Sunflower oil		8% HPMC Triacetin		8% Carbomer Triacetin		10% HPMC 10% PEG 1000	
	[%]	g	[%]	g	[%]	g	[%]	g	[%]	g
Aeroperl 300	52.27	15.22	55.95	15.47	56.92	14.02	55.28	13.14	75.61	14.51
Optamint liquid	2.16	0.63	5.46	1.51	2.11	0.52	2.44	0.58	31.79	0.61
Sunflower oil	36.78	10.71	30.49	8.43						
Triacetin					32.93	8.11	34.03	8.09		
PEG 1000									10.58	2.03
Polymer	8.79	2.56	8.10	2.24	8.04	1.98	8.25	1.96	10.63	2.04

Table 36. Composition of mucoadhesive carrier system with Optamint solid

Formulation:	Carbomer 10% Sunflower oil	
	[%]	g
Aeroperl 300	39.97	15.21
Optamint solid	7.07	2.69
Carbomer	42.34	16.11
Polymer	10.62	4.04

Table 37. Composition of mucoadhesive carrier systems with Aeroperl 300 and CBD

Formulation:	10% HPMC		10% Carbomer		6% Chitosan		Aeroperl 300 CBD	
	[%]	g	[%]	g	[%]	g	[%]	g
Aeroperl 300	34.00	12.09	33.89	11.98	33.10	5.93	83.39	15.16
CBD	9.59	3.41	9.56	3.38	9.33	1.67	16.61	3.02
Sunflower oil	45.14	16.05	45.21	15.98	51.50	9.23		
Polymer	11.28	4.01	11.34	4.01	5.68	1.02		

Table 38. Composition CBD-loaded Aeroperl 300 carrier systems with enhancer

Formulation:	SLS 1%C		Oleic acid 5%		Propylene glycol 10%	
	[%]	mg	[%]	mg	[%]	mg
Aeroperl 300	81.86	86.99	79.83	86.06	74.21	801.99
CBD	16.62	17.66	14.77	15.92	15.40	166.44
Enhancer	1.52	1.62	5.40	5.82	10.39	112.24

Table 39. Composition of CBD-loaded mucoadhesive carrier systems with 5% propylene glycol (PG)

Formulation:	10% HPMC PG		10% Carbomer PG		6% Chitosan PG		Aeroperl 300 CBD PG	
	[%]	g	[%]	g	[%]	g	[%]	g
Aeroperl 300	32.36	11.42	33.57	12.06	32.26	11.16	79.00	0.79
CBD	5.44	1.92	5.62	2.02	5.41	1.87	15.47	0.15
Propylene glycol	5.04	1.78	4.93	1.87	5.06	1.75	5.49	0.05
Sunflower oil	45.54	16.07	44.56	16.04	51.37	17.77		
Polymer	11.59	4.09	10.97	9.34	5.92	2.05		

Table 40. Composition of CBD- and flavor-loaded carrier systems

Formulation:	10% Carbomer		6% Chitosan		Aeroperl 300 CBD	
	[%]	g	[%]	g	[%]	g
Aeroperl 300	37.52	13.37	32.37	10.60	83.38	37.80
CBD	1.85	0.66	1.62	0.53	4.17	1.88
Optamint liquid	5.36	1.91	4.64	1.52	12.00	5.41
Sunflower oil	44.09	15.71	55.25	18.09		
Polymer	11.17	3.98	6.11	2.00		